
Tesi doctoral

Nanoparticles: The next step in endodontic medicaments.

Firas Elmsmari



Aquesta tesi doctoral està subjecta a la licència [Reconeixement-NoComercial-SenseObraDerivada 4.0 Internacional \(CC BY-NC-ND 4.0\)](https://creativecommons.org/licenses/by-nc-nd/4.0/)

Esta tesis doctoral está sujeta a la licencia [Reconocimiento-NoComercial-SinObraDerivada 4.0 Internacional \(CC BY-NC-ND 4.0\)](https://creativecommons.org/licenses/by-nc-nd/4.0/)

This doctoral thesis is licensed under the [Attribution-NonCommercial-NoDerivatives 4.0 International \(CC BY-NC-ND 4.0\)](https://creativecommons.org/licenses/by-nc-nd/4.0/)



NANOPARTICLES: THE NEXT STEP IN ENDODONTIC
MEDICAMENTS.

FIRAS ELMSMARI



NANOPARTICLES: THE NEXT STEP IN ENDODONTIC MEDICAMENTS.

Department of Endodontics - Faculty of Dentistry

Doctorate in Health Sciences

Universitat Internacional de Catalunya

Doctoral thesis

Firas Elmsmari

Sant Cugat del Vallés 2021

Director: Dr José Antonio González Sánchez

Codirector: Dra Elena Sánchez López

﴿ وَقُلْ رَبِّ زِدْنِي عِلْمًا ﴾

القرآن الكريم – سورة طه ﴿١١٤﴾

“Our discussion will be adequate if it has as much clearness as the subject-matter admits of, for precision is not to be sought for alike in all discussions,...for it is the mark of an educated man to look for precision in each class of things just so far as the nature of the subject admits.”

Aristotle (350 BC) *Nicomachean Ethics*.

Translated by: W D Ross

ACKNOWLEDGEMENTS

ACKNOWLEDGEMENTS

First and foremost, I want to thank the almighty god for guiding me and making all of this possible. I owe everything I have, and I will be to him and my parents Hussein and Amina. Mom and dad, words cannot describe how much I am grateful for everything you have done for me, I will be eternally indebted. Thank you for supporting me and helping me become the person I am today. Thank you for making me strive to be a better human begin which each passing day. You both are my role models and no amount of “thank you’s” will ever be enough.

I want to thank my thesis director José Antonio, for all his help and guidance throughout the years, first as a master student then as my doctorate director. One could not have asked for a better more understating and helping director. You were always there for me with everything whenever I needed you, day or night. With your infectious smile and positive attitude, you always made everything seem possible. Sincerely, thank you.

I would also like to thank my thesis co-director Elena, for all her support and assistance throughout my doctorate project. Thank you for your will and appetite in teaching me things I had no idea about from absolute scratch. Thank you for your patience and eagerness to explain every single thing for me over and over and over again. Your work ethic and professionalism are at extraordinary levels that I wish I can reach someday. I will be perpetually thankful.

Ultimately, I want to express special thanks to Luis Delgado for all his help and guidance in the experiments carried out in UIC. Thank you very much Luis.

ABSTRACT

ABSTRACT

ABSTRACT

Aim: The aim of the current study was to develop two formulations loading calcium hydroxide (Ca(OH)₂) and Clobetasol Propionate into poly lactic-co-glycolic acid (PLGA) biodegradable nanoparticles (NPs) to be used in the field of endodontics as an intracanal medications, including NPs optimization and characterization, plus drug release profile of the NPs compared to free drug counterpart. Additionally, comparison of the depth and area of penetration of the NPs inside the dentinal tubules against the free drug was carried out. Furthermore, the therapeutic efficacy for both formulations were examined using antibacterial and anti-inflammatory assays.

Methodology: NPs were prepared using the solvent displacement method. Optimization of the NPs was carried out with a central composite design to obtain a final optimized formulation. The NPs morphology was examined under transmission electron microscopy (TEM), plus characterization was done by x-ray diffraction (XRD), fourier transform infrared spectroscopy (FTIR) and differential scanning calorimetry (DSC). Moreover, the optimal conditions and cryoprotectants for freeze drying of the NPs were examined and tested. The drug release profile of the NPs and free drug was evaluated up to 48 hours. Additionally, the depth and area of penetration inside the dentinal tubules was examined for both the NPs and free drug. Antibacterial testing was performed on the antibacterial NPs to evaluate their efficacy in eliminating different bacterial strains. Agar disk-diffusion and broth dilution were used to determine the inhibition growth zones and the minimal inhibitory concentration (MIC). Likewise, anti-inflammatory testing was performed on the Clobetasol Propionate anti-inflammatory NPs, in which their response and reaction against inflammatory cells, in particular against macrophages was tested using the enzyme-linked immunosorbent assay (ELISA) to examine the cytokine release of IL-1 β and TNF- α .

Results: Using the solvent displacement method, both formulations of NPs were successfully optimized. The characteristics of the NPs utilizing the optimized formula showed a polydispersity index (PI) value lower than 0.2, characteristic of monodisperse systems and an average size

below 200 nm along with a highly negative surface charge (measured as zeta potential, ZP) and maximum entrapment efficiency (EE) percentage. For both the Ca(OH)₂/PLGA and the clobetasol propionate/PLGA NPs, the characterization of the NPs was performed, and the spherical morphology was confirmed using TEM. Moreover, interaction studies were carried out including XRD, FTIR and DSC to examine the profile of the NPs. These studies confirmed that no covalent bonds were formed during the preparation process and that the drug appeared to be encapsulated inside the NPs. Examining the drug release profile for the Ca(OH)₂/PLGA NPs, the Ca(OH)₂ NPs exhibited a prolonged and steady release with higher concentrations than those obtained with the free Ca(OH)₂, that remained stable up to 48 hours. Moreover, clobetasol propionate/PLGA NPs, exhibited a prolonged and steady release with only around 21 % of the encapsulated drug released after 48 hours, in comparison the free drug that was completely released after just 6 hours. For the freeze drying of the Ca(OH)₂/PLGA NPs, the combination of 5% of (2-Hydroxypropyl)- β -cyclodextrin and 15% D-mannitol gave rise to the most stable outcome and the best appearance after lyophilization being able to recover the initial physicochemical characteristics of the NPs after their resuspension. Unfortunately, for the clobetasol propionate/PLGA NPs, we were not able to achieve a suitable combination. Using the confocal laser scanning microscopy, it was shown that both the Ca(OH)₂/PLGA and the clobetasol propionate/PLGA NPs had a better depth and area of penetration inside the dentinal tubules when compared to the free drug. Plus, the NPs displayed higher values mean fluorescence intensity (MFI) and integrated density compared to the free drug. Assessing the antibacterial efficiency of the Ca(OH)₂/PLGA NPs using the agar diffusion test, it was noted that the NPs showed clear maximal zones of growth inhibition around the filter papers comparable only to the positive group of antibiotics. Additionally, the MIC of the NPs was measured in regard to inhibiting bacterial growth for 3 bacterial species. It was noted that after 24 hours of incubation the NPs were able to inhibit bacterial growth at all tested concentrations. The anti-inflammatory capacity of the clobetasol propionate/PLGA NPs was also examined, in which ELISA assays were used to evaluate the inflammatory cytokines release of the macrophages in response to the NPs. The releases of TNF- α was reduced considerably to almost undetectable amounts with NPs compared to the LPS negative control, displaying results similar and even less than the TCP positive control after 48 hours. However, resulted in the release of IL-1 β in higher amounts which were similar to the TCP positive control and lesser than the LPS negative control

group. Additionally, the inflammatory cytokines release of IL-1 β and TNF- α from the LPS pretreated macrophages, was not reduced with the NPs at all tested concentration to limits below the amounts obtained by the LPS pretreated macrophages or the TCP positive control group after 48 hours.

Conclusions: In the present study, Ca(OH)₂ loaded PLGA NPs and clobetasol propionate loaded PLGA NPs were successfully optimized and characterized, and their therapeutic efficacy was tested with aims to increase the antibacterial and anti-inflammatory effect through controlled drug release and reach areas of complicated root canal anatomy due to the smaller mean nanoscopic size. However, further future studies are still required in order for the developed NPs to take the next step to be utilized in a clinical condition and to achieve its goal as an intracanal medicament.

Objetivo: El objetivo del presente estudio ha sido el desarrollo de dos formulaciones de nanopartículas para ser usadas en el campo de la endodoncia como medicación intra-conducto. La primera formulación se basa en la encapsulación de *hidróxido de calcio* ($Ca(OH)_2$) en nanopartículas (NPs) biodegradables de ácido poli(láctico-co-glicólico) (PLGA), la segunda formulación se basa en la encapsulación de *propionato de clobetasol* en nanopartículas (NPs) biodegradables de ácido poli(láctico-co-glicólico) (PLGA). También se ha realizado la optimización y caracterización de las NPs y el perfil de liberación del principio activo en comparación con el fármaco libre. Además se ha comparó la cantidad y el área de penetración de las NPs en el interior de los túbulos dentinarios. Por último se evaluó la capacidad terapéutica de ambas formulaciones mediante test antibacterianos y antiinflamatorios.

Metodología: Las NPs fueron preparadas por el método de desplazamiento de solvente. La optimización fue realizada mediante un diseño factorial central compuesto, mediante el cual se pudo obtener la formulación final. Se realizó un estudio de la morfología de las NP mediante microscopía electrónica de transmisión (MET). Además, las NPs se caracterizaron mediante cristalografía de Rayos X, espectroscopía infrarroja de Fourier y calorimetría diferencial de barrido. También se llevó a cabo el estudio de las condiciones óptimas para el proceso de liofilización de las NP. En ambas formulaciones se evaluó el perfil de liberación del fármaco desde el interior de las NP comparándolo con el del fármaco libre, hasta las 48 horas. El examen de penetración dentro de los túbulos dentinarios de las NP en comparación con el fármaco libre se realizó mediante microscopía confocal. Para evaluar la capacidad antibacteriana de las NP de hidróxido de calcio se realizaron los test mediante el método Kirby-Bauer (Test de difusión en agar) y la concentración mínima inhibitoria (CMI). La capacidad anti-inflamatoria de las NP de propionato de clobetasol se evaluó mediante la respuesta y reacción frente a células inflamatorias, en particular frente a macrófagos, utilizando el ensayo inmunoabsorbente ligado a enzimas (ELISA) para examinar la liberación de citocinas de IL -1 β y TNF- α .

Resultados: Las formulaciones de NPs con hidróxido de calcio y propionato de clobetasol se consiguieron preparar utilizando el método de desplazamiento de solvente. Las características de las formulaciones optimizadas presentaron una población homogénea con un valor de índice de

poli-dispersión (PI inferior a 0,2) y tamaño promedio adecuado, inferior a 200 nm. Además, su carga superficial medida en base al potencial zeta fue altamente negativa y se obtuvo una eficiencia de asociación elevada en ambos casos, superior para el clobetasol. Tanto para las NP de $(Ca(OH)_2)$ / PLGA como para las NP de propionato de clobetasol / PLGA, se confirmó la morfología esférica y la superficie lisa mediante MET. Se realizaron diferentes estudios de interacción fisicoquímica confirmando que ambos fármacos se encontraban en el interior de la matriz polimérica y que no se producían nuevos enlaces en la formación de los sistemas nanoestructurados. Se examinó el perfil de liberación para ambas formulaciones. En el caso de las NP de $(Ca(OH)_2)$ / PLGA, mostraron una liberación prolongada y constante del fármaco con concentraciones más altas que en el caso del fármaco libre, que permanecieron estables hasta 48 horas después. Las NP de propionato de clobetasol / PLGA exhibieron una liberación prolongada y constante con una liberación del 21 % del fármaco encapsulado después de 48 horas, en comparación con el fármaco libre que se liberó por completo después de solo 6 horas. Para el proceso de liofilización de las NP de $(Ca(OH)_2)$ / PLGA, se obtuvo un mejor resultado con la combinación de 5% de (2-hidroxipropil) β -ciclodextrina y 15% de D-manitol. Estas formulaciones pudieron ser re-suspendidas de forma instantánea consiguiendo los parámetros originales. Desafortunadamente, para los NP de propionato de clobetasol / PLGA, no se pudieron lograr una combinación adecuada de crioprotectores y condiciones de liofilización óptimas. Las pruebas de penetración mediante microscopía confocal, demostraron que tanto el $Ca(OH)_2$ / PLGA como el propionato de clobetasol / PLGA, tenían una mejor profundidad y área de penetración dentro de los túbulos dentinarios en comparación con el fármaco libre. Además, las NP mostraron valores más altos de intensidad de fluorescencia media y densidad integrada (*mean fluorescence intensity, MFI*) en comparación con el fármaco libre. Al evaluar la eficacia antibacteriana de las NP de $Ca(OH)_2$ / PLGA utilizando la prueba de difusión en agar, se observó que las NP mostraban zonas claras máximas de inhibición del crecimiento alrededor de los papeles de filtro comparables solo al grupo positivo de antibióticos. Además, se midió la concentración mínima inhibitoria (CMI) de las NP con respecto a la inhibición del crecimiento bacteriano para 3 especies bacterianas. Se observó que después de 24 horas de incubación, las NP inhibieron el crecimiento bacteriano en todas las concentraciones probadas. Se realizaron estudios para medir la capacidad anti-inflamatoria de las NPs de propionato de clobetasol

/PLGA, para lo cual se utilizaron test ELISA para evaluar la respuesta de los macrófagos en la liberación de citoquinas inflamatorias en presencia de las NP. Se observó que las liberaciones de TNF- α se redujeron considerablemente a cantidades casi indetectables con NPs en comparación con el control negativo (LPS), mostrando resultados similares e incluso menores que el control positivo (TCP) después de 48 horas. Sin embargo, se obtuvo la liberación de IL-1 β en cantidades mayores que eran similares al control positivo de TCP y menores que al grupo de control negativo de LPS. La liberación de citoquinas inflamatorias de IL-1 β y TNF- α de los macrófagos pre-tratados con LPS no se redujo con las NP en ninguna concertación probada a límites por debajo de las cantidades obtenidas por los macrófagos pre-tratados con LPS o el grupo de control positivo de TCP después de 48 horas.

Conclusiones: En el presente estudio, las NP de PLGA encapsulando ($Ca(OH)_2$) y las NP de PLGA encapsulando propionato de clobetasol han sido optimizadas y caracterizadas con éxito, y se ha probado su eficacia terapéutica con el objetivo de aumentar el efecto antibacteriano y anti-inflamatorio. La penetración de las mismas en áreas de anatomía complicada del conducto radicular (túbulos dentinarios) ha sido demostrada, debido al tamaño nanoscópico de las mismas. Sin embargo, aún se requieren más estudios futuros para que las NP formuladas puedan ser utilizados en una condición clínica.

PATENT

PATENT

PATENT

European patent for the $\text{Ca(OH)}_2/\text{PLGA}$ nanoparticles:

DURÁN-SINDREU TEROL Fernando Salvado, GONZÁLEZ SÁNCHEZ José Antonio, PÉREZ ANTOÑANZAS Román, ELMSMARI Firas, SÁNCHEZ LÓPEZ Elena GARCÍA LÓPEZ María Luisa B; inventors; Universitat Internacional de Catalunya, assignee. COMPOSITION COMPRISING NANOPARTICLES, METHOD FOR THE PREPARATION OF A COMPOSITION COMPRISING NANOPARTICLES AND USES OF THE COMPOSITION FOR DENTAL TREATMENT (Under submission) (Patent number: #EP20382504).

GENERAL INDEX

GENERAL INDEX

GENERAL INDEX

1. ABBREVIATION LIST	31
2. JUSTIFICATION	35
3. INTRODUCTION	41
3.1 ENDODONTIC TREATMENT OBJECTIVE: MICROBIAL INFECTION	41
3.2 CALCIUM HYDROXIDE AS AN ANTIBACTERIAL AGENT	45
3.3 AVULSED TEETH WITH EXTENDED EXTRA ORAL TIME	48
3.4 TREATMENT OPTIONS FOR AVULSED TEETH WITH EXTENDED EXTRA ORAL TIME	53
3.5 NANOTECHNOLOGY AND ITS DENTAL APPLICATION	56
3.6 PLGA BIODEGRADABLE NANOPARTICLES: A NOVEL APPROACH IN DRUG DELIVERY	59
4. OBJECTIVES	63
4.1 PRIMARY OBJECTIVES.....	63
4.1.1 <i>Antibacterial calcium hydroxide (Ca(OH)₂/PLGA) NPs to be used as an intracanal antibacterial medication.....</i>	63
4.1.2 <i>Anti-inflammatory clobetasol propionate (clobetasol/PLGA) NPs to be used as an intracanal medication in cases of avulsed teeth with extended extra oral time.....</i>	63
4.2 SECONDARY OBJECTIVES.....	63
5. HYPOTHESIS	67
5.1 NULL HYPOTHESIS (<i>H</i> ₀)	67
5.2 ALTERNATIVE HYPOTHESIS (<i>H</i> ₁).....	68
6. MATERIALS AND METHODS	73
6.1 MATERIALS.....	74
6.2 PREPARATION OF THE NANOPARTICLES	74
6.3 DEVELOPMENT OF CALCIUM HYDROXIDE QUANTIFICATION METHOD FOR CALCIUM HYDROXIDE/PLGA NANOPARTICLES	75
6.4 ENTRAPMENT EFFICIENCY OF CALCIUM HYDROXIDE/PLGA NANOPARTICLES USING INDUCTIVELY COUPLED PLASMA OPTICAL EMISSION SPECTROSCOPY	76
6.5 DEVELOPMENT OF CLOBETASOL PROPIONATE QUANTIFICATION METHOD FOR CLOBETASOL PROPIONATE/PLGA NANOPARTICLES	78
6.5.1 <i>Entrapment efficiency of Clobetasol Propionate/PLGA Nanoparticles using High Performance Liquid Chromatography.....</i>	79
6.6 PREFORMULATION STUDIES	80
6.7 DESIGN OF EXPERIMENTS.....	81
6.8 NANOPARTICLES MORPHOLOGY STUDIES	81
6.9 NANOPARTICLES CHARACTERIZATION AND INTERACTION STUDIES	81
6.10 STABILITY STUDIES	82
6.11 <i>IN VITRO</i> DRUG RELEASE.....	82
6.12 FREEZE DRY OF THE NANOPARTICLES	83
6.13 STERILIZATION ASSAYS	83
6.14 CONFOCAL LASER SCANNING MICROSCOPY TEST	84

6.15	ANTIBACTERIAL CAPACITY OF THE CALCIUM HYDROXIDE/PLGA NANOPARTICLES	86
6.15.1	Agar diffusion test	87
6.15.2	Minimal inhibitory concentration.....	88
6.16	IN VITRO INFLAMMATORY RESPONSE ASSESSMENT OF THE CLOBETASOL PROPIONATE/PLGA NANOPARTICLES	90
6.16.1	Cytotoxicity assays: cell morphology and metabolic activity using alamarBlue®	90
6.16.2	Enzyme-linked immunosorbent assays	90
7.	RESULTS	95
7.1	RESULTS OF THE CALCIUM HYDROXIDE/PLGA NANOPARTICLES	95
7.1.1	Preformulation studies.....	95
7.1.2	Entrapment efficiency using ICP-OES.....	96
7.1.3	Design of experiments (DoE) approach.....	97
7.1.3.1	Independent variables analysis.....	99
7.1.3.1.1	Calcium hydroxide concentration.....	99
7.1.3.1.2	PLGA concentration.....	101
7.1.3.1.3	Lutrol concentration	102
7.1.3.1.4	pH value	103
7.1.4	Reproducibility of the optimized formulation	104
7.1.5	Nanoparticles morphology studies	105
7.1.6	Nanoparticles characterization and interaction studies	106
7.1.7	Stability studies.....	108
7.1.8	In vitro drug release	109
7.1.9	Freeze dry of the nanoparticles	111
7.1.10	Sterilization assays	114
7.1.11	Confocal laser scanning microscopy study	114
7.1.12	Therapeutic efficacy: Antibacterial capacity.....	118
7.1.12.1	Agar diffusion test.....	118
7.1.12.2	Minimal inhibitory concentration.....	119
7.2	RESULTS OF THE CLOBETASOL PROPIONATE/PLGA NANOPARTICLES	122
7.2.1	Preformulation studies.....	122
7.2.2	Entrapment efficiency measurement	123
7.2.2.1	Clobetasol propionate quantification method.....	123
7.2.2.2	Entrapment efficiency measurement using clobetasol quantification method.....	124
7.2.3	Design of experiments (DoE) approach.....	125
7.2.3.1	Independent variables analysis.....	127
7.2.3.1.1	Clobetasol propionate concentration	127
7.2.3.1.2	PLGA concentration.....	129
7.2.3.1.3	Tween®80 concentration	130
7.2.3.1.4	pH value	131
7.2.4	Reproducibility of the optimized formulation	132
7.2.5	Nanoparticles morphology studies	133
7.2.6	Nanoparticles characterization and interaction studies	134
7.2.7	Stability studies.....	136
7.2.8	In vitro drug release	137
7.2.9	Freeze dry of the nanoparticles	138
7.2.10	Sterilization assays	139
7.2.11	Confocal laser scanning microscopy test	140
7.2.12	In vitro inflammatory response assessment of the Clobetasol Propionate/PLGA nanoparticles	142
7.2.12.1	Cytotoxicity assays: cell morphology and metabolic activity using alamarBlue®	142
7.2.12.2	Enzyme-linked immunosorbent assays	144
8.	DISCUSSION.....	151

8.1	DISCUSSION OF THE CALCIUM HYDROXIDE/PLGA NANOPARTICLES	151
8.2	DISCUSSION OF THE CLOBETASOL PROPIONATE/PLGA NANOPARTICLES	157
9.	CONCLUSIONS	165
9.1	FUTURE PERSPECTIVES	167
10.	REFERENCES	171
11.	LIST OF FIGURES AND TABLES	191
11.1	LIST OF FIGURES	191
11.2	LIST OF TABLES.....	195
12.	ANNEXES.....	199
12.1	ANNEXES I: APPROVAL LETTER OF THE PHD PROJECT.....	199
12.2	ANNEXES II: APPROVAL LETTER OF ETHIC COMMITTEE	200
12.3	ANNEXES III: PATENT APPLICATION FOR CALCIUM HYDROXIDE/PLGA NANOPARTICLES	201
12.4	ANNEXES IV: STUDY OF THE PATENTABILITY OF THE CLOBETASOL/PLGA NANOPARTICLES	202

ABBREVIATION LIST

ABBREVIATION LIST

1 . ABBREVIATION LIST

AAE	American Association of Endodontics
BHI	Agar heart infusion agar
Ca	Calcium
Ca(OH) ₂	Calcium hydroxide
CFU	Colony forming units
C _{max}	Maximum drug release
DMSO	Dimethyl sulfoxide anhydrous
DoE	Design of experiments
DSC	Differential scanning calorimetry
EE	Entrapment efficiency
Ef	Enterococcus faecalis
ELISA	Enzyme-linked immunosorbent assays
Fn	Fusobacterium nucleatum
FTIR	Fourier transform infrared
HNO ₃	Nitric acid
HPLC	High performance liquid chromatography
HPβCD	(2-Hydroxypropyl)-β-cyclodextrin
IADT	International Association of Dental Traumatology
ICP-OES	Coupled plasma optical emission spectroscopy
LPS	Lipopolysaccharide

Abbreviation list

LTA	Lipoteichoic acid
MFI	Mean fluorescence intensity
MIC	Minimal inhibitory concentration
NaOCl	Sodium hypochlorite
NPs	Nanoparticles
PCS	Photon correlation spectroscopy
PEG	Polyethylene glycol 3350
PG	Peptidoglycan
Pg	Porphyromonas gingivalis
PI	Polydispersity index
PLGA	Poly(lactic-co-glycolic acid)
TCP	Tissue culture plastic
TEM	Transmission electron microscopy
XRD	X-ray diffraction
Z _{av}	Average size
ZP	Zeta potential

JUSTIFICATION

JUSTIFICATION

2. JUSTIFICATION

Our ultimate aim and goal as endodontic clinicians is to save and preserve all teeth from extraction (1,2). In our daily clinical practice, we deal with an array of emergency situations that require our intervention, this could be either in cases of routine endodontic infections or even in cases of dental trauma. We achieve our goal by eliminating or preventing microbial infection and apical periodontitis (3). However, as hard as we try, we still have many limitations in dealing with these situations (3).

Calcium hydroxide ($\text{Ca}(\text{OH})_2$) has been used for decades as the go-to antibacterial intracanal medication for emanating and eradicating bacteria and their by-products inside the root canal system (4). Nevertheless, the limitations and shortcomings of calcium hydroxide, especially in clinical situations is well documented (5). This could not be highlighted more clearly then when examining the success rates obtained in endodontics throughout the decades (6). With all the innovations and advancements of modern endodontics, the success rate of our endodontic treatment has not increased in the last 5 decades (6). Emphasizing the need to try and improve on our current antibacterial arsenal.

Moreover, another situation that is deemed as hopeless, are avulsed teeth with extended dry extra oral time (7,8). In those cases, reimplantation presents an extremely poor prognosis and ankylosis due to replacement resorption is a forgone conclusion (7,8). However, more recently several attempts have been made to try and develop a solution to this problem. More specifically the use of potent corticosteroids like Clobetasol Propionate in animal studies, presented very favourable results in preventing and reversing the resorptive process of the avulsed teeth once they are reimplanted (9,10).

Justification

Conventional drug delivery in general which include the traditional administration of Ca(OH)_2 and clobetasol propionate has major drawbacks. Those include undesirable side effects, deficiency of selectivity, restricted effectiveness and diminished drug release (11). In order to overcome these problems, innovative advances in drug delivery systems have been recently undertaken. In this sense, the most recent nanotechnological approaches focuses on the development of techniques to target the specific cells responsible of the disease by means of individually designed carriers loading the drug. Advancements like nanotechnology had shown great potential in solving beforehand mentioned problems. Nanoparticles (NPs) are nanoscopic elements between 1-1000 nm with one or more external dimensions. Compared to their bulk or powder counterparts, nanomaterials offer unique physiochemical properties, some of which are ultra-small size, large surface area to mass ratio and increased chemical reactivity (12). Moreover, different vehicles have been used to administer Ca(OH)_2 , ranging from water-soluble, viscous and oil based vehicles (5). However, even some of these vehicles do prolong the action of Ca(OH)_2 , unfortunately all of them propose a certain degree of negative effect that carry the risk of altering the physical and chemical properties of Ca(OH)_2 , thus ultimately affecting their clinical performance (5). From this sense the need for a different vehicle like NPs, that maintains the properties of Ca(OH)_2 and induce prolonged action is urgently needed in this scope.

It can be assumed that optimizing two NPs (antibacterial and anti-inflammatory) by applying and utilizing the antibacterial properties of a material like Ca(OH)_2 and the anti-inflammatory properties of clobetasol propionate, with the the prolonged drug delivering ability, plus the targeted release and specificity of the polymeric NPs, can overcome the well documented shortcomings and limitations of Ca(OH)_2 and perhaps provide an appropriate treatment for avulsed teeth with extended extra oral dry time. Additionally, the ultra-small size of these NPs could permit more penetration inside the dentinal tubules and reaching areas of complicated anatomy like isthmuses, accessory, and lateral canals.

Accordingly, the aim of this research is the development and optimization of two novel different biodegradable polymeric NPs to be used in the field of endodontics, using PLGA polymers

loaded with two different drugs. In which, one will be an antibacterial calcium hydroxide (Ca(OH)₂/PLGA) NPs to be used as an intracanal antibacterial medication, and the other an anti-inflammatory NPs using clobetasol propionate and PLGA polymers to be used as an intracanal medication in cases of avulsed teeth with extended extra oral time.

INTERPRETATION

INTRODUCTION

3. INTRODUCTION

3.1 Endodontic treatment objective: microbial infection

According to the American Association of Endodontics (AAE) there are over 15.1 million root canal therapy procedures performed annually in the united states alone (13). Even with this vast number of treatments performed, we are fortunate as clinicians to encounter a relatively predictable favourable outcome of the procedure, with studies reporting success rates reaching as high as 95%. (14–17). However, when further examining the results of these studies we can notice that the percentages of success rate relatively decreases in cases diagnosed with necrotic non vital pulp tissue (18). This is mainly attributed to the presence of pathogenic microorganisms that cause the necrosis of the pulpal tissue (19). Normally, the root canal system is an aseptic sterile environment clear of any microorganisms and the oral flora (3) as its protected by the enamel, dentine and cementum surrounding it. But when there is a breach in the integrity of the surrounding tissues by the form of dental caries, restorative procedures, trauma-stimulated fractures and cracks, root planning and scaling procedures, attrition or abrasion, a pathway for the microorganisms and oral flora is formed to invade the sterile pulp canal space (3). Most endodontic infections are formed in this manner and depending on the progression of the disease different presentation could arise. as early progression of the microorganisms can present that cases with vital pulp tissues and clinical signs and symptoms of pain and discomfort due to the inflammatory process in the pulp tissue in response to the microorganisms' assault (20). Were in cases of late progression, the pulp tissue is necrotic, and the root canal space is infected and filled with microorganisms with no clinical signs and symptoms (20) (Figure 1).

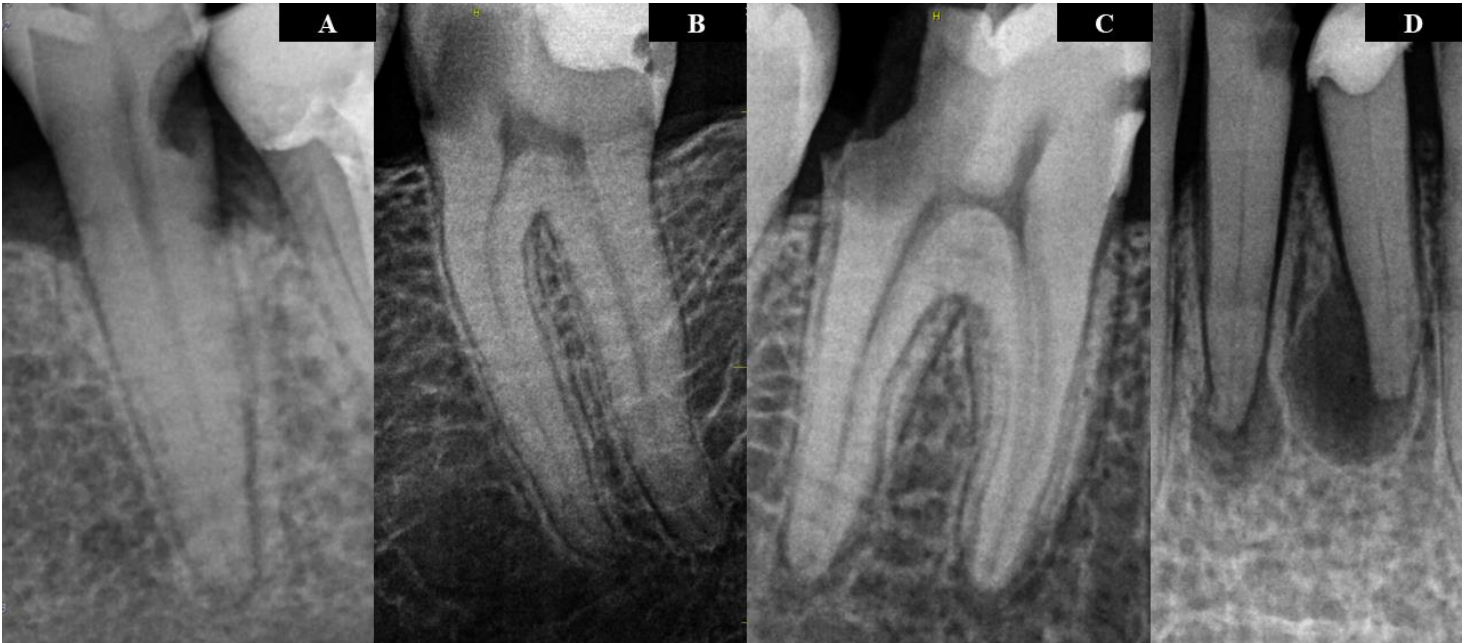


Figure 1 Dynamics of the pulpal response to microbial assault (A) Response from caries exposure (B) Pulp inflammation (C) Pulpal necrosis (D) Apical periodontitis formation.

Accordingly, the essence of endodontic treatment is to eliminate the infection by preventing the invading microorganisms from infecting the root canal space (21). However, the complete elimination of the intracanal microorganisms and their by-products has been a constant challenge (22). This has been further complicated by the complex anatomy of the root canal system and the location in which the bacteria and microorganisms are present at. In general, bacteria located as planktonic cells roaming freely in the main root canal are eliminated rather easily throughout chemo-mechanical preparation of instrumentation and irrigation (23–25). However, those bacteria and microorganisms that are located inside isthmuses, accessory, and lateral canals, and dentinal tubules much more complicated to remove or eradicate as accessibility to those locations is not simple (23–25).

Arguably the most common anatomical complexity that harbour and contain bacteria is the dentinal tubules, which travel through the width of the entire dentine, establishing this pathway that has a conical tapering shape (26,27) (Figure 2). As the smallest diameter of the tubules of around $0.9\ \mu\text{m}$ is located near the enamel and the largest diameter of the tubules of around $2.5\ \mu\text{m}$ is located near the pulp (26,27). These numbers are significant as even the smallest diameter of the tubules at around $0.9\ \mu\text{m}$ is enough to shelter and conceal oral bacteria that by average

have a diameter the ranges from 0.2 to 0.7 μm (26,27). This is even more important in cases of non-vital necrotic pulp, as it has been documented that bacteria invade much rapidly in those cases as compared to cases that contain vital pulp tissue (28). The main reason for this is the presence of the dentinal fluid inside the dentinal tubules in case of vital pulp tissue. As the outwards movement of the dentinal fluid inside the tubules will decrease their permeability and their rate of invasion (28).

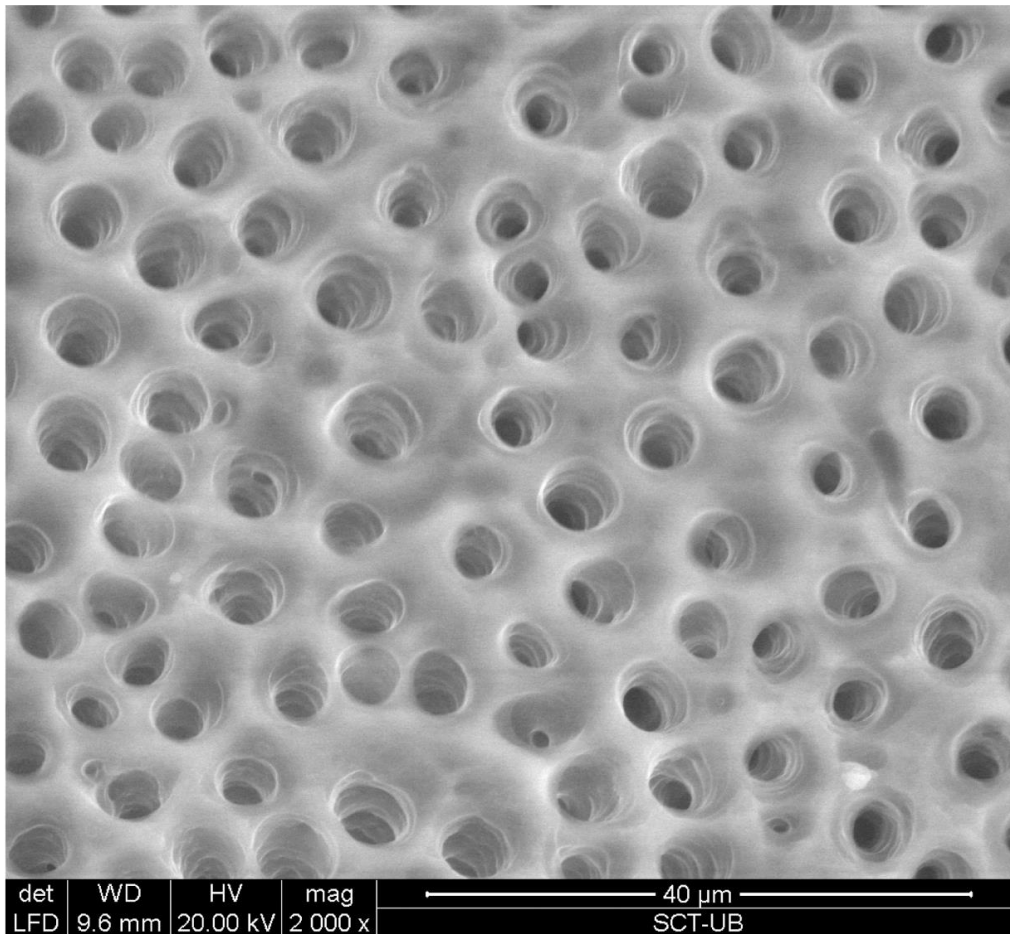


Figure 2 Scanning electron microscope image of dentinal tubules cross sectional view with $\times 2000$ magnification. (Courtesy of Dr Juan Gonzalo Olivieri).

To this very day the main reason for endodontic failure is the persistent of microbial infection inside the root canal (29,30). Even in cases of clinical mishaps and procedural errors like

Introduction

separated files, ledges, perforations, apical transportation, overextended fillings, and son on, even in those cases the main reason for failure is the persistent microbial infection insides the canal. As it has been documented, in most cases those errors and mishaps do not compromise the outcome of the endodontic treatment unless they are combined with a present microbial infection (31). In other terms, those errors and mishaps are not the reason of failure, they simply complicate or impede the process of bacterial and microbial elimination inside the canal (31). Hence, the possibility of failure of the endodontic treatment after a procedural error or mishap increase significantly in cases of infected teeth with necrotic non-vital pulp tissue.

Furthermore, these microorganisms can possess the ability to tolerate, overcome and survive against disinfectant solutions and our host defense (32). they can cause what is known as indirect tissue damages that is caused by the host defense due to many components they possess in the bacterial wall like lipopolysaccharide (LPS), peptidoglycan (PG) and lipoteichoic acid (LTA) (33,34). Additionally, bacteria have the ability to grow, aggregate and attach to each other and to a dense substratum, whilst implanted in an extracellular matrix forming a community that is known as bacterial biofilm (35). Biofilms are notoriously more resistant to all forms of disinfection as they possess the ability to survive under scarce environments and conditions, making the process of endodontic disinfection even more complicated (36).

In our efforts to achieve optimal root canal treatment, we try to remove all the bacterial microbes from inside the root canal system (2,37). This is attempted with a combination of mechanical debridement through root canal instrumentation and a chemical cleaning though irrigation solutions and intracanal medications (2). However, despite our relentless efforts thus far, we have not succeeded in the complete elimination of the bacterial microbes from the root canal (22). That is why the use of intracanal medications are resorted as an interappointment medicament between visits, in order to achieve greater decrease in the bacterial load (38). Many studies have well documented the inefficacy of our intracanal antibacterial medications in the elimination of the bacteria especially the ones that resides inside anatomical complexities like the dentinal tubules (39–42). And despite all the innovations and advances in endodontics in recent history, when examining the success rate through the decades, we can observe that similar

success rates were obtained from 1920's till our present day and no trend of a progressively increasing favourable outcome was documented (6). This could highlight that despite the many developments and improvement in modern endodontics, our current intracanal medications still has many limitations and cannot achieve the desirable effect.

3.2 Calcium hydroxide as an antibacterial agent

Calcium hydroxide (Ca(OH)_2) is the most commonly used interappointment intracanal antibacterial medication in eliminating bacterial species and their by-products in endodontics (43). The first reports for Ca(OH)_2 use in dentistry dates back to as far as 1838 (44), when Nygren tried to use the material to treat "fistula dentalis". However, it was Hermann that first introduced Ca(OH)_2 officially to be used in dentistry in 1920 (45). Throughout the 30s the material have been promoted heavily to be used as a pulp healing material with many reports between 1930 and 1941 (46–50). Subsequently numerous studies have documented their antibacterial qualities in eradicating microbes and their by-products from the human root canal (51–54). Since that time and especially in the period after the second world war the clinical use of Ca(OH)_2 has increased significantly and has been considered as the gold standard material for promoting healing of the pulp tissue, inducing hard tissue formation and as a intracanal antibacterial medicament (55).

Ca(OH)_2 originates from a natural rock known as limestone, which is mainly made of calcium carbonate (CaCO_3). This usually materializes whenever the existing CaCO_3 in oceans and mountains crystallizes (56). Consequently, when limestone is ignited and subjected to temperatures between 900 and 1200 °C, the subsequent reaction is formed:



Moreover, this calcium oxide (CaO) that is formed, is also known as quicklime, which possesses powerful corrosive capacity. Whenever this CaO is contact with water it will result in the subsequent reaction:



Ca(OH)₂ is essentially a white inodorous powder with a molecular weight of 74.093 g/mol (57,58). Moreover, it has low solubility in water of about 1.2 g L⁻¹ at 25 °C which further declines in case of any temperature raise and completely insoluble in alcohol (57,58). Due to its low solubility, it could be dubbed as a good clinical trait, as it takes extended periods to become soluble in tissue fluids whenever it comes in immediate contact with vital tissues (57,58). Ca(OH)₂ has a high pH value of around 12.5 to 12.8 which is one of its defining characteristics and it is categorized as a strong base (57,58).

The antibacterial capacity of Ca(OH)₂ depends on its alkalinity and the subsequent release of highly oxidant free radicals hydroxyl ions which acts on the bacterial cell wall (4,5,59). They act on the bacterial cells causing damage to the cytoplasmic membrane through protein denaturation plus causing damage to the DNA (4). Furthermore, a high basic pH has to be retained in order for the hydroxyl ions to sustain their antibacterial capacity (5). As the pH gradient of the cytoplasmic membrane is altered by the high concentration of hydroxyl ions, which causes protein denaturation by acting on the proteins of the membrane (5). Additionally, the integrity of the cytoplasmic membrane is altered by the high pH of Ca(OH)₂ through chemical injury to the organic components and transport of nutrients (59). Additionally, the hydroxyl ions will react with the DNA of the bacteria causing splitting of the genes strands, which then become lost (60). This will result in the inhibition of DNA replication and can cause destructive mutations, also triggering disruptions in the cellular activity (60). However, examining the best available evidence, it is suggested the three mechanisms of damage to the bacterial cytoplasmic membrane, protein denaturation and damage to the DNA may all happen simultaneously, and it

is exceedingly difficult to establish a chronological order in which the events take place (60–62). In short, it is more as a combination of all these mechanisms that Ca(OH)_2 apply their antibacterial properties. Additionally, this uncoupling of Ca(OH)_2 into calcium and hydroxyl ions is highly dependent on the vehicle used for application (63), as it can affect the pH value and the degree of penetration inside the tubules (64). Ideally the optimal vehicle should allow for slow and steady release of the calcium and hydroxyl ions with gradual diffusion into the tissues combined by low solubility in tissue fluids, plus having no undesirable effects on the initiation of hard tissue formation if it is intended (65). Moreover, different vehicles have been used to administer Ca(OH)_2 , ranging from water-soluble, viscous and oil based vehicles (5). However, even though some of these vehicles do prolong the action of Ca(OH)_2 , unfortunately all of them propose a certain degree of negative effect that carry the risk of altering the physical and chemical properties of Ca(OH)_2 , thus ultimately affecting their clinical performance (5). From this scope the need for a different vehicle, that maintains the properties of Ca(OH)_2 and induce prolonged action is needed.

Throughout the years, several studies have been conducted to evaluate the antibacterial efficiency of Ca(OH)_2 in eliminating bacteria from the root canal system with mixed results. As many studies reported the high efficiency of Ca(OH)_2 as an antibacterial agent (38,66–71), on the other hand numerous studies reported the opposite and documented the inefficacy of Ca(OH)_2 in eradicating bacterial and their by-products (41,59,80,72–79), especially when tested in conditions similar to the clinical environment in which they are applied. Furthermore, it has been routinely demonstrated with several studies that Ca(OH)_2 is ineffective in eliminating bacteria the subsides inside the dentinal tubules (39–42). This could be due to their inability to establish direct contact with the bacteria inside the tubules, which is a vital aspect in applying their antibacterial properties (4), as it has been shown Ca(OH)_2 can only penetrate up to 28 and 126 μm inside the dentinal tubules (81), which is not nearly enough since we know that bacteria can penetrate to around 400 μm in some circumstances (82,83).

Another possible reason that could also explain the well documented shortcomings of the conventional $\text{Ca}(\text{OH})_2$ in bacterial elimination in endodontics is the reduction in their alkalinity clinically inside the root canal system. It has been reported that the dentin and hydroxyapatite have a buffering effect against substances with high pH values like $\text{Ca}(\text{OH})_2$, in which their alkalinity is reduced, resulting in decreased antibacterial potential and subsequently diminished diffusion of the hydroxyl ions (72,84,85). As it has been reported, in order for the $\text{Ca}(\text{OH})_2$ to be effective as an antibacterial intracanal medication, high concentrations of hydroxyl ions needs to be released with direct contact with the bacteria for a considerable amount of time (4). Unfortunately, this is not attained clinically, in a systematic review by Sathorn et al (86), the antibacterial efficiency of $\text{Ca}(\text{OH})_2$ was assessed in clinical trials, in which they concluded that $\text{Ca}(\text{OH})_2$ had limited effectiveness in eliminating bacteria from human root canal when assessed by culture techniques. This is due to the buffering effect that is exerted by the dentine and hydroxyapatite clinically, which will reduce their alkalinity and subsequently their antibacterial capacity inside the root canal system, presumably because sustained levels of pH cannot be achieved (72,84,85).

3.3 Avulsed teeth with extended extra oral time

As a dental clinic and particularly as our professional practices as endodontic clinicians, dealing with and managing dental trauma is of the utmost importance (87). It is considered as one of the most frequent reasons for emergency appointments in our clinical practice (87). It is our responsibility as dentists and endodontists to try our best to ensure the survival of traumatized teeth with selecting the appropriate treatment measurement (88). However, this will depend on the degree and more importantly the type of the dental trauma. One of the most sever types of dental trauma that has a very questionable prognosis is tooth avulsion. In the permanent dentition avulsion injuries present with a prevalence of around 0.5 to 3% of all dental injuries (89,90). This occurs when a tooth has been completely removed from the socket due to severe trauma (Figure 3). This act of separation from the socket will lead to tearing of the periodontal ligaments, leaving feasible periodontal ligament cells on most the surface of the avulsed root (8).

Additionally, localized areas of cemental damage will arise due to the crushing action of the tooth against the socket (8). In normal dentition, there is a thin layer of connective tissue that is called the periodontal membrane or periodontal ligaments, they separate the root surface from the alveolar bone, forming an attachment and maintains the integrity of the root (91). Additionally, it contains a collection of epithelial cells known as the epithelial rest cells of Malassez (92). When this zone gets damaged and becomes absent, a union between the root surface and bone will occur which is known as ankylosis (93). Moreover, examining the dental cementum we can observe that collagen fibres form an important part for the attachment of periodontal ligaments (94,95). Further assessing the outer layer of the root that contains the cementum, intermediate cementum, and the granular layer of Tomes, it was proposed that the intermediated cementum is key to the process of root and periodontal regeneration and affecting its likelihood once it gets damaged like in the case of tooth avulsion injury (94,95).

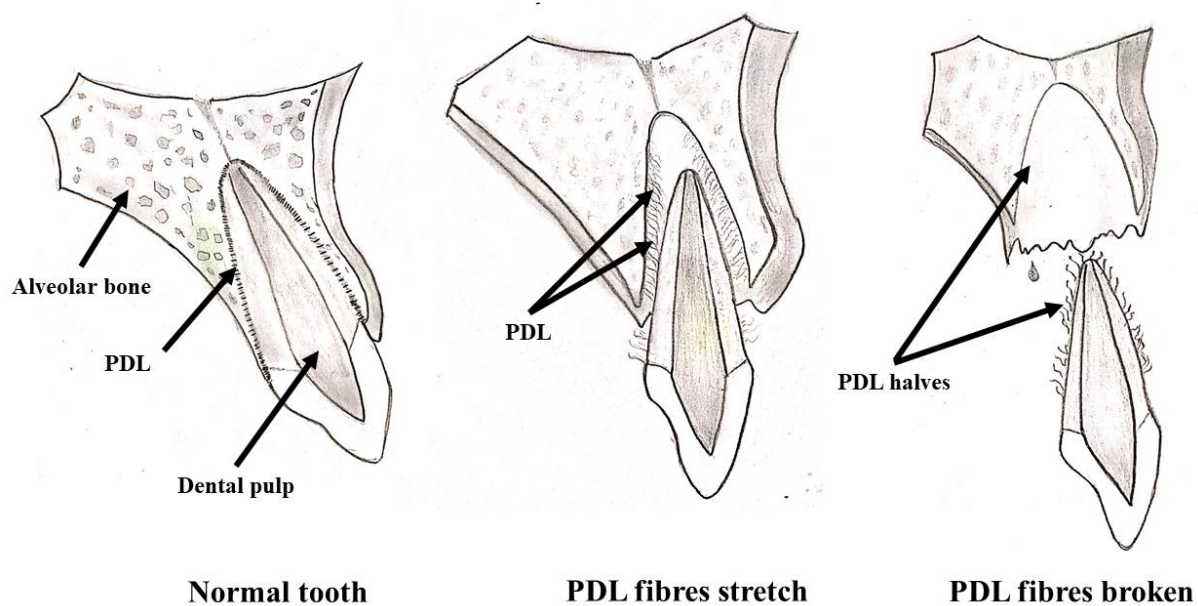


Figure 3 Dynamics of tooth avulsion injury.

Avulsion injuries are considered one of the most serious and unpredictable dental traumas, due to the fact that the prognosis is heavily dependent on the action taken place at the site of the incident and the urgency in performing them (8,88,90,96–99). In most situations reimplantation of the avulsed tooth is the treatment of choice but this is not applied in all cases (8). It is important to understand what exactly happens with the avulsed tooth and the supporting tissue. When the tooth is avulsed the pulp becomes necrotic and as described before injury will occur to supporting tissues of periodontal ligaments and localized cemental damage (8). Nevertheless, the two most important factors affecting the prognosis of avulsed teeth is the extra oral time and the degree of dryness of the root surface (8,88,90,96–99). In case the supporting tissue of periodontal ligaments are left hydrous on the root surface, the prognosis of the avulsed tooth is elevated significantly (8,96–99). As the hydrous periodontal ligament will preserve their capability which allows them to reattach properly after tooth reimplantation without causing considerable damage due to the slight inflammation produced (8). This can be explained as the crushing injury that is caused will be limited to a localized area, the subsequent inflammation caused by the damage will be also limited, indicating that healing and formation of new replacement cementum is expected to happen once the inflammations has receded (8).

However, this is completely different in the case of avulsed teeth with extended dry extra oral time as they present will the a very poor prognosis with ankylosis regarded almost as a foregone conclusion (100,101). This is because when the extreme dryness of the periodontal ligaments occurs in those cases, they will induce a severe inflammatory reaction diffused all over the root area once they are reimplanted (93,97,102). Additionally, here the area that is required to repair after the inflammation is large hence it can only be repaired with new tissue formation. Unfortunately, cementoblasts have a slow onset and they are not able to cover the whole surface of the damaged root area in time, which will lead to uncovered areas that bone tissue will be attaching itself directly in those areas (93,97,102).

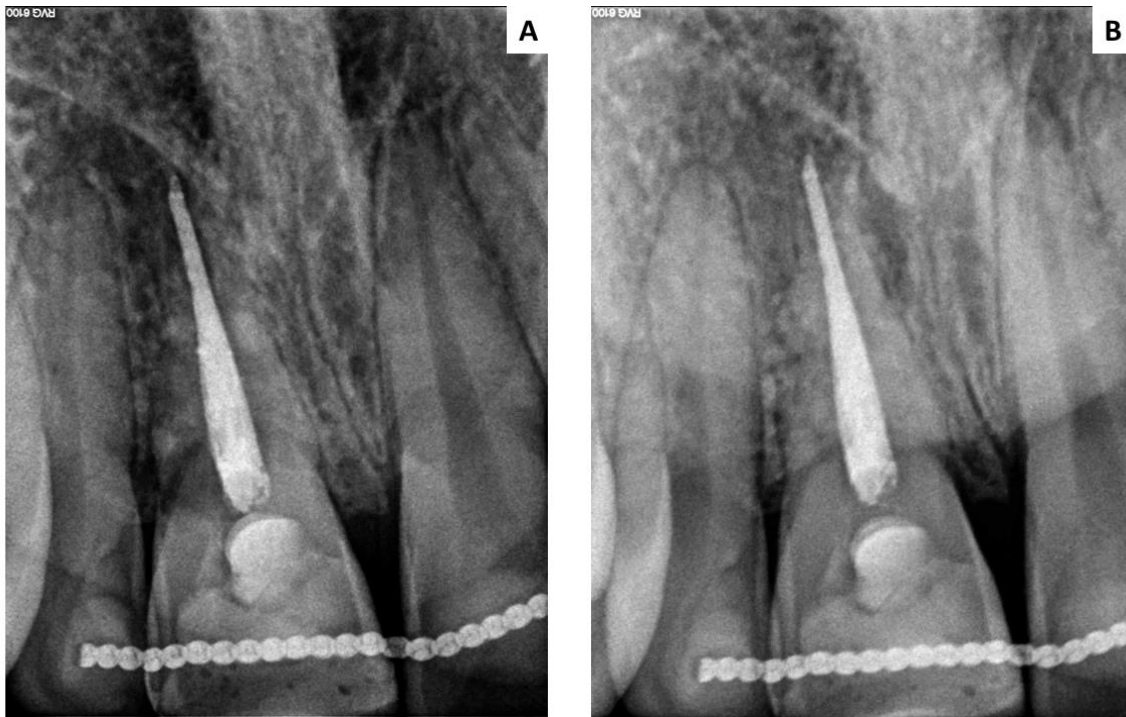


Figure 4 Preapical radiographs displaying a case of replacement resorption after an avulsed tooth with extended dry extra oral time was reimplanted. (A) Tooth immediately after reimplantation. (B) Tooth at follow up appointment displaying signs of replacement resorption around the root. (Courtesy of Dr José Antonio González Sánchez).

After a time of physiological recontouring the whole root will be replaced by bone leading to what is known as replacement resorption of the root (93,97,102) (Figure 4). Overall, it is important to point out, that in its essence replacement resorption is an inflammatory process in itself (93,97,102). Moreover, after avulsion injury the tooth always become necrotic, which will inevitably will lead to the total infection of the root canal space if appropriate endodontic treatment measures are not performed (8).

If this happens, the amalgamation of the bacteria inside the root canal space and the injury on the external cemental layers due to impact from the trauma, will result in an elevated state of external inflammatory resorption that can lead to very serious consequences like the loss of the tooth very rapidly (103) (Figure 5). Due to the inflammatory component, some authors (9,10) have chosen to utilize therapies based on the use of intra-radicular corticoids.

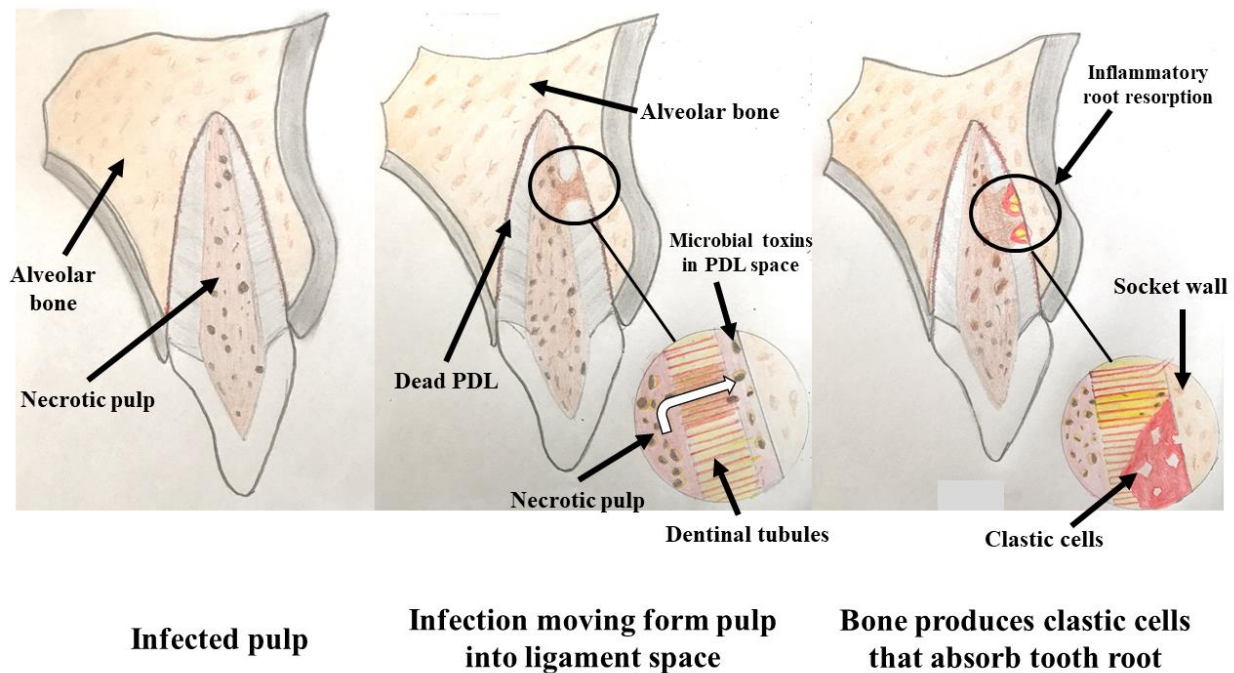


Figure 5 Progression of external inflammatory root resorption for an avulsed tooth after reimplantation.

3.4 Treatment options for avulsed teeth with extended extra oral time

Avulsed teeth with more than 60 minutes of extra oral dry time have always been considered to present a poor prognosis and replacement resorption and ankylosis is regarded a foregone conclusion in those cases (100). Numerous attempts and efforts to overcome this problem and enhance the prognosis of teeth with more than 60 minutes dry extra oral time have been proposed, but none of them thus far have been proven clinically to prevent the inevitable replacement resorption and ankylosis of the tooth (100). This is more common in cases where the damaged area is larger than 20% of the root surface or extended extra oral dry time that will cause an additional inflammatory stimulus and will lead to ankylosis or replacement resorption (8,93). Thus, if this additional inflammatory stimulus could be stopped this can help in preventing the unfavourable outcome of resorption or ankylosis.

According to the most recent guidelines published in 2020 by the International Association of Dental Traumatology (IADT) for the management of avulsion in permanent teeth (7), reimplantation of teeth with extended dry extra oral time more than 60 minutes has a very poor long term prognosis. And the inevitable outcome in those case is ankylosis due to replacement resorption (104). Nevertheless, they recommend reimplanting the avulsed tooth even with extended dry extra oral time, but only temporarily serve for the purpose of aesthetics and functionality, as it can help in maintaining the height of the alveolar bone especially in growing children (7). The rationale behind this, is that it can keep the options open later on for other treatment strategies like decoronation or autotransplantation. However the chances of actually saving the tooth are non-existent (7). Previous proposals, like applying 2 % of sodium fluoride on the root surface before reimplantation, in the hope of slowing the resorptive process are no longer recommended in the most recent updated guidelines, due to their clear ineffectiveness in achieving their goals (7).

However, researchers and clinicians still continue searching for a more appropriate treatment or cure, in the hopes of managing to save the avulsed teeth in those conditions. Several animal studies investigated the use of different intracanal medicaments like corticosteroids in the treatment of replacement resorption of avulsed teeth with delayed reimplantation (9,10), it has also been suggest by the IADT as a future expectation (7). Chen et al. (9) evaluated the individual influence of Ledermix[®] and the drugs contained in it individually on external root resorption after extended extra-oral dry time. Ledermix[®] contains 1% Triamcinolone which is a glucocorticoid and 3% Demeclocycline which is a tetracycline antibiotic. Furthermore, they found that groups treated with Ledermix[®], Triamcinolone and Demeclocycline individually had statistically significantly more favourable healing and more remaining root structure than the control groups, with the Ledermix[®] group obtaining the highest results, which could indicate that both Triamcinolone and Demeclocycline are synergic and obtain better results when used together. Kirakosova et al. (10) investigated the effect of potent intracanal corticosteroids (0.05% clobetasol and 0.05% fluocinonide) on periodontal healing of replanted avulsed teeth and evaluated the systemic absorption of these corticosteroids. They concluded that teeth treated with 0.05% clobetasol and 0.05% fluocinonide exhibited significantly more favourable healing than the control group. They also observed **no change** in the systemic corticosteroid blood concentration after intracanal use of high potency corticosteroids. It is stated that the trauma sustained by the root during the extra oral dry time will serve as a potent inflammatory stimulus following replantation and causes a more sever inflammation than the initial injury itself (9). This will lead to a more destructive inflammatory response including root resorption. The results of the previous studies (9,10) suggest that the use of corticosteroids, as anti-inflammatory and anti-resorptive agents, will shut down or minimize the inflammatory reaction including clastic-cells mediated resorption, thus promote more favourable healing than the positive control group. They also indicate that the use of systematic antibiotics in these cases is not warranted or needed, and just by the use of corticoids these cases could be resolved.

Further elaborating on one of the investigated proposed medicaments for this condition, Clobetasol Propionate, is a potent corticosteroid that is used for treating various skin diseases and it has the ability of affecting the growth and the differentiation of many cells and inhibit the

production of cytokine by possessing anti-inflammatory, immunosuppressive and antimetabolic effects (105). Clobetasol propionate (0,05%) acts by releasing certain anti-inflammatory proteins that will inhibit the synthesis of phospholipase A₂, this is done after activation of the glucocorticoid mediated gene expression by the act of binding to the suspected receptors (105). By inhibiting the release of phospholipase A₂, it will lead to the control of the release of arachidonic acid, which is an inflammatory precursor from membrane phospholipids (105) (Figure 6), and by controlling this it will subsequently lead to the control of cyclooxygenase and lipoxygenase inflammatory enzymes and their succeeding mediators.

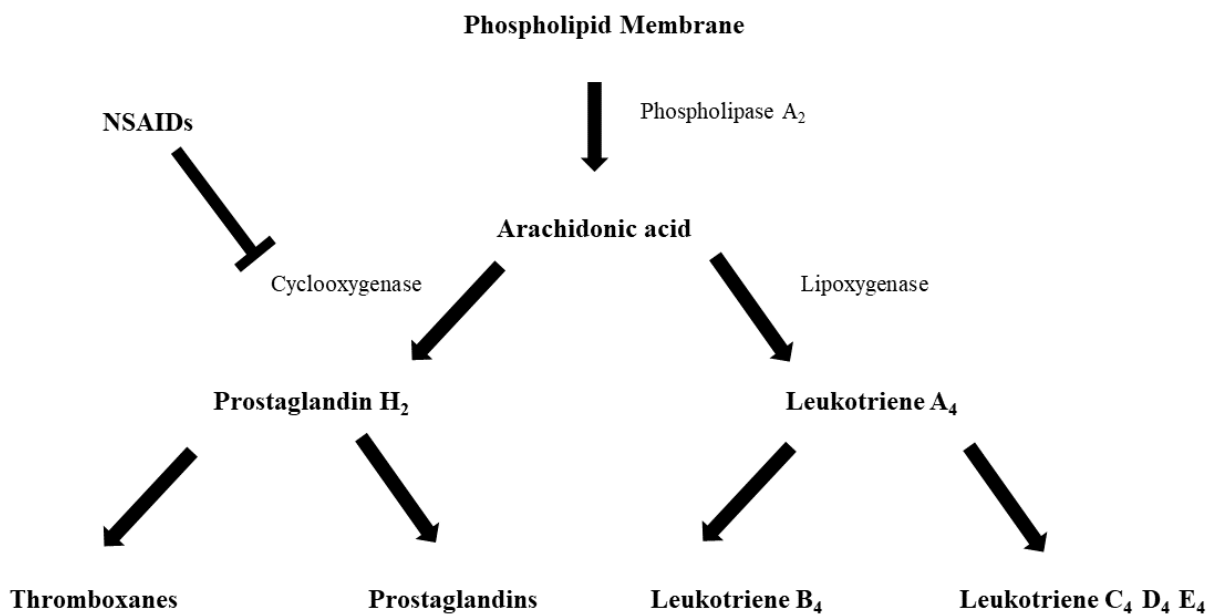


Figure 6 Main biochemical pathways of arachidonic acid.

However, long term administration of systematic corticoids can cause a variety of unpleasant effects like osteoporosis, hypertension, diabetes, weight gain and increased vulnerability to infection to name a few (106). To avoid any corticosteroids adverse effects, drug delivery systems represent an interesting approach in order to also increase the therapeutic efficacy of the drug (11). In addition, these systems would provide an advantage over traditional strategies for long-term treatments such as prolonged and focused drug release on the target site. There are

several types of drug delivery systems such as liposomes, lipid nanoparticles or polymeric nanoparticles (NPs) (11).

3.5 Nanotechnology and its dental application

Nano is a word that originated from the latin language that means “dwarf”, in this sense nanotechnology is characterized as the application of scientific knowledge, predominantly on an atomic, molecular and supramolecular scale, of matter that involves the design, development, characterization and application of different nanoscale materials in different potential fields, providing novel technological advancements (11,107). In other words, nanotechnology is the science that deal with material of the sizes ranging from 1-1000 nm (11). Nanotechnology has been used in our everyday lives for some time now, from cosmetics to sunscreens, toothpastes and food, as it has been used to improve food stability and consistency (108–110). More recently, this has been mainly focused on the field of medicine, which became known as nanomedicine that is defined as the controlled application of nanotechnologies in healthcare, contributing to novel pathways for diagnosing and treating human diseases utilizing what is known as nanoparticles (NPs) (111–113).

In general NPs can be classified according to their structural configuration (11). Accordingly NPs can be differentiated in general into carbon nanotubes, dendrimers, liposomes, metallic NPs, amphiphilic cyclodextrins, quantum dots, micelles, polymeric and lipid nanoparticles (Figure 7). All these different NPs are utilized as ultra-small carriers acting as these colloidal systems, transporting different therapeutic agents to specific sites. These agents can differ ranging from a drug, protein, gene or even a vaccine (114).

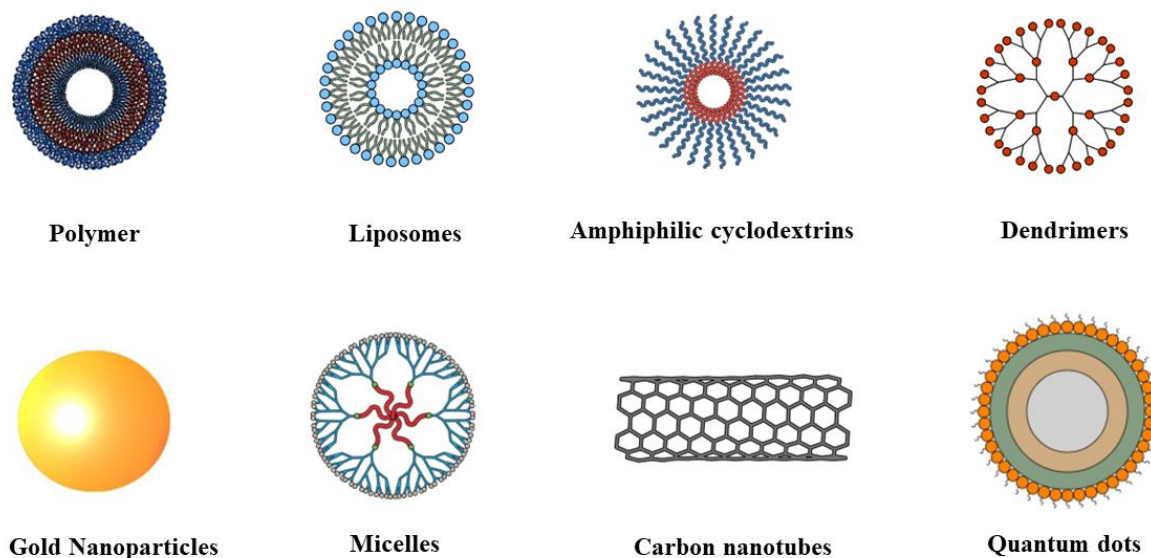


Figure 7 Different types of NPs classified in accordance to their structural configuration.

Following with the latest scientific innovations, nanotechnology has been gaining increasing importance in dentistry (115,116). They have been introduced to improve a variety of aspects in the dental field. From dental materials to increase the ability to polish and the gloss stability of resin composites (117), to elements of scaffold used for tissue engineering (118). All in all, nanotechnology is applied in about 3500 dental materials, from composites, cements and impression material (115). In 2000 the term “*nanodentistry*” was coined by Dr Freitas Jr (119), he helped paving the way by introducing and advocating the models of nanomaterials and NPs in dentistry. All these concepts were first thought of as impractical and farfetched but more recently they are being recognized as viable alternatives and solutions to our dental problems by dental practitioners and it has been applied to many dental fields (120) (Figure 8). In endodontics, it has mainly been applied as an antibacterial element, to try to overcome our shortcomings in eliminating microorganisms during root canal treatment (121,122). NPs in this case can offer an inventive answer because of their large surface to area ratio, ultra-small size and their charged outer surface (123). Back in 2008, Kishen et al (124) first introduced the use of nontechnology in

eliminating bacterial microorganisms, and ever since many authors and studies have tried developing and advancing in this regard utilizing different nanomaterials from chitosan, bioactive glass and silver (125–127).

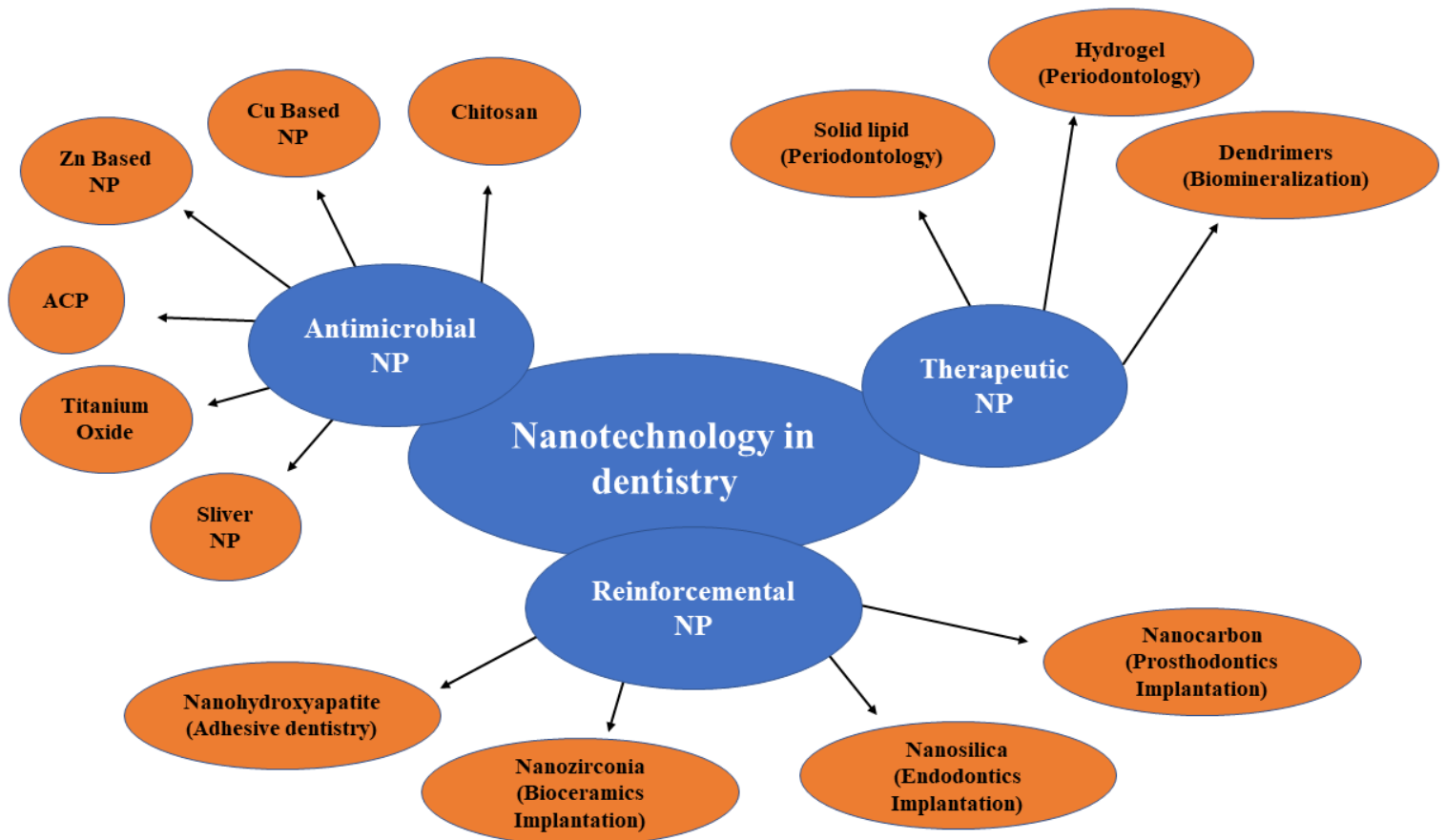


Figure 8 Different types of dental applications for NPs.

3.6 PLGA biodegradable nanoparticles: A novel approach in drug delivery

By and large, conventional drug delivery in general which include the traditional administration of $\text{Ca}(\text{OH})_2$ and clobetasol propionate has major drawbacks. Those include undesirable side effects, deficiency of selectivity, restricted effectiveness and diminished drug release (11). In order to overcome these problems, innovative advances in drug delivery systems have been recently undertaken. In this sense, the most recent nanotechnological approaches focuses on the development of techniques to target the specific cells responsible of the disease by means of individually designed carriers loading the drug (11). This also lead to the reduction in the administered dose, since less drug is lost, and can reduce any potential side effects that could be caused by the drug (11,128). These improvements could help in preventing or reducing the buffering effect caused by dentin and hydroxyapatite and help to maintain a high alkaline pH value in which $\text{Ca}(\text{OH})_2$ can sustain their antibacterial capacity (5). Additionally, they can help in avoiding any corticosteroids adverse effects like osteoporosis, hypertension, diabetes, weight gain and increased vulnerability to infection to name a few (106), after administration of corticosteroids like clobetasol propionate.

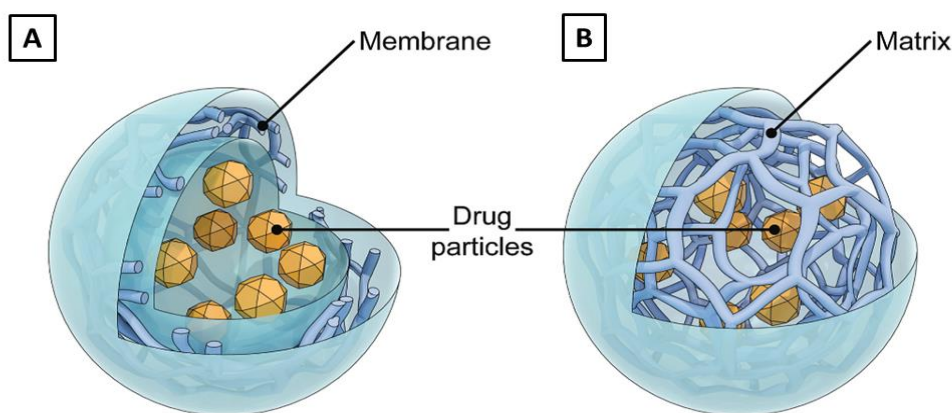


Figure 9 Polymeric biodegradable nanoparticles. (A) Nanocapsules. (B) Nanospheres (129).

Introduction

Advancements in nanotechnology had shown great potential in solving beforehand mentioned problems. Nanoparticles (NPs) are nanoscopic elements between 1-1000 nm with one or more external dimensions. Compared to their bulk or powder counterparts, nanomaterials offer unique physiochemical properties, some of which are ultra-small size, large surface area to mass ratio and increased chemical reactivity (12) (Figure 9). As mentioned before, this technology has been applied into dentistry to what is known as *nanodentistry* which has been used with aims of improving many aspects like dentin hypersensitivity, periodontal infections and implantology (130), plus it is considered an innovative approach in endodontic disinfection (122).

One of the most successfully used synthetic polymers for targeted drug delivery and synthesizing polymeric NPs is PLGA or poly(lactic-co-glycolic acid) (131). PLGA is a biocompatible, biodegradable polymer which is approved by the Food and Drug Administration (FDA) and its used as a carrier for controlled drug release (132). It is deemed simple to formulate and can be reproduced easily with minimal side effects (133). It can be assumed that applying and utilizing these principles and by combining the antibacterial properties of a material like $\text{Ca}(\text{OH})_2$ and the anti-inflammatory properties of clobetasol propionate, with the the prolonged drug delivering ability, plus the targeted release and specificity of the PLGA polymers it can overcome the well documented shortcomings and limitations of $\text{Ca}(\text{OH})_2$ and perhaps provide an appropriate treatment for avulsed teeth with extended extra oral dry time. Additionally, the ultra-small size of these NPs could permit more penetration inside the dentinal tubules and reaching areas of complicated anatomy like isthmuses, accessory, and lateral canals.

OBJECTIVES

OBJECTIVES

4. OBJECTIVES

4.1 Primary Objectives

The aim of this research is the development and optimization of two novel different biodegradable polymeric NPs to be used in the field of endodontics, using PLGA polymers loaded with two different drugs.

4.1.1 Antibacterial calcium hydroxide (Ca(OH)₂/PLGA) NPs to be used as an intracanal antibacterial medication.

4.1.2 Anti-inflammatory clobetasol propionate (clobetasol/PLGA) NPs to be used as an intracanal medication in cases of avulsed teeth with extended extra oral time.

4.2 Secondary Objectives

1. Analyzing the characterization, stability and drug release of the antibacterial Calcium Hydroxide (Ca(OH)₂/PLGA) NPs.
2. Analyzing the characterization, stability and drug release of the anti-inflammatory Clobetasol Propionate/PLGA NPs.
3. Achieving the optimal conditions for the process of freeze drying of the antibacterial Calcium Hydroxide (Ca(OH)₂/PLGA) NPs.
4. Achieving the optimal conditions for the process of freeze drying of the anti-inflammatory Clobetasol Propionate/PLGA NPs.
5. Evaluate the pH values of the antibacterial Calcium Hydroxide (Ca(OH)₂/PLGA) NPs during the first week after their preparation.
6. Evaluating the biocompatibility, cytotoxicity and the biostability of the anti-inflammatory Clobetasol Propionate/PLGA NPs.

7. Performing antibacterial testing to assess the antibacterial performance of the antibacterial Calcium Hydroxide ($\text{Ca}(\text{OH})_2/\text{PLGA}$) NPs in regard to elimination of different bacterial strains.
8. Performing anti-inflammatory testing to assess the anti-inflammatory therapeutic efficacy of Clobetasol Propionate/PLGA NPs in regard to their response against macrophages.
9. Test penetration and the mean fluorescence intensity inside the dentinal tubules for the antibacterial Calcium Hydroxide ($\text{Ca}(\text{OH})_2/\text{PLGA}$) NPs against their counterpart free drug using confocal laser scanning microscopy.
10. Test penetration and the mean fluorescence intensity inside the dentinal tubules for the anti-inflammatory Clobetasol Propionate/PLGA NPs against their counterpart free drug using confocal laser scanning microscopy.

HYPERTHESIS

HYPOTHESIS

5. HYPOTHESIS

5.1 Null Hypothesis (H_0)

1. There will not be a possibility to successfully load, optimize and formulate Calcium Hydroxide (Ca(OH)_2)/PLGA NPs to increase the antibacterial effect of Ca(OH)_2 through controlled drug release and superior reach to areas of complicated root canal anatomy due to the nanoscopic size.
2. There will not be a possibility to successfully load, optimize and formulate Clobetasol Propionate /PLGA NPs to be used as an intracanal anti-inflammatory medication in cases of avulsed teeth with extended extra oral time.
3. There will not be a possibility to characterize both the Calcium Hydroxide (Ca(OH)_2 /PLGA) and the Clobetasol Propionate/PLGA NPs by examining their morphology, any possible drug interactions and ensuring that the drug is encapsulated inside.
4. There will not be a possibility to examine the drug release profile for the Calcium Hydroxide (Ca(OH)_2 /PLGA) NPs in comparison to the free drug.
5. There will not be a possibility to examine the drug release profile for the Clobetasol Propionate/PLGA NPs in comparison to the free drug..
6. There will not be a possibility to achieve the optimal conditions for the process of freeze drying of the antibacterial Calcium Hydroxide (Ca(OH)_2 /PLGA) NPs.
7. There will not be a possibility to achieve the optimal conditions for the process of freeze drying of the anti-inflammatory Clobetasol Propionate/PLGA NPs.
8. There will not be a possibility to evaluate the pH values of the antibacterial Calcium Hydroxide (Ca(OH)_2 /PLGA) NPs during the first week after their preparation.
9. There will not be a possibility to evaluate the biocompatibility, cytotoxicity and the biostability of the anti-inflammatory Clobetasol Propionate/PLGA NPs.

10. There will not be a possibility to perform the antibacterial testing to assess the antibacterial effects of Calcium Hydroxide (Ca(OH)_2 /PLGA) NPs in regard to elimination of different bacterial strains.
11. There will not be a possibility to perform the anti-inflammatory testing to assess the anti-inflammatory effects of the Clobetasol Propionate/PLGA NPs in regard to their response against macrophages.
12. Calcium Hydroxide (Ca(OH)_2 /PLGA) NPs will not be able to achieve a superior depth of penetration inside the dentinal tubules or higher mean florescent intensity in comparison to their respective free counterpart using confocal laser scanning microscopy.
13. Clobetasol Propionate/PLGA NPs will not be able to achieve a superior depth of penetration inside the dentinal tubules or higher mean florescent intensity in comparison to their respective free counterpart using confocal laser scanning microscopy.

5.2 Alternative Hypothesis (H1)

1. There will be a possibility to successfully load, optimize and formulate Calcium Hydroxide (Ca(OH)_2)/PLGA NPs to increase the antibacterial effect of Ca(OH)_2 through controlled drug release and superior reach to areas of complicated root canal anatomy due to the nanoscopic size.
2. There will be a possibility to successfully load, optimize and formulate Clobetasol Propionate /PLGA NPs to be used as an intracanal anti-inflammatory medication in cases of avulsed teeth with extended extra oral time.
3. There will be a possibility to characterize both the Calcium Hydroxide (Ca(OH)_2 /PLGA) and the Clobetasol Propionate/PLGA NPs by examining their morphology, any possible drug interactions and ensuring that the drug is encapsulated inside.
4. There will be a possibility to examine the drug release profile for the Calcium Hydroxide (Ca(OH)_2 /PLGA) NPs in comparison to the free drug.
5. There will be a possibility to examine the drug release profile for the Clobetasol Propionate/PLGA NPs in comparison to the free drug..
6. There will be a possibility to achieve the optimal conditions for the process of freeze drying of the antibacterial Calcium Hydroxide (Ca(OH)_2 /PLGA) NPs.

7. There will be a possibility to achieve the optimal conditions for the process of freeze drying of the anti-inflammatory Clobetasol Propionate/PLGA NPs.
8. There will be a possibility to evaluate the pH values of the antibacterial Calcium Hydroxide (Ca(OH)_2 /PLGA) NPs during the first week after their preparation.
9. There will be a possibility to evaluate the biocompatibility, cytotoxicity and the biostability of the anti-inflammatory Clobetasol Propionate/PLGA NPs.
10. There will be a possibility to perform the antibacterial testing to assess the antibacterial effects of Calcium Hydroxide (Ca(OH)_2 /PLGA) NPs in regard to elimination of different bacterial strains.
11. There will be a possibility to perform the anti-inflammatory testing to assess the anti-inflammatory effects of the Clobetasol Propionate/PLGA NPs in regard to their response against macrophages.
12. Calcium Hydroxide (Ca(OH)_2 /PLGA) NPs will be able to achieve a superior depth of penetration inside the dentinal tubules or higher mean florescent intensity in comparison to their respective free counterpart using confocal laser scanning microscopy.
13. Clobetasol Propionate/PLGA NPs will be able to achieve a superior depth of penetration inside the dentinal tubules or higher mean florescent intensity in comparison to their respective free counterpart using confocal laser scanning microscopy.

MATERIALS AND METHODS

6. MATERIALS AND METHODS

For the following *in vitro* laboratory study, the part of preparation, optimization, characterization, penetration depth and *in vitro* drug release of NPs was carried out in the Department of Pharmacy and Pharmaceutical Technology and Physical Chemistry of the Faculty of Pharmacy and Food Sciences in the University of Barcelona (Barcelona, Spain). Freeze drying, cytotoxicity studies, antibacterial capacity assays and anti-inflammatory capacity assays were carried out in the Bioengineering institute of technology and Department of Endodontics in the Universitat Internacional de Catalunya (UIC, Sant Cugat del Valles, Barcelona, Spain). Additionally, the following *in vitro* laboratory study was carried out with the ethical committee approval code (END-ELB-2020-01).

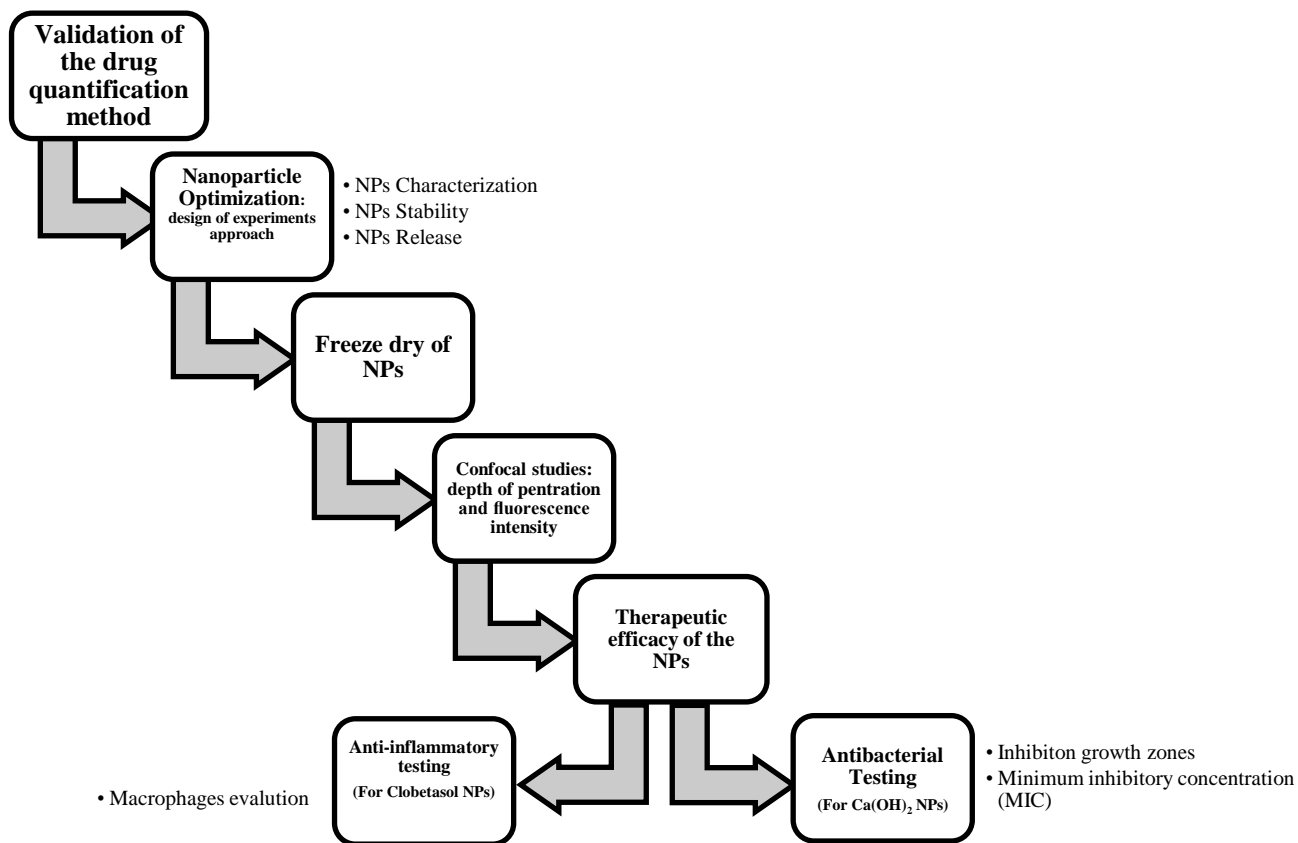


Figure 10 Scheme showing the steps and the experiments that were carried out.

6.1 Materials

Poly(D,L-lactide-co-glycolide) (Evonik Industries, Resomer® RG 503 H), Calcium hydroxide 98% extra pure ACROS Organics™ (Fisher Scientific, USA), Poloxamer 188 (P188) (Sigma-Aldrich, USA), Acetone (Fisher Scientific, USA), Clobetasol 17-Propionate 98 % (Capot Chemical Co.Ltd, China), Tween®80 (Sigma-Aldrich, USA), Dimethyl sulfoxide anhydrous ≥99.9% (Sigma-Aldrich, USA), Nitric acid reagent grade, fuming, >70% (Sigma-Aldrich, USA), Polyethylene glycol 3350 (Sigma-Aldrich, USA), D-mannitol (Sanofi, France), (2-Hydroxypropyl)-β-cyclodextrin (Sigma-Aldrich, USA). All the formulations were carried out using Milli-Q water (MilliporeSigma, USA). All the other reagents were of analytical grade.

6.2 Preparation of the nanoparticles

The solvent displacement method was used to prepare both Ca(OH)₂/PLGA and Clobetasol Propionate/PLGA NPs (134). For the Ca(OH)₂/PLGA NPs the drug (Calcium hydroxide) was firstly placed in 1 mL Dimethyl sulfoxide anhydrous (DMSO) and vortexed until it was totally dissolved. This was added to a 4 mL solution of the co-polymer (PLGA) dissolved in acetone. This 5 mL solution was placed in an ultrasonic bath (Elma Digital Ultrasonic Cleaners®) forming the organic phase. In case of the Clobetasol Propionate/PLGA NPs, the co-polymer (PLGA) and the drug (Clobetasol propionate) were directly dissolved in 5 mL acetone and positioned in an ultrasonic bath (Elma Digital Ultrasonic Cleaners®) producing the organic phase. This organic phase was then added dropwise, under moderate stirring, into 10 mL of an aqueous solution of sterile water (Milli-Q water) and surfactant which was Lutrol (P188) for the Ca(OH)₂/PLGA NPs and Tween®80 for the Clobetasol Propionate/PLGA NPs, which constitutes the aqueous phase (Figure 11). After that, organic solvents (Acetone and DMSO) were evaporated using Rotavapor® R-210/215 (Buchi, Switzerland), and the NPs were concentrated to 10 mL under reduced pressure. Empty NPs were prepared using the same procedure but without the addition of the drug (Calcium hydroxide or Clobetasol Propionate).

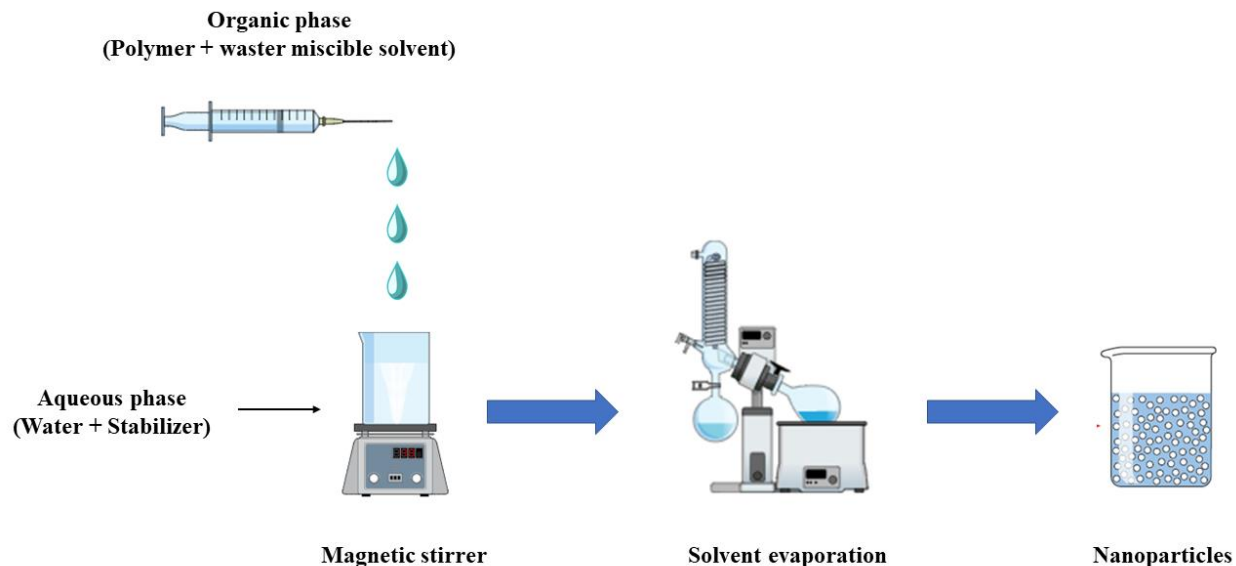


Figure 11 Solvent Displacement Method.

6.3 Development of Calcium hydroxide quantification method for Calcium Hydroxide/PLGA Nanoparticles

Quantification of calcium hydroxide was performed using inductively coupled plasma optical emission spectroscopy (ICP-OES). This technique allows the determination of low concentrations of calcium in samples, and it is highly regarded for its speed and accuracy. It uses the inductively coupled plasma to produce excited atoms and ions that emit electromagnetic radiation at wavelengths characteristic of a particular element. Subsequently, the intensity of these emissions are proportional to the concentrations of the elements within the sample (135). An Optima 8300 ICP-OES (PerkinElmer, USA) was used to measure to the concentrations of calcium inside the samples. Explaining the method briefly, the liquid sample converted in the nebulizer into aerosol spray, were finer droplets are directed towards the hot plasma (135). In the plasma, the sample aerosol vaporizes, and its atoms and ions are excited so that their characteristic wavelength are emitted. The light is transferred into the high resolution no purge sealed optical system which separates the light into specific wavelengths for the elements to be measured (135). As these wavelengths strike the detector array, light intensity for each different wavelength is quantified and the software converts them into concentration units by means of reference validated standards (135) (Figure 12).

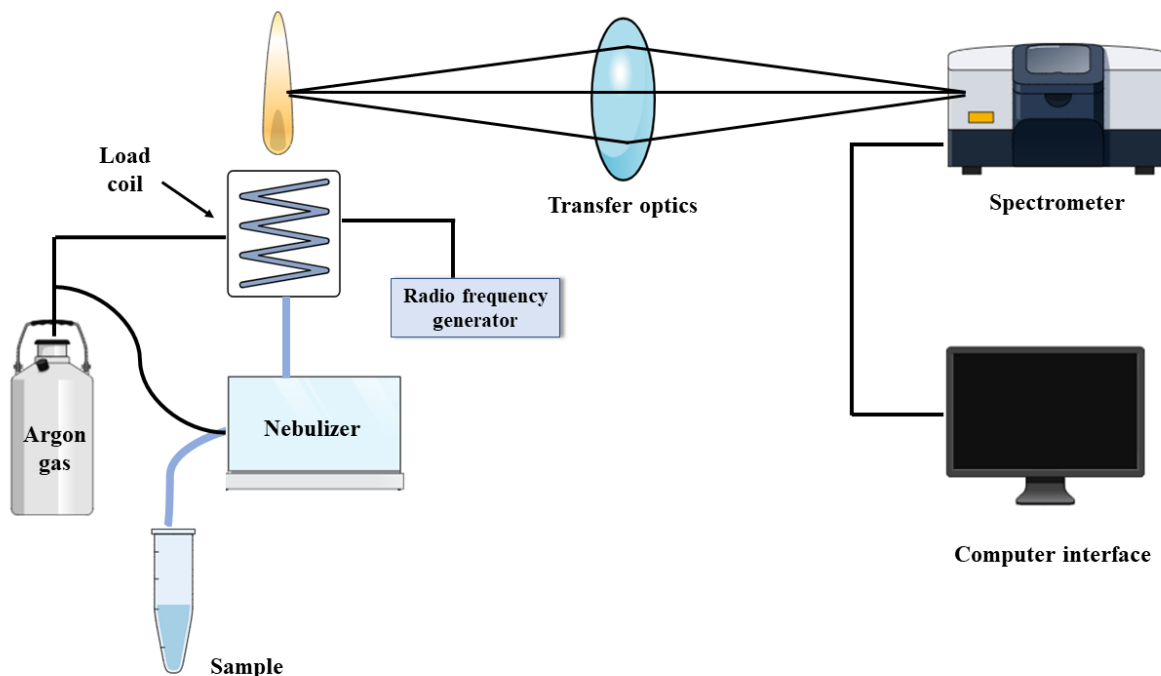


Figure 12 Inductively Coupled Plasma Optical Emission Spectroscopy.

6.4 Entrapment efficiency of Calcium Hydroxide/PLGA Nanoparticles using Inductively Coupled Plasma Optical Emission Spectroscopy

The Entrapment efficiency (EE) which is the amount of the drug that is encapsulated inside the NPs, was determined indirectly by measuring the concentration of the free drug in the dispersion medium (136). The non-encapsulated drug was separated by a filtration/centrifugation technique by using an Ultracell–100 K (AmiconR Ultra; Millipore Corporation, Massachusetts) centrifugal filter devices at 1400 rpm for 15 min (Heraeus, Multifuge 3 L-R, Centrifuge. Osterode, Germany). The EE was calculated using the following Equation /1/:

$$EE(\%) = \frac{\text{Total amount of drug} - \text{Free drug}}{\text{Total amount of drug}} \times 100$$

These sample were prepared by adding 1 % Nitric acid ($\text{HNO}_3 > 90 \%$) to guarantee the dissolution and stability of Calcium. Consequently, in order to measure and quantify Calcium hydroxide. Samples were diluted with 1 % Nitric acid ($\text{HNO}_3 > 90 \%$) to obtain enough volume for measurements. Instrument was calibrated using 5 standard solutions prepared by dilution of certified Calcium standard solution (1g/l Inorganic Ventures) covering samples concentration range. Additionally, in order to elucidate the recovery after the sample preparation process, 5 standards were used and compared with the amount of the Calcium measured by the instrument. In which, $\text{Ca}(\text{OH})_2$ standard were prepared in a range of 0.2, 0.6, 1, 1.4 and 1.8 mg/ml plus, 1 % Nitric acid (HNO_3) was added for each standard following the same procedure applied for the samples.

Since the concentration of Calcium hydroxide concentration inside the standards is established, using the known molecular weight ($\text{Ca} = 40.08 \text{ g/mol}$) we were able to calculate the theoretical Calcium concentration. This was divided by the real Calcium concentration in the standards obtained in the method to determine the ratio. Obviously in this case, a ratio closer to 1 is considered precise. The ratio was determined to know the recovery % of the samples after manipulation and it was applied to the samples because they have been subjected to the same manipulation. Then, using the molecular weight ($\text{Ca}(\text{OH})_2 = 74.093 \text{ g/mol}$) these adjusted concentrations were converted back to obtain the real Calcium hydroxide concentration inside the samples (Figure 13).

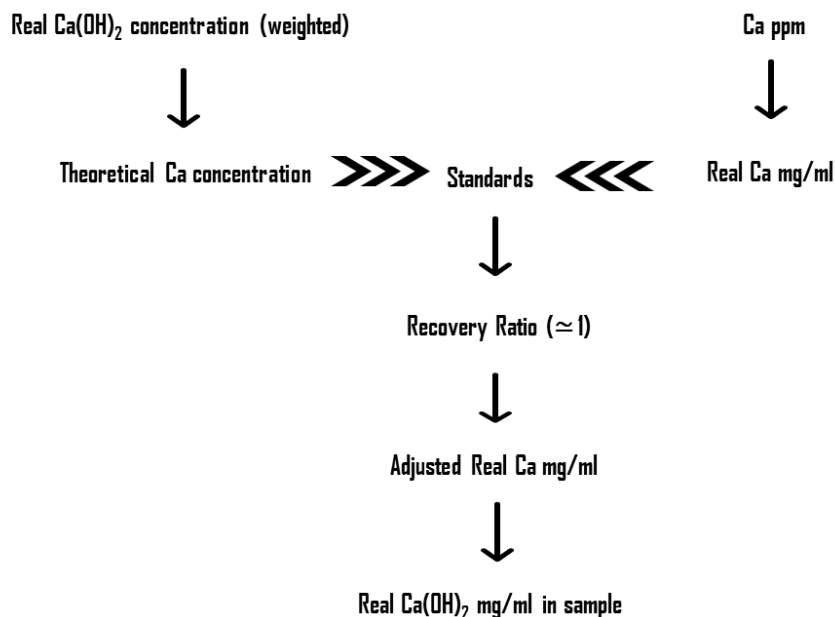


Figure 13 Scheme explaining the step for calculating the concentration of Calcium hydroxide in the samples.

6.5 Development of Clobetasol propionate quantification method for Clobetasol Propionate/PLGA Nanoparticles

Samples were evaluated by high performance liquid chromatography (HPLC). Briefly, samples were quantified using HPLC Waters 2695 separation module and a Hypersil™ C₁₈ column (150 × 3.9 mm) with a mobile phase of methanol/water (74:26) at a flow rate of 1 ml/min and a wavelength of 240 nm. Standards were prepared in methanol:H₂O (90:10) from a stock solution of 1 mg/ml Clobetasol. Quantification range was calculated.

6.5.1 Entrapment efficiency of Clobetasol Propionate/PLGA Nanoparticles using High Performance Liquid Chromatography

Due to the solubility of Clobetasol propionate which is 3.86 $\mu\text{g/ml}$, the suitable dilution would be 1:1000. However, 1:1000 dilution is extremely high as we will be under the quantification limit of the HPLC method. Also, in case the dilution was less, we risk the fact of the formation of crystals that could cause filter collapse. In this sense, before the optimization of the NPs, several assessments were performed. The following formulations were prepared in order to optimize the entrapment efficiency (EE):

1. NPs were diluted to 1:1000 in water. This solution was placed on the Vortex mixer and 300 μl were placed in a filtration-centrifugation device. Filtration-centrifugation was carried out at 4000 rpm for 15 min. Finally, the supernatant solution was placed in an HPLC vial with insert.
2. NPs were diluted to 1:100 in water. This solution was placed on the Vortex mixer and 300 μl was placed in a filtration-centrifugation device. Filtration-centrifugation was carried out at 4000 rpm for 15 min. Finally, this solution was placed in an HPLC vial with insert.
3. NPs were diluted to 1:100 in methanol. This solution was placed on the Vortex mixer and 300 μl was placed in a filtration-centrifugation device. Filtration-centrifugation was carried out at 4000 rpm for 15 min. Finally, the supernatant solution was placed in an HPLC vial with insert.
4. NPs were diluted to 1:10 in methanol. This solution was placed on the Vortex mixer and 300 μl was placed in a filtration-centrifugation device. Filtration-centrifugation was carried out at 4000 rpm for 15 min. Finally, this solution was placed in an HPLC vial with insert.
5. NPs were diluted to 1:10 in DMSO. A subsequent dilution 1:10 methanol:H₂O was carried out. Then, 50 μl of NPs + 450 μl methanol:H₂O were pipetted again and placed in an HPLC vial with insert. Using this procedure, we attempted to dissolve the polymer and measure the total amount of drug.
6. NPs were diluted to 1:10 in DMSO. This solution was placed on the Vortex mixer and 300 μl was placed in a filtration-centrifugation device. Filtration-centrifugation was

carried out at 4000 rpm for 15 min. Finally, this solution was placed in an HPLC vial with insert.

7. 500 μ l of the NPs were placed in a weighted Eppendorf. This solution was placed on the Vortex mixer and 300 μ l was placed in a filtration-centrifugation device. Filtration-centrifugation was carried out at 14000 rpm for 30 min.

7.1 The supernatant was removed and a 1:2 dilution in methanol:H₂O was carried out. This was placed in an HPLC vial. Theoretically, this should measure the non-encapsulated drug.

7.2 To the pellet, DMSO was added until it reaches the initial weight earlier (with a micropipette of 20 μ l). This was placed in an ultrasonic bath or on the Vortex mixer to make sure it is solved. From here, a 1:2 dilution with methanol:H₂O was carried out. This was placed in an HPLC vial. Theoretically, the polymeric matrix is solved with DMSO and since the free drug was previously removed, only the encapsulated drug will be measured.

6.6 Preformulation studies

NPs average size (Z_{av}), polydispersity index (PI) and zeta potential (ZP) were assessed in order to characterize the formulation. Z_{av} and PI of NPs were determined by photon correlation spectroscopy (PCS) after a 1:10 dilution with a Zetasizer Nano ZS (Malvern Instruments, Malvern, UK) at 25 °C using disposable quartz cells and (Malvern Instruments). NPs surface charge, measured as ZP, was evaluated by using laser-Doppler electrophoresis with M3 PALS system in Zetasizer Nano ZS. This was performed by further diluting the previous solution with 1000 μ l of Milli-Q water. All the experiments were prepared by triplicate (137–139).

6.7 Design of experiments

Design of experiments (DoE) is frequently used to plan research because it provides maximum information, whilst requiring a minimal number of experiments (140). Therefore, in order to optimize the formulation, the DoE approach was used. Thus, a factorial design was applied, and a suitable formulation was obtained. The effect of the variables involved in the formulation process were assessed on the dependent variables of Z_{av} , PI, ZP and EE. Using this approach, a composite design matrix was generated using Statgraphics Centurion XV software (StatPoint Technologies, Inc., Warrenton, VA, USA).

6.8 Nanoparticles morphology studies

To visualize the NPs, negative staining was carried out with uranyl acetate (2 %) on copper grids activated with UV light. NPs morphology was determined by transmission electron microscopy (TEM), performed on a JEOL 1010 microscope (Akishima, Japan) (134).

6.9 Nanoparticles characterization and interaction studies

X-ray diffraction (XRD) was used to analyze the state (amorphous or crystalline) of the samples (centrifuged NPs or formulation compounds). Compounds were sandwiched between polyester films of 3.6 μm and exposed to Cu $K\alpha$ radiation (45 kV, 40 mA, $\lambda = 1.5418 \text{ \AA}$) in the range from 2° to 70° with a step size of 0.026° and a measuring time of 200 seconds per step (141,142).

Fourier transform infrared (FTIR) spectra of different samples (NPs formulations or compounds separately) were obtained using a Thermo Scientific Nicolet iZ10 with an ATR diamond and DTGS detector. The scanning range was $400\text{--}4000 \text{ cm}^{-1}$ (141,143)

In order to analyse the thermic profile of the NPs, differential scanning calorimetry (DSC) was performed in which, thermograms were obtained on a Mettler TA 4000 system (Greifensee,

Switzerland) equipped with a DSC 25 cell. Temperature was calibrated by the melting transition point of indium prior to sample analysis. All samples were weighed (Mettler M3 Microbalance) directly in perforated aluminum pans and were conducted under a nitrogen flow heating rate of 10 °C / min up to 1000 °C for the Ca(OH)₂/PLGA NPs (144) and a range of 5 to 325 °C for the Clobetasol Propionate/PLGA NPs (142).

6.10 Stability studies

Short-term stability of the NPs was assessed at three different temperatures (4, 25 and 37 °C) which represent the refrigerator temperature, room temperature and the incubation temperature, measuring the Z_{av} , PI, ZP and EE of the NPs once a month by triplicate. All the temperature studies were carried out, and visual observation of the samples was also undertaken (134).

6.11 *In vitro* drug release

In vitro drug release of the Ca(OH)₂/PLGA NPs and the Clobetasol Propionate/PLGA NPs was studied against the free Ca(OH)₂ drug in PBS and free Clobetasol Propionate in 90:10 methanol:H₂O in a bulk equilibrium direct dialysis bag technique under sink conditions for 48 hours (n =3/group). Briefly, a volume of 8 mL of each formulation was placed directly into a dialysis bag (Visking Size 3 Inf Dia 20/32\ - 15.9 mm : 30 m, Medicell International Ltd, UK) and each bag was placed on 150 mL of isotonic phosphate-buffered saline (PBS) 0.1 M, pH 7.4 at 37 °C for the Ca(OH)₂/PLGA NPs and in 90:10 methanol:H₂O at 37 °C for the Clobetasol Propionate/PLGA NPs to ensure sink conditions for each drug. At predetermined intervals, 300 µl of sample were withdrawn from the stirred release medium and simultaneously replaced with 300 µl of fresh buffer at the same temperature. Later, the amounts and percentages of drug released at each time were determined and the data were adjusted with the GraphPad Prism 8 program (GraphPad Software, USA). Furthermore, data was adjusted to the most common kinetic models for Clobetasol NPs using Prism software. On the other hand, for Ca(OH)₂ NPs,

accounting for the conversion of the drug, a pharmacokinetics one compartment model analysis was performed to predict and evaluate the behaviour of the drug, utilizing the PKSolver excel add-in program (145).

6.12 Freeze dry of the nanoparticles

Due to the limited stability of polymeric NPs in aqueous suspension, the removal of water from the solution is recommended. This was done by freeze drying the NPs using the laboratory freeze dryer Lyomicron: Cylindric chamber configuration (Coolvacuum Technologies, Spain). Mild-aggressive standard conditions were utilized and optimization were carried out for the best fitting cryoprotectants for the NPs (146). All the formulations were tested at the same conditions utilizing the laboratory freeze dryer Lyomicron: Cylindric chamber configuration (Coolvacuum Technologies, Spain) (Table 1).

Table 1 Conditions utilized for freeze-drying.

Phase	Time (hours)	Temperature (°C)	Pressure (mBar)
Freezing	8	-80	-
Freezing	1	-30	-
Primary drying	3	-30	0.350
Secondary drying	12	+10	0.350

6.13 Sterilization assays

Freeze-dried NPs were γ -irradiated using 60 °C as irradiation source (Aragogamma, Barcelona, Spain) and received a dose of 25 kGy. According to the European Pharmacopoeia, 25 kGy represents the adequate absorbed dose for the purpose of sterilizing pharmaceutical products when bioburden is not known. Furthermore, it is considered a standard γ -irradiation dose

recommended for terminal sterilization of medical products that maintain a valid sterility assurance level of 10^{-6} SAL (147).

6.14 Confocal laser scanning microscopy test

The maximum depth of penetration, the area the drug covered, the percentage of area covered compared to the total root canal, the mean fluorescence intensity (MFI) and the integrated density of the polymeric NPs was measured *in vitro* using extracted human teeth in comparison to their free drug counterpart. Both the $\text{Ca}(\text{OH})_2/\text{PLGA}$ NPs and the clobetasol propionate/PLGA NPs were prepared by adding 17.40 % of PLGA labelled with rhodamine 110 to the total concentration of PLGA (148). Moreover, the free drug ($\text{Ca}(\text{OH})_2$ or clobetasol propionate) was mixed with rhodamine 6G as a control (149). In this case, 12.5 % of rhodamine 6G was added with the same concentration of the free drug present in the NPs, after that the solution was dissolved in sterile saline. Moreover, teeth that were extracted for reasons nonrelated to this study, were decoronated with a diamond disk (Kerr Dental, California, USA) to obtain roots with a standardized length of 16 mm. A double varnish layer of Fluor protector (Ivoclar Vivadent, Schaan, Liechtenstein) was applied externally avoiding the root apex to simulate cementum. Subsequently, all root canals were instrumented using RECIPROC size 40 files (VDW, GmbH, Munich, Germany), during which they were irrigated continuously using 4.25 % Sodium hypochlorite (NaOCl) solution (1 ml). After finishing the instrumentation process, a final irrigation sequence was adopted for all the teeth in the following order: NaOCl (1 ml), 10 % citric acid (1 ml), NaOCl (1 ml) and sterile saline (1 ml) followed by finally drying the canals using RECIPROC Paper Points (VDW, GmbH, Munich, Germany), obtaining an average irrigation time of 8 to 10 minutes for each tooth. Afterwards, teeth were placed in resin blocks and divided into five groups (two NPs groups and two free drug groups and one control) with the sample size and distribution for each group presented in table 2. Teeth that were in the control group were irrigated with sterile saline solution only and were used as a negative control group. However, for the other groups 1 ml solution of each medicament was introduced into the canal as an intracanal medication and it was sonically activated using EndoActivator (Dentsply Sirona, USA) and teeth were incubated at 37 °C. Later, teeth were sectioned using a precise Diamond

Section machine (Buehler, Waukegan Road Lake Bluff, Illinois, USA) using a diamond blade with a radius of 17.9 mm and a thickness of 1.3 mm, applying a speed in between 350-400 rpm, creating a clean and reproducible cut in all the samples (Figure 14). Each sample was set to cut at 1.7 mm, 4.7 mm, and 7.7 mm from the anatomical apex, taking into consideration the thickness of the blade, the visible section was made at exactly 3, 6 and 9 mm. This process was repeated for all samples. Afterwards, teeth were examined using a Carl Zeiss LSM 880 spectral confocal microscope (Carl Zeiss AG, Germany) evaluating the depth and the area of penetration inside the dentinal tubules (149). Using the ImageJ image processing software (GNU General Public License, USA), the depth of penetration was calculated as the deepest point of penetration measured from the canal wall to the point of the maximum medicament penetration inside the tubules. Whilst the area was calculated by measuring the area of the drug penetration using the freehand selection tool in ImageJ. Additionally, the percentage of area covered by the drug in relation to the total area of the root canal was calculated, in which the area of the drug penetration was divided by the total area of the root canal after subtracting the area of the hollow middle canal space. Finally, the MFI and the integrated density was calculated for the area of drug penetration to evaluate the concentration of the medicament inside the dentinal tubules. Mann-Whitney U test and the Two-Sample t-test were used to perform mean comparisons between the NPs and the free drug in order to identify any significant differences.

Table 2 Distribution of the samples used for the confocal laser scanning microscopy test.

Group	Sample size	Section place
Free calcium hydroxide	5	3 mm (n = 1) 6 mm (n = 3) 9 mm (n = 1)
Calcium hydroxide nanoparticles	6	3 mm (n = 1) 6 mm (n = 4) 9 mm (n = 1)
Free clobetasol propionate	2	6 mm (n = 1) 9 mm (n = 1)
Clobetasol propionate nanoparticles	3	3 mm (n = 1) 6 mm (n = 1) 9 mm (n = 1)
Sterile Saline	4	3 mm (n = 1) 6 mm (n = 2) 9 mm (n = 1)

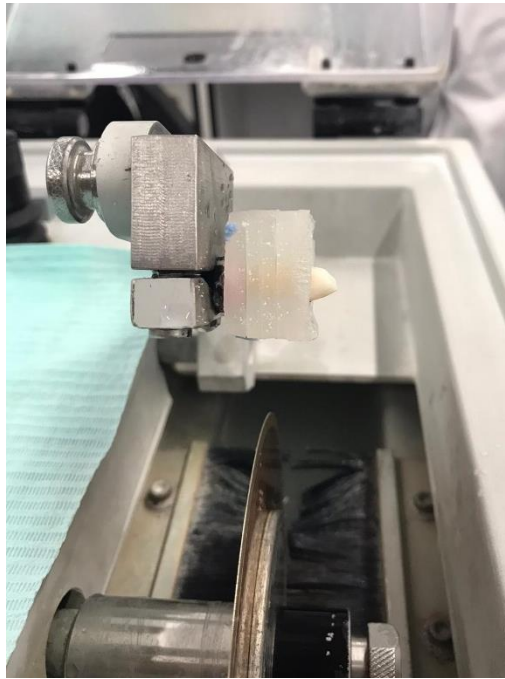


Figure 14 Teeth sectioning using Diamond Section machine.

6.15 Antibacterial capacity of the Calcium Hydroxide/PLGA nanoparticles

The antibacterial effect of the Ca(OH)_2 /PLGA NPs was assessed in order to elucidate whether they are suitable for endodontics disinfection procedures. In order to evaluate the antibacterial efficacy of the NPs, several antibacterial tests were carried out using three bacterial strains: *Porphyromonas gingivalis* (Pg) (ATCC 33277), *Fusobacterium nucleatum* (Fn) (ATCC 25586) and *Enterococcus faecalis* (Ef) (ATCC 19433) (150–152). All the testing procedures were performed following the guidelines proposed by the Clinical and Laboratory Standards Institute (CLSI) (153,154).

6.15.1 Agar diffusion test

Firstly, we measured the growth inhibition zones by using the agar disk-diffusion testing. In this commonly used antibacterial testing, agar plates were prepared using brain heart infusion agar (BHI Agar) (Condalab, Spain) and were injected with the test microorganism in this case Pg bacterium. Pg was chosen here because of its unique dual dental threat, firstly it has a high prevalence in cases of necrotic endodontic infections (155,156), secondly for begin part of what is known as the '*red complex*' of bacterial species that are responsible for sever forms of periodontal disease (157,158). After that, filter papers were placed in the agar plates containing different drugs. The antibacterial Calcium Hydroxide (CaOH₂/PLGA) NPs, Amoxicillin antibiotic 500 mg, Calcicur (VOCO, Germany), Calcium hydroxide 98 % extra pure ACROS Organics™ (Fisher Scientific, USA) mixed with sterile saline and a BHI agar as a blank control were all placed onto sterile filter papers (153). Amoxicillin antibiotics were used as guaranteed positive control group, in which it provide conditions that are certain for bacterial inhibition, whilst Calcicur was used as a representative and one of the most common commercially available brands of Ca(OH)₂ that are utilized in our daily clinical practice. The plates were incubated at 37 °C and under anaerobic conditions for 24 and 48 hours. Then, the diameters of the growth inhibition were measured for each medicament. All experiments were performed by triplicate (Figure 15).

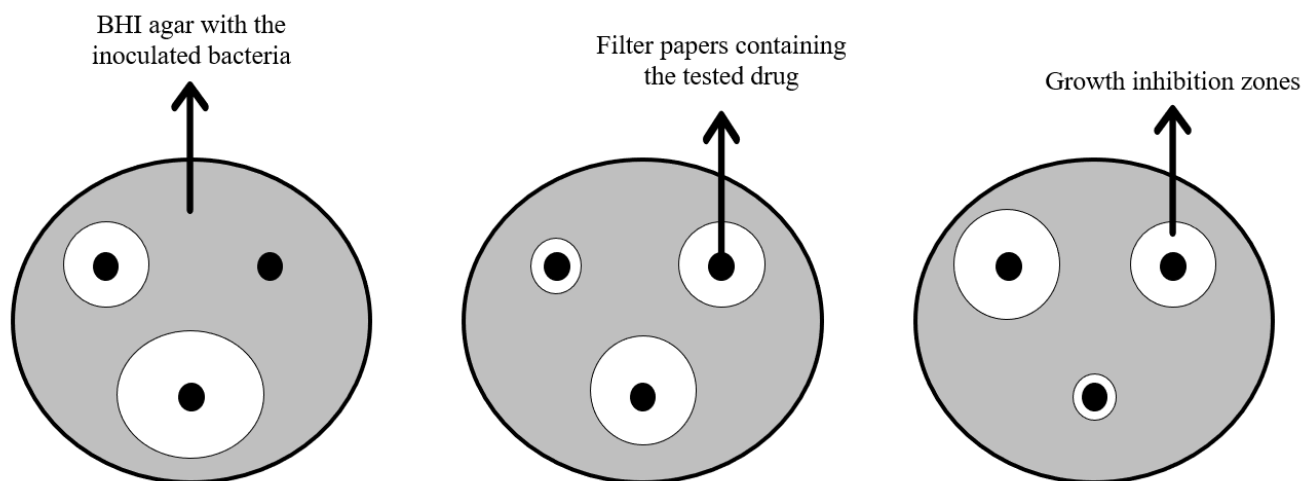


Figure 15 Scheme explaining the agar diffusion test.

6.15.2 Minimal inhibitory concentration

In order to determine the minimal inhibitory concentration (MIC), a broth microdilution method was used in accordance to the guidelines proposed by the CLSI (154) (159) (Figure 16). A serial dilution (1:1, 1:2, 1:5, 1:10, 1:20, 1:50, 1:100, 1:200 and 1:500) was applied for both the antibacterial (CaOH₂/PLGA) NPs and Calcium hydroxide 98 % extra pure ACROS Organics™ (Fisher Scientific, USA) mixed with Milli-Q water at the same concentrations. Subsequently, 100 µl from each dilution were added in a 96-Well Microplate (Fisher Scientific, USA). Furthermore, for the three bacterial strains *Porphyromonas gingivalis*, *Fusobacterium nucleatum* and *Enterococcus faecalis*, the bacterial suspension turbidity was adjusted to 0.5 McFarland by adding BHI media and measuring absorbance in a spectrophotometer (Cary 60 UV-Vis Spectrophotometer, Agilent) at a wavelength of 600 nm. Then, each diluted well was inoculated with 100 µl of the adjusted bacterial suspensions. All the experiments were prepared by triplicate. After 24 hours, the bacterial growth was assessed in terms of turbidity that was measured at 600 nm using a plate spectrophotometer (BioTek Synergy™ HT, Vermont USA) . Wells

containing the broth medium only were used as a negative control to examine the equipment and the medium sterility. And some wells containing the broth growing medium and bacteria were used as a positive control to test the growing ability of the medium. MIC was defined as the lowest concentration of the antimicrobial agent that inhibited the bacterial growth (154).

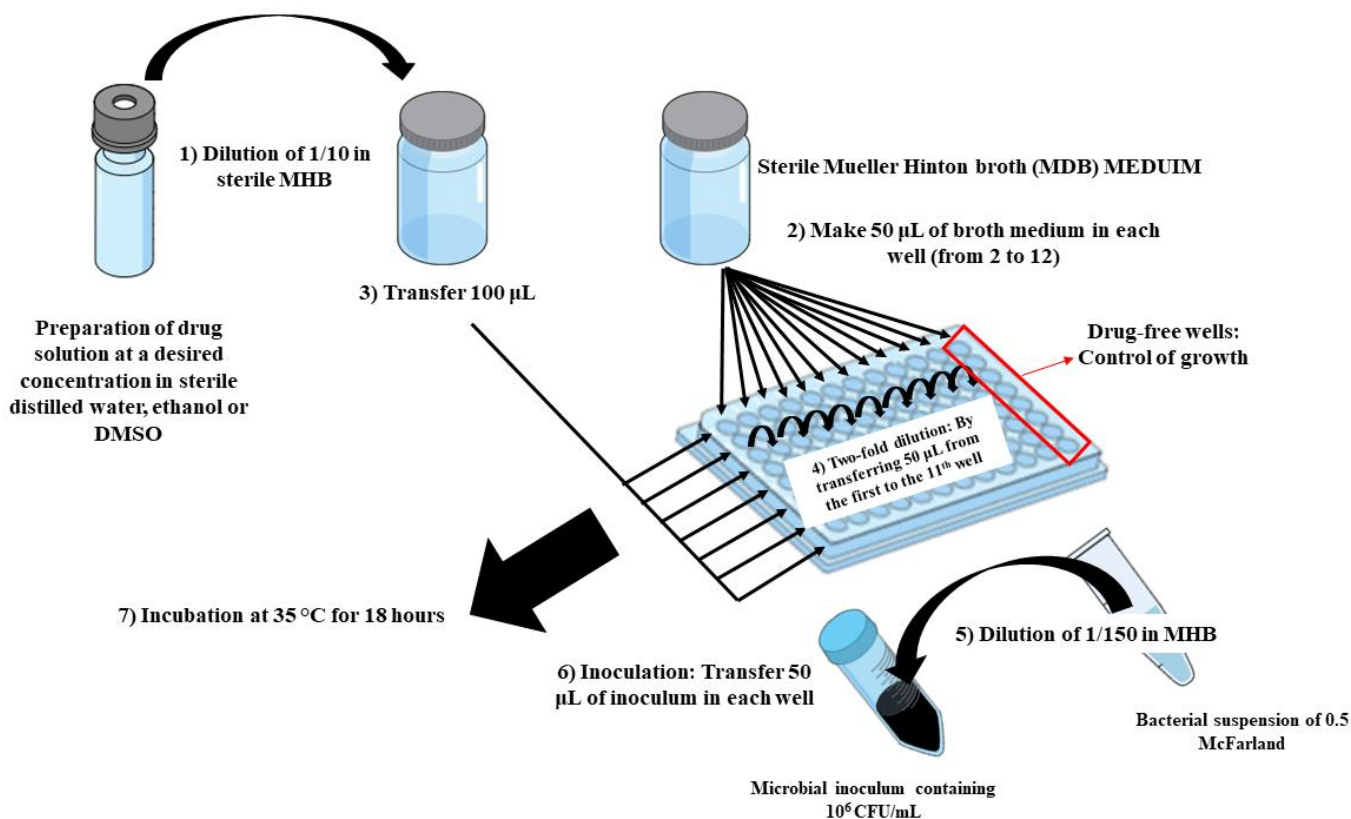


Figure 16 Scheme showing broth microdilution for antibacterial testing as recommended by CLSI protocol.

6.16 *In vitro* inflammatory response assessment of the Clobetasol Propionate/PLGA nanoparticles

6.16.1 Cytotoxicity assays: cell morphology and metabolic activity using alamarBlue®

The cytotoxicity of the Clobetasol Propionate/PLGA NPs was using *in vitro* cell culture of macrophages, in which cell morphology and metabolic activity were assessed using alamarBlue® (Invitrogen, USA). As it has been formerly explained (160,161), human derived leukemic monocyte cells (THP-1, ATCC, USA) were grown in RPMI-1640 supplemented with 10 % foetal bovine serum (FBS), 1 % penicillin/streptomycin. Cells were seeded onto collagen films at a density of 26×10^3 cells per cm^2 . Mature macrophage-like state was induced by treating cells with phorbol 12-myristate 13-acetate (PMA) at 100 ng/ml for 6 hours. Subsequently, plastic adherent cells were washed with HBSS and incubated with supplemented media at 37 °C, 5 % CO₂ and 95 % humidified air for 24 and 48 hours. Clobetasol Propionate/PLGA NPs (1 mg/ml, 0.5 mg/ml, 0.2 mg/ml, 0.1 mg/ml, 0.05 mg/ml, 0.02 mg/ml and 0.01 mg/ml) were placed into each well of 24-well plates. Activated control was induced with 100 ng/ml of lipopolysaccharide (LPS) in supplemented media. Macrophage morphology analysis was performed using phase contrast microscopy. Cell metabolic activity was measured by 2 hours incubation at 37 °C with 10 % alamarBlue® (Invitrogen, USA) following manufacturer's instructions. Cell metabolic activity was expressed in terms of reduction of alamarBlue®, considering metabolic activity of cells in tissue culture plastic (TCP) at each time point as 100 %.

6.16.2 Enzyme-linked immunosorbent assays

Enzyme-linked immunosorbent assays (ELISA) were used to evaluate the inflammatory cytokines release of the macrophages in response to the Clobetasol Propionate/PLGA NPs. In which two experiments were carried out, firstly the macrophages response was tested after getting exposed to different concentrations of the Clobetasol Propionate/PLGA NPs (1 mg/ml,

0.5 mg/ml, 0.2 mg/ml, 0.1 mg/ml, 0.05 mg/ml, 0.02 mg/ml and 0.01 mg/ml), additionally they were exposed to TCP and LPS as controls. Furthermore, another experiment was carried out in which macrophage were pretreated with LPS for 24 hours to induce an inflammatory condition; subsequently, LPS was removed, and the macrophages exposed to different concentrations of the Clobetasol Propionate/PLGA NPs (1 mg/ml, 0.5 mg/ml, 0.2 mg/ml, 0.1 mg/ml, 0.05 mg/ml, 0.02 mg/ml and 0.01 mg/ml). As control, we could determine the basal level with the positive control of TCP and the ultimate pro-inflammatory stimulus with LPS prem from the first experiment as a negative control. Invitrogen ELISA kits (Thermo Fisher, USA) measuring the release pro-inflammatory cytokines of IL-1 β and TNF- α were used for both experiments as per manufactures instructions. In brief, cell free supernatants of each sample and supplied standard curve were incubated on Invitrogen plates for 2 hours followed by a wash. Then, plates were incubated with detection antibody solution for 1 hour on a microplate shaker. The plates were then washed and read using BioTek Synergy™ HT instrument (Vermont, USA). Additionally, Mann-Whitney test was carried out to perform mean comparisons analysis in order to identify any significant differences between the groups.

RESULTS

RESULTS

7. RESULTS

7.1 Results of the Calcium Hydroxide/PLGA nanoparticles

7.1.1 Preformulation studies

All the experiments were prepared by triplicate. Different NPs batches were prepared using different concentrations of drug and surfactant (Table 3) before the development of the factorial design in order to confirm that the preparation method works and yields to consistent results regarding Z_{av} , PI and ZP of the NPs.

Table 3 Concentrations used for the prepared samples

Sample	Calcium hydroxide (mg/ml)	PLGA (mg/ml)	Lutrol (mg/ml)	pH
1	0.25	8	1.5	12
2	0.25	8	1.5	12
3	1.00	8	10	12

The aim of the optimized formulation was a Z_{av} of ≤ 250 nm, PI of ≤ 0.1 and ZP of ≈ -10 mV. The results of the samples were similar to the target ones as can be observed in Table 4. However, optimization of the formulation is still necessary to achieve suitable results.

Table 4 Physicochemical parameters of the preformulated samples

Sample	Average size (Z_{av}) (nm)	Polydispersity index (PI)	Zeta potential (ZP)
1	250.6 ± 1.41	0.083 ± 0.012	- 22.4 ± 0.05
2	116.5 ± 1.45	0.121 ± 0.020	- 19.1 ± 0.65
3	234.0 ± 2.19	0.061 ± 0.035	- 18.0 ± 0.25

7.1.2 Entrapment efficiency using ICP-OES

For the entrapment efficiency, inductively coupled plasma optical emission spectroscopy (ICP-OES) was utilized. $\text{Ca}(\text{OH})_2$ standards were prepared in a range of 0.2, 0.6, 1, 1.4 and 1.8 mg/ml plus, 1 % Nitric acid (HNO_3) was added for each standard. Since the concentration of $\text{Ca}(\text{OH})_2$ inside the standards is established, using the known molecular weight we were able to calculate the theoretical Calcium concentration (Table 5). This was divided by the Calcium concentration in the standards obtained in the method to determine the ratio. The mean ratio in this case was 0.753. This ratio was applied to the Calcium concentration obtained in the formulations analysed in order to apply this recovery ratio into the sample's calculation. Afterwards, calcium of the samples was converted to $\text{Ca}(\text{OH})_2$ again using the molecular weight. In this way, the method proved to be reproducible being able to measure efficiently $\text{Ca}(\text{OH})_2$ samples.

Table 5 Calculating the ratio of Calcium concentration

Standard number	Calcium hydroxide concentration (mg/ml)	Theoretical Calcium concentration (mg/ml)	Calcium ppm (mg/l)	Real Calcium (mg/ml)	Ratio
Std 1	0.2	1.064	1115	1.115	0.954
Std 2	0.6	3.382	4188	4.188	0.807
Std 3	1.0	5.393	7113	7.110	0.758
Std 4	1.4	8.143	12627	12.627	0.644
Std 5	1.8	9.937	15472	15.471	0.642

7.1.3 Design of experiments (DoE) approach

Design of experiments (DoE) approach was used to optimize the formulation. Thus, a central composite factorial design was applied, undertaking a total of 26 experiments. The studied experimental responses were the result of the individual influence and the interaction of the four independent variables which were the concentrations of Calcium hydroxide, PLGA and Lutrol, and also pH values. These interactions were studied and analyzed to assess their effect against the dependent variables of Z_{av} , PI, ZP and EE. Results of the factorial design can be observed in Table 6.

Table 6 Values of the matrix of a factorial design of concentration parameters and measured response.

Formula	Calcium hydroxide		PLGA		Lutrol		pH		Z _{av} (nm)	PI	ZP (mV)	EE %
	Coded level	mg/ml	Coded level	mg/ml	Coded level	mg/ml	Coded level	Level				
F1	+2	1.8	0	8.5	0	10	0	11	199.9 ± 1.35	0.174 ± 0.021	-6.41 ± 0.10	24.98
F2	+1	1.4	-1	7	+1	12	-1	9	180.2 ± 0.55	0.132 ± 0.006	-6.90 ± 0.14	20.34
F3	-1	0.6	+1	10	-1	8	-1	9	186.0 ± 1.70	0.088 ± 0.009	-10.90 ± 0.25	23.41
F4	+1	1.4	+1	10	+1	12	-1	9	181.9 ± 0.95	0.083 ± 0.014	-7.36 ± 0.17	24.05
F5	-1	0.6	+1	10	+1	12	-1	9	188.2 ± 0.90	0.078 ± 0.020	-9.92 ± 0.39	23.63
F6	+1	1.4	+1	10	-1	8	+1	13	151.4 ± 1.83	0.140 ± 0.022	-4.71 ± 0.17	32.16
F7	-1	0.6	-1	7	+1	12	-1	9	165.4 ± 1.55	0.095 ± 0.016	-10.5 ± 0.00	18.58
F8	-1	0.6	-1	7	+1	12	+1	13	141.8 ± 1.71	0.131 ± 0.018	-6.74 ± 0.14	19.06
F9	0	1	-2	5.5	0	10	0	11	157.5 ± 0.32	0.077 ± 0.016	-8.11 ± 0.04	17.14
F10	+1	1.4	-1	7	+1	12	+1	13	3063 ± 392.7	0.590 ± 0.400	-7.01 ± 1.11	20.03
F11	-1	0.6	-1	7	-1	8	-1	9	165.4 ± 0.87	0.098 ± 0.009	-11.2 ± 0.41	22.94
F12	0	1	+2	11.5	+1	10	0	11	190.2 ± 1.57	0.096 ± 0.013	-10.2 ± 0.31	30.94
F13	+1	1.4	-1	7	-1	8	-1	9	205.0 ± 1.71	0.224 ± 0.014	-7.22 ± 0.11	28.21
F14	-1	0.6	+1	10	-1	8	+1	13	150.1 ± 1.36	0.108 ± 0.019	-8.48 ± 0.41	31.65
F15	-2	0.2	0	8.5	0	10	0	11	173.3 ± 1.47	0.094 ± 0.027	-16.3 ± 0.37	90.84
F16	+1	1.4	-1	7	-1	8	+1	13	3699 ± 3685	0.916 ± 0.145	-3.02 ± 0.53	30.36
F17	0	1	0	8.5	0	10	0	11	167.7 ± 0.55	0.072 ± 0.016	-22.2 ± 1.42	9.39
F18	0	1	0	8.5	0	10	0	11	169.7 ± 1.86	0.078 ± 0.013	-20.0 ± 0.08	36.01
F19	+1	1.4	+1	10	-1	8	-1	9	183.9 ± 2.31	0.112 ± 0.026	-11.4 ± 0.25	33.06
F20	-1	0.6	+1	10	+1	12	+1	13	144.9 ± 1.51	0.115 ± 0.021	-11.0 ± 0.28	27.51
F21	0	1	0	8.5	+2	14	0	11	178.7 ± 1.50	0.081 ± 0.011	-11.7 ± 0.05	96.21
F22	-1	0.6	-1	7	-1	8	+1	13	The count rate is too low for the measurement		-4.34 ± 0.19	40.52
F23	+1	1.4	+1	10	+1	12	+1	13	158.4 ± 1.97	0.167 ± 0.012	-5.60 ± 0.19	36.49
F24	0	1	0	8.5	-2	6	0	11	184.1 ± 1.02	0.098 ± 0.021	-10.8 ± 0.10	28.16
F25	0	1	0	8.5	0	10	+2	15	430.2 ± 48.61	0.458 ± 0.066	-4.85 ± 1.43	92.74
F26	0	1	0	8.5	0	10	-2	7	178.6 ± 1.71	0.097 ± 0.013	-14.5 ± 0.83	35.99

7.1.3.1 Independent variables analysis

7.1.3.1.1 Calcium hydroxide concentration

Examining the pareto's chart, it was noted the concentration of Ca(OH)_2 only had a significant effect on the PI values ($P < 0.05$). In which the increase in the concentration of Ca(OH)_2 resulted in higher PI values (Figure 17). Furthermore, analyzing the surface response diagrams the trends followed when modifying this parameter were found out. It was noted that when Lutrol concentration is fixed at 11 mg/ml and pH value is fixed at 12, the percentage of EE was proportional to the concentration of Ca(OH)_2 regardless of the PLGA concentration. The EE percentage increased around 90 % when maintaining a high concentration of Ca(OH)_2 of 1.8 mg/ml (Figure 18). Also, it was noted that when the Lutrol concentration is fixed at 11 mg/ml and the pH value is fixed at 12, the Z_{av} will increase significantly when maintaining a low PLGA concentration of up to 7 mg/ml regardless of the Ca(OH)_2 concentration (Figure 18). Finally, it was observed that when the Lutrol concentration is fixed at 11 mg/ml and the pH value is fixed at 12 the PI will increase significantly when decreasing the PLGA concentration regardless of the concentration of Ca(OH)_2 (Figure 18). Attending the analysis to the influence of Ca(OH)_2 , high concentrations of Ca(OH)_2 will result in high EE percentages, with little effect on other parameters like Z_{av} and PI values.

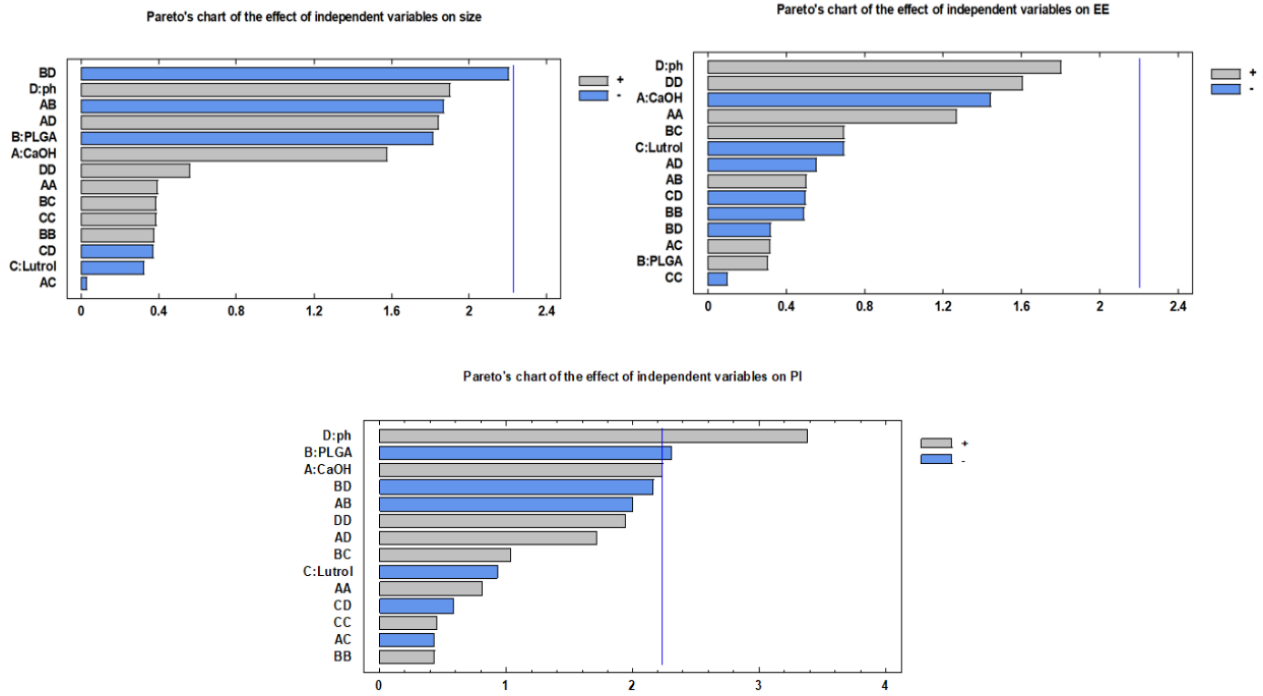


Figure 17 Pareto's charts of the effect of the independent variables.

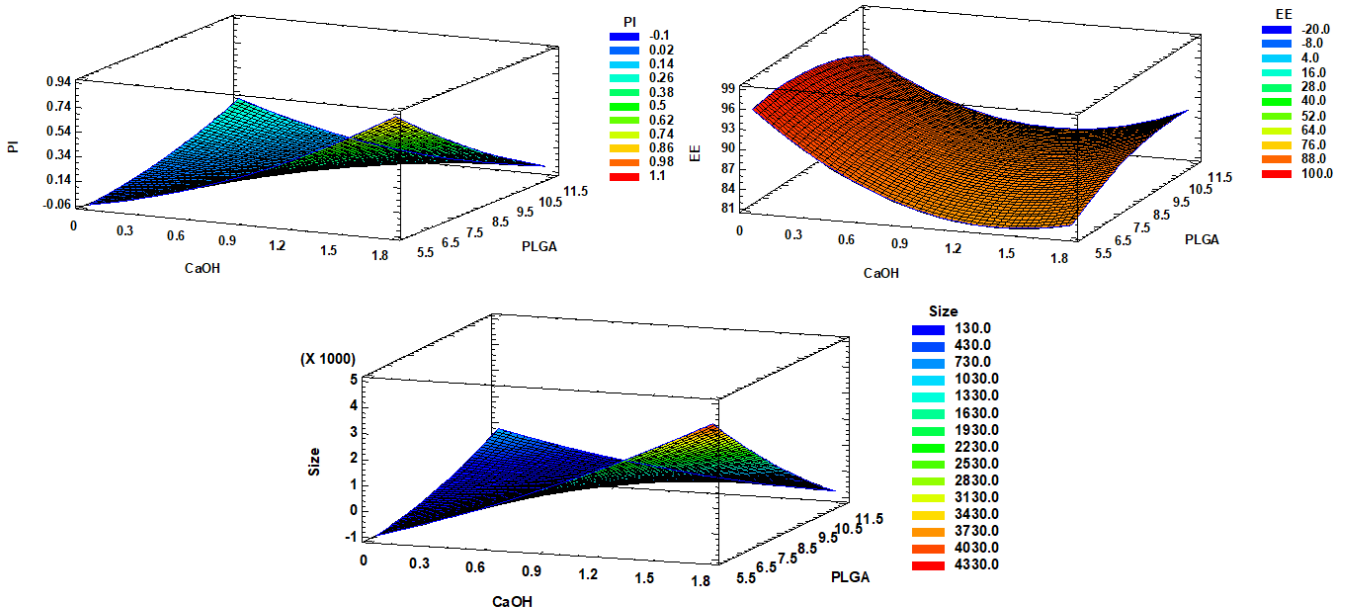


Figure 18 Surface response diagrams for Calcium hydroxide concentration.

7.1.3.1.2 PLGA concentration

Examining the pareto's chart, it was noted the concentration of PLGA only had a significant effect on the PI values ($P < 0.05$). In which the increase in the concentration of PLGA resulted in lower values of PI. (Figure 17). Furthermore, surface response diagrams were analyzed to examine any trends. It was noted that when Lutrol concentration is fixed at 11 mg/ml and Ca(OH)_2 concentration is fixed at 1.8 mg/ml, the percentage of EE is increased to around 90 % regardless of the PLGA concentration or pH value (Figure 19). Also, it was noted that when the Lutrol concentration is fixed at 11 mg/ml and Ca(OH)_2 concentration is fixed at 1.8 mg/ml, the Z_{av} will increase significantly when maintaining a low PLGA concentration of up to 7 mg/ml and it will decrease significantly when maintaining a high concentration PLGA of 11 mg/ml regardless of the pH value (Figure 19). Finally, it was noted that when the Lutrol concentration is fixed at 11 mg/ml and Ca(OH)_2 concentration is fixed at 1.8 mg/ml, the PI decreases significantly when maintaining a high concentration of PLGA of around 11 mg/ml and a pH value of around 11 – 12 (Figure 19). Attending the analysis to the influence of PLGA, high concentrations of PLGA will result in lower Z_{av} and PI values, with little effect on the EE percentages.

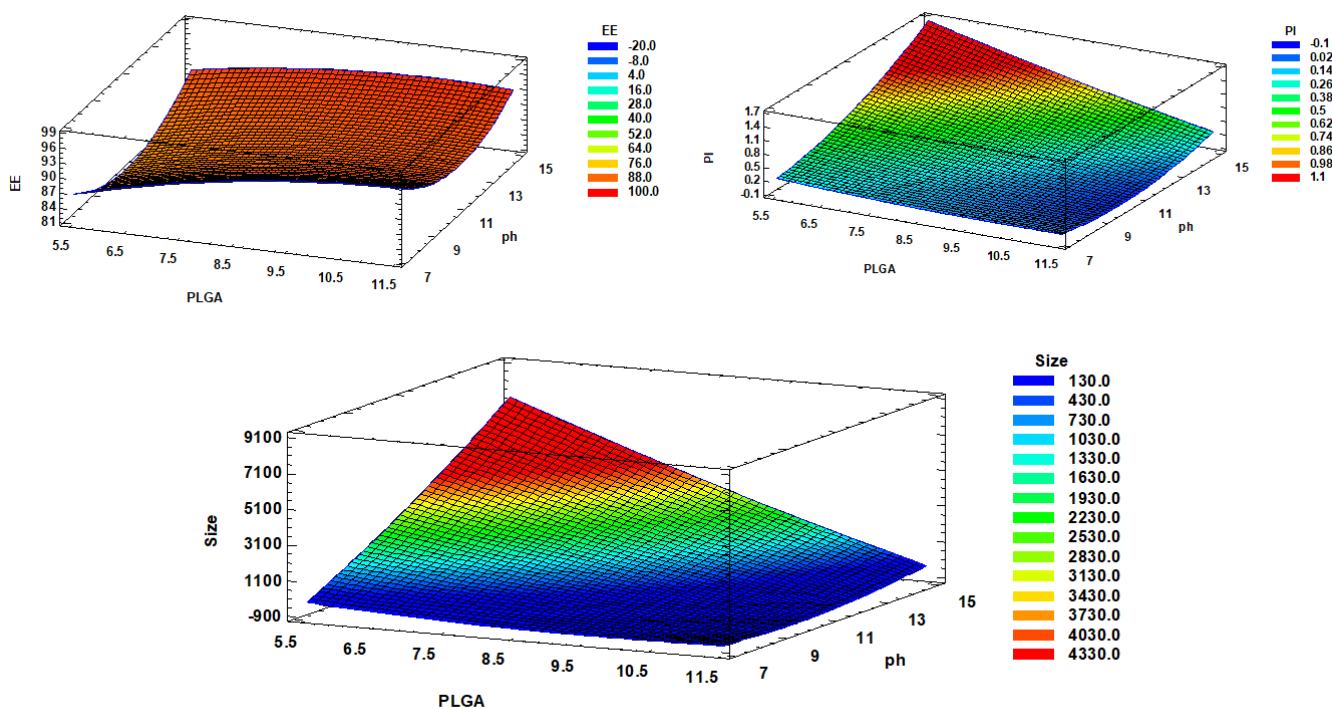


Figure 19 Surface response diagrams for PLGA concentration.

7.1.3.1.3 Lutrol concentration

Examining the pareto's chart, it was noted the concentration of Lutrol did not have a significant effect on any of the dependent variables (Figure 17). Furthermore, analyzing the surface response diagrams to examine any trends. It was noted that when PLGA concentration is fixed at 11.5 mg/ml and Ca(OH)₂ concentration is fixed at 1.8 mg/ml the EE percentage will be fixed at around 90 % regardless of the Lutrol concentration or the pH value (Figure 20). Also, it was noted that when the Ca(OH)₂ concentration is fixed at 1.8 mg/ml and the pH value is fixed at 11, the Z_{av} will increase significantly when maintaining a low PLGA concentration of up to 7 mg/ml regardless of the Lutrol concentration (Figure 20). Finally, it was noted that when the Ca(OH)₂ concentration is fixed at 1.8 mg/ml and the pH value is fixed at 11 the PI will increase significantly when decreasing the PLGA concentration regardless of the concentration of Lutrol (Figure 20). Attending the analysis to the influence of Lutrol, maintaining high concentrations seemed to have little influence on Z_{av}, PI values or EE percentages.

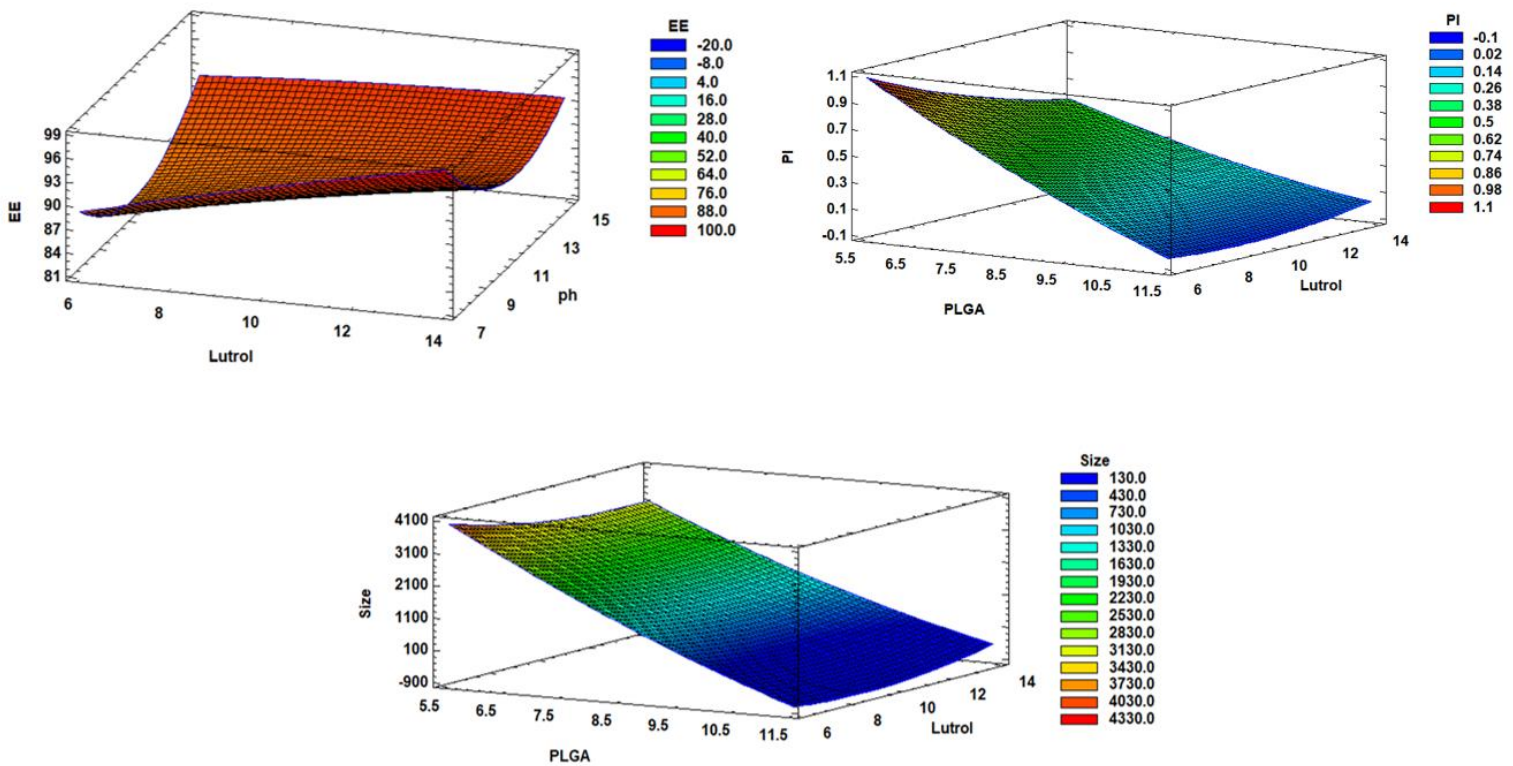


Figure 20 Surface response diagrams for Lutrol concentration.

7.1.3.1.4 pH value

Examining the pareto's chart, it was noted that the pH value only had a significant effect on the PI values ($P < 0.05$). In which higher basic pH levels resulted in higher values of PI (Figure 17). Furthermore, analyzing the surface response diagrams to examine any trends. It was noted that when PLGA concentration is fixed at 11.5 mg/ml and Ca(OH)_2 concentration is fixed at 1.8 mg/ml, the EE percentage will be fixed at around 90 % regardless of the Lutrol concentration or the pH value (Figure 21). Also, it was noted that when the PLGA concentration is fixed at 11.5 mg/ml and the Lutrol concentration if fixed at 11 mg/ml, the Z_{av} will decrease to the desired limit only when maintaining a high Ca(OH)_2 concentration of 1.5 mg/ml and upwards, regardless of the pH value (Figure 21). Finally, it was noted that when the PLGA concentration is fixed at 11.5 mg/ml and the Lutrol concentration if fixed at 11 mg/ml, the PI will increase significantly when decreasing the Ca(OH)_2 concentration regardless of the pH value (Figure 21). Attending the analysis to the influence of pH, maintaining high values seemed to have little influence on Z_{av} , PI values or EE percentages.

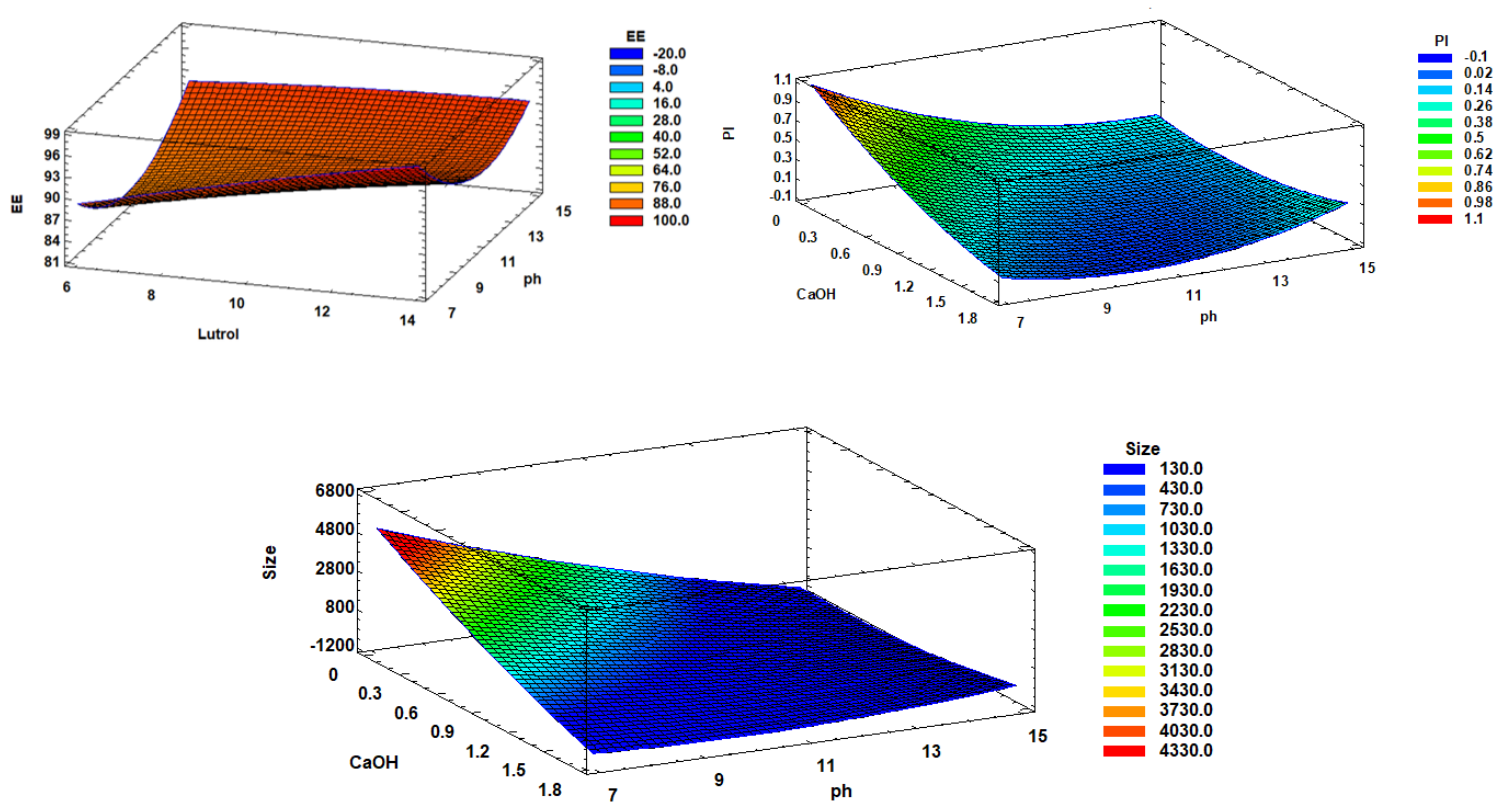


Figure 21 Surface response diagrams for pH values.

After analyzing all the surface response diagrams and examining all the possible trends and interactions. It was decided in order to achieve the desired characteristics of the NPs of a Z_{av} of ≤ 250 nm, PI of ≤ 0.1 , ZP ≈ -10 mV and EE as high as possible, we had to maintain a high Ca(OH)_2 and PLGA concentrations with maintaining a medium concentration of Lutrol and a pH value as high as possible. Accordingly, the optimal formulation should be as following, Ca(OH)_2 concentration of 1.7 mg/ml, PLGA concentration of 11.5 mg/ml, Lutrol concentration of 11 mg/ml and a pH value of 12.

7.1.4 Reproducibility of the optimized formulation

To confirm the reproducibility and effectiveness of the optimized formulation, three more samples were prepared according to the optimized formulation. Subsequently, the different dependent variables of Z_{av} , PI and ZP were assessed using Zetasizer Nano ZS (Malvern Instruments, Malvern, UK) after proper dilution of the sample as mentioned before. Finally, the EE of the samples were evaluated using the ICP-OES method and the beforementioned quantification method. All the results of these different variables are presented in Table 7. Samples were prepared by triplicate to confirm reproducibility. Additionally, the levels of pH of NPs were observed and measured for a duration of 1 week, in which the NPs were able to maintain their high basic pH retaining values in the range of 10 to 11 after 1 week.

Table 7 Physicochemical parameters of Ca(OH)_2 NPs optimized formulation

Sample	Calcium hydroxide (mg/ml)	PLGA (mg/ml)	Lutrol (mg/ml)	pH	Average size (Z_{av}) (nm)	Polydispersity index (PI)	Zeta potential (mV)	Entrapment efficiency (%)
1	1.7	11.5	11	12	168.2 ± 1.15	0.120 ± 0.003	-11.40 ± 0.17	30.53
2	1.7	11.5	11	12	165.2 ± 5.14	0.095 ± 0.062	-8.05 ± 0.04	24.62
3	1.7	11.5	11	12	169.5 ± 0.36	0.115 ± 0.008	-9.56 ± 0.35	30.94

7.1.5 Nanoparticles morphology studies

For the visualization of the NPs by negative staining followed by TEM (Figure 22) the images obtained revealed that the optimized NPs displayed a uniformly spherical shape without any signs of aggregation. Furthermore, the mean size of the NPs was similar to that acquired by the PCS (< 200 nm) (Figure 22b).

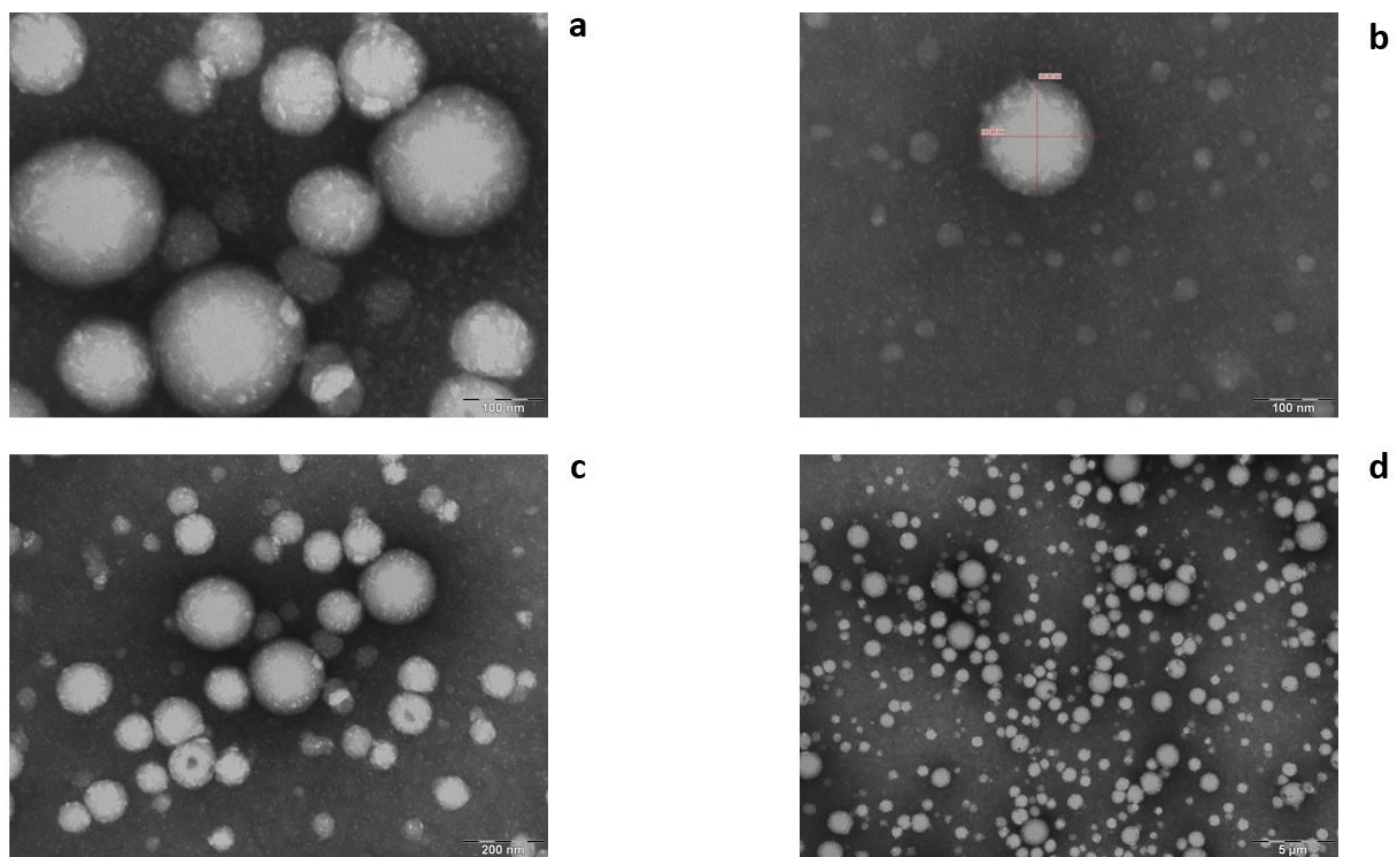


Figure 22 Transmission electron microscopy of Calcium hydroxide nanoparticles. (a) Visualization of the Calcium hydroxide nanoparticles at 100nm scale bar. (b) Measurement of the size of the Calcium hydroxide nanoparticle with dimensions of 141.91 nm X 143.85 nm at 100nm scale bar. (c) Visualization of the Calcium hydroxide nanoparticles at 200nm scale bar. (d) Visualization of the Calcium hydroxide nanoparticles at 5µm scale bar.

7.1.6 Nanoparticles characterization and interaction studies

Regarding the XRD (Figure 23) the powder free drug ($\text{Ca}(\text{OH})_2$) displayed a profile with sharp crystalline peaks at $2\theta = 18^\circ, 28^\circ, 34^\circ, 47^\circ$ and 50° , likewise the surfactant (Lutrol) displayed sharper crystalline peaks at $2\theta = 19^\circ$ and 22° . Moreover, the polymer (PLGA) displayed an amorphous profile. Both the drug loaded, and empty NPs ($\text{Ca}(\text{OH})_2$ NPs) displayed an amorphous profile with no sharp peaks correlating to the free drug were detected. This may indicate that the drug is completely encapsulated. However, broad peaks could be detected at $2\theta = 17^\circ - 24^\circ$ which can correspond to the interaction between the drug and the surfactant.

Examining the FTIR (Figure 24) to evaluate any possible interactions between the drug, polymer, and the surfactant, it was observed that no evidence of new strong bonds is displayed between them. The $\text{Ca}(\text{OH})_2$ powder displayed a solitary sharp peak at around 3640 cm^{-1} and a small peak at around 1545 cm^{-1} . Furthermore, the surfactant (Lutrol) displayed intense peaks at 1100 and 2880 cm^{-1} , whilst the polymer (PLGA) showed sharp peaks at 1090 and 1750 cm^{-1} and an intense band at 3300 cm^{-1} . Only the drug loaded $\text{Ca}(\text{OH})_2$ NPs displayed a small peak similar to the one obtained by free drug at around 1545 cm^{-1} . However, both the drug loaded, and empty NPs displayed peaks corresponding to the ones obtained by the polymer and the surfactant at around 1100 and 1750 cm^{-1} , plus an intense band at around 3300 cm^{-1} .

Evaluating the DSC profiles (Figure 25), we can notice that the surfactant (Lutrol) exhibited an endothermic peak corresponding to the melting transition at $54.76\text{ }^\circ\text{C}$, whilst the polymer (PLGA) exhibited a smaller peak at $53.01\text{ }^\circ\text{C}$. However, the pure powder free drug ($\text{Ca}(\text{OH})_2$) displayed an amorphous behaviour, which is in agreement with previous studies (162,163). Both the drug loaded, and empty NPs ($\text{Ca}(\text{OH})_2$ NPs) displayed an onset of glass transition temperature (T_g) at $48.39\text{ }^\circ\text{C} - 55.06\text{ }^\circ\text{C}$, which can be mainly attributed to the presence of the surfactant and polymer within the NPs. Additionally, the slight increase in the T_g with the drug loaded NPs from $48.39\text{ }^\circ\text{C}$ to $55.06\text{ }^\circ\text{C}$ compared to the empty NPs, can be attributed to the presence of $\text{Ca}(\text{OH})_2$ inside the NPs.

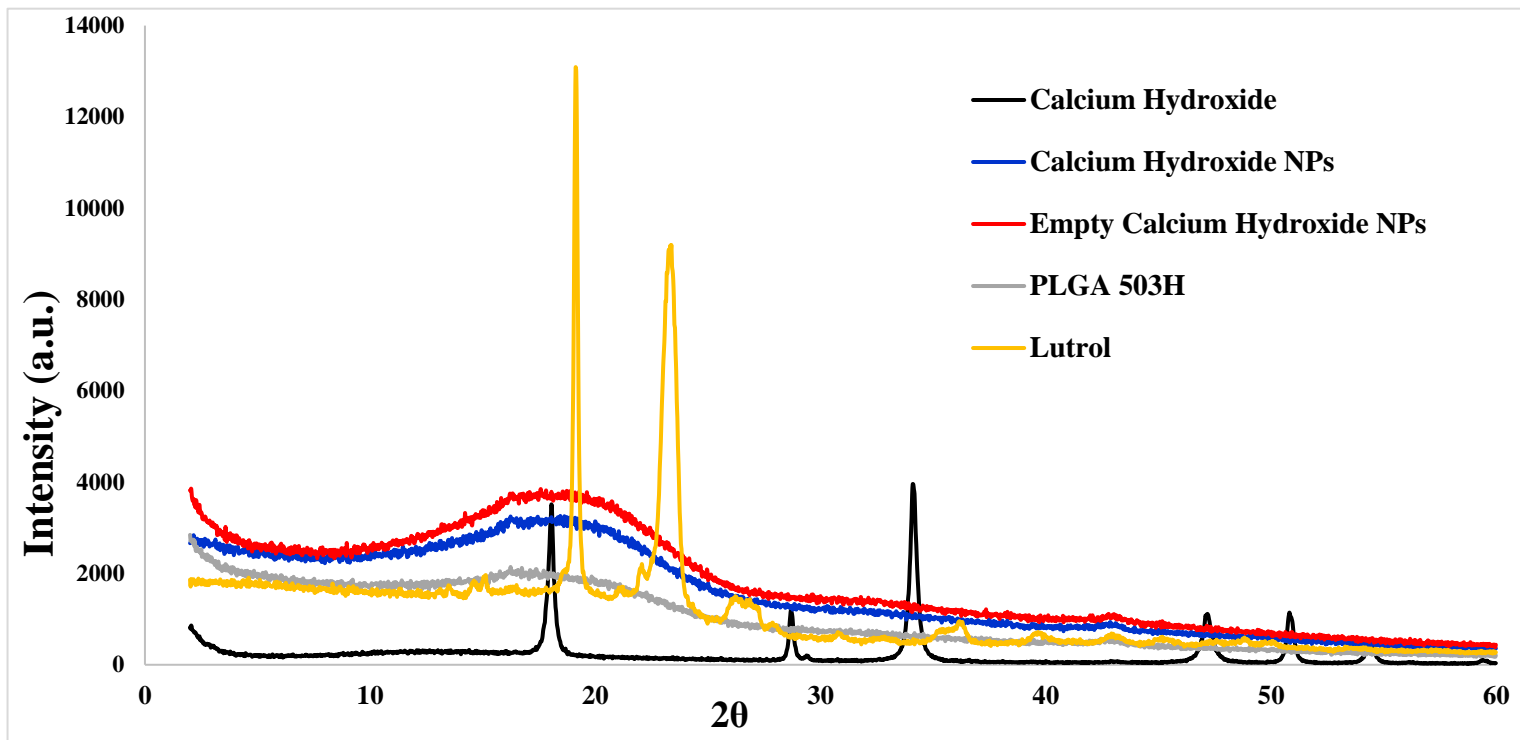


Figure 23 X-ray diffraction analysis of calcium hydroxide nanoparticles nanoparticles and free drug.

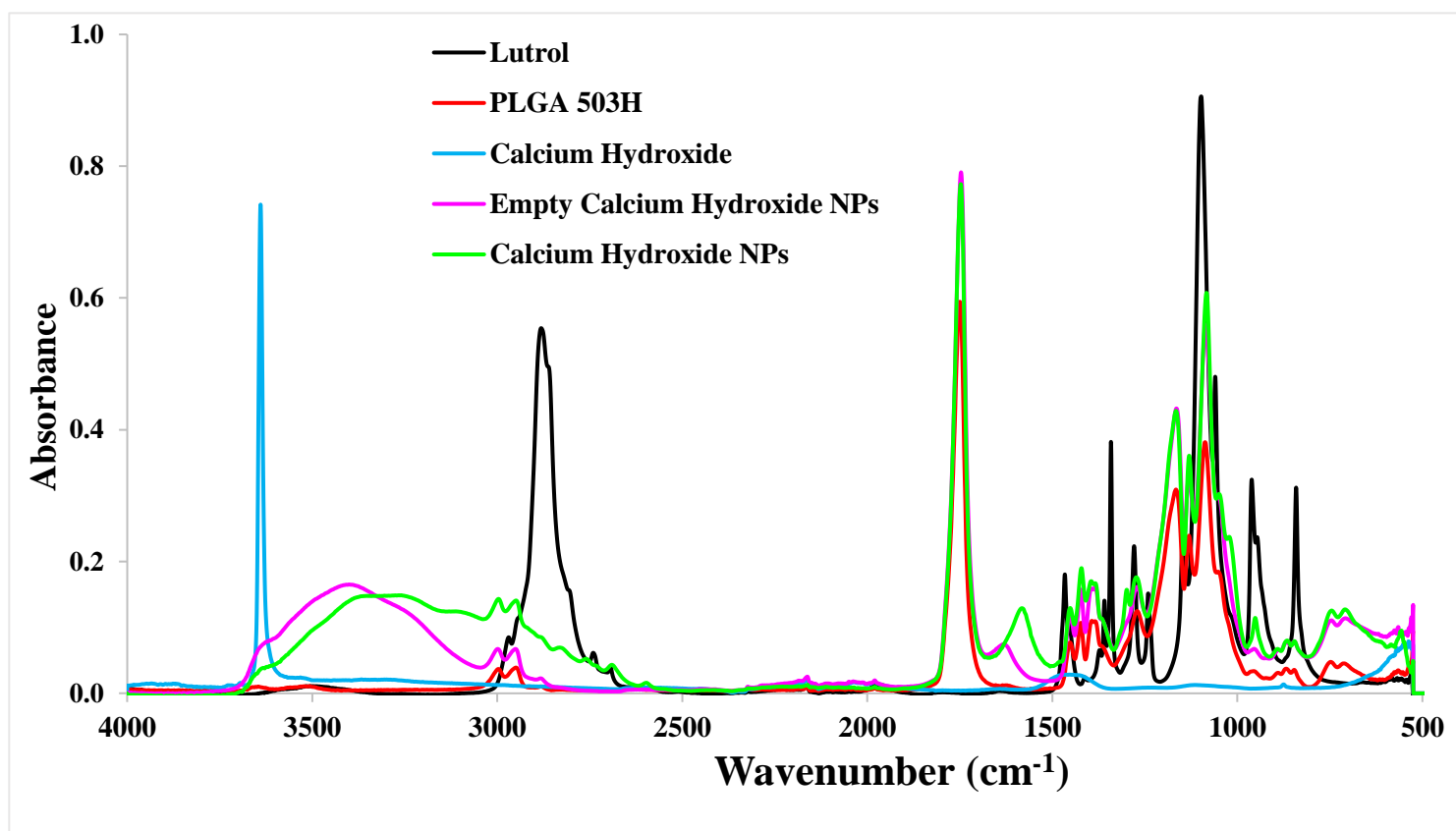


Figure 24 Fourier transformed infra-red analysis of calcium hydroxide nanoparticles nanoparticles and free drug.

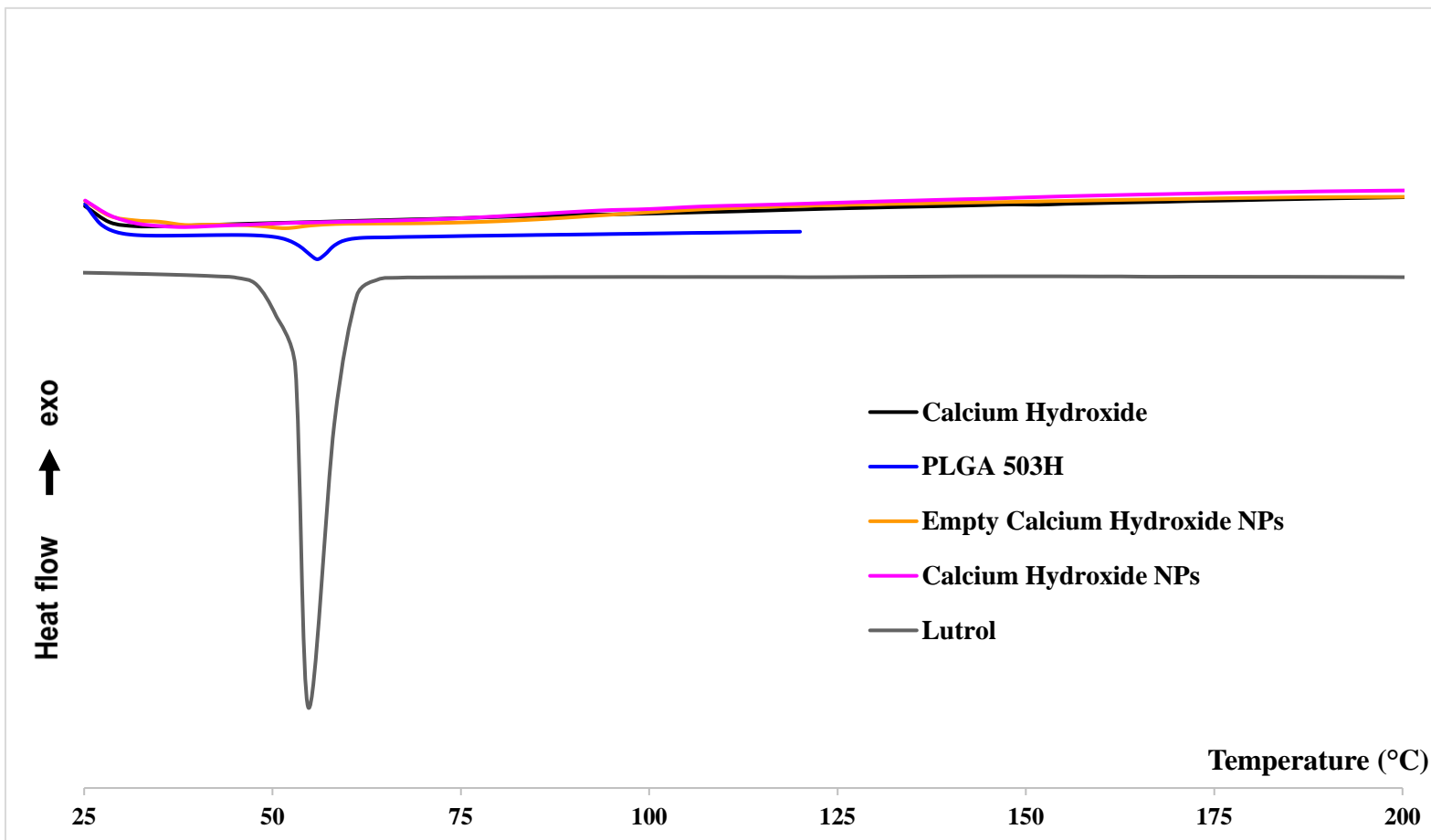


Figure 25 Differential scanning calorimetry analysis of calcium hydroxide nanoparticles nanoparticles and free drug.

7.1.7 Stability studies

Results of the short-term stability of the NPs are presented in table 8, in which the Z_{av} , PI and ZP were measured and assessed at two different temperatures (4 and 25 °C) once a month. Samples stored at 4 and 25 °C kept all their parameters Z_{av} , PI and ZP at the desired limits for 2 months. Additionally, after visual inspection, it was noted that samples stored at 4 and 25 °C remained visually unchanged during the first 2 months of storage.

Table 8 Physicochemical parameters of the samples stored at different temperatures

Temperature	4 °C			25 °C		
Parameter	Average size (Z_{av}) (nm)	Polydispersity index (PI)	Zeta potential (mV)	Average size (Z_{av}) (nm)	Polydispersity index (PI)	Zeta potential (mV)
Month 1	168.9 ± 1.34	0.083 ± 0.064	-8.45 ± 0.34	176.5 ± 1.06	0.115 ± 0.025	-8.34 ± 0.92
Month 2	173.8 ± 1.98	0.077 ± 0.037	-6.49 ± 0.20	121.4 ± 2.93	0.114 ± 0.010	-7.90 ± 0.77

7.1.8 In vitro drug release

The release profile of the free $\text{Ca}(\text{OH})_2$ was compared to that of the $\text{Ca}(\text{OH})_2$ NPs. The release profile was quantified by the cumulative released volume (Figure 26). Comparing the results after 12 hours (Figure 26a), we can see an initial burst effect of the $\text{Ca}(\text{OH})_2$ NPs, which can be attributed to fraction of drug being adsorbed on the surface of the PLGA NPs. Afterwards, the release profile of the NPs remained stable showing high concentrations. In comparison, the free drug exhibited a slight initial burst in the first 30 minutes and exhibited lower concentrations throughout the remaining observation period. After 48 hours (Figure 26b), we can observe that the $\text{Ca}(\text{OH})_2$ NPs were able to maintain a constant volume of drug released achieving a steady state with higher concentrations compared to the free $\text{Ca}(\text{OH})_2$. A slight drop in the concentration can be noticed after 48 hours, which can be attributed to $\text{Ca}(\text{OH})_2$ conversion into clinically inactive phosphate salts. Comparing the results of the one compartmental model, we can observe that the $\text{Ca}(\text{OH})_2$ NPs (Figure 26c), displayed a prolonged and steady release with higher concentrations resulting in a better degree of fit between the observed and the predicted concentrations compared to the free $\text{Ca}(\text{OH})_2$ (Figure 26d), which exhibited a linear and rapid release with lower concentrations. Furthermore, the maximum drug release (C_{\max}) was higher in $\text{Ca}(\text{OH})_2$ NPs (3518.6 $\mu\text{g}/\text{ml}$) than in the free $\text{Ca}(\text{OH})_2$ (843.7 $\mu\text{g}/\text{ml}$). Moreover, NPs release achieved during a longer period also, as the T_{\max} for the $\text{Ca}(\text{OH})_2$ NPs was (1.88 h) compared to

(0.43 h) with the free $\text{Ca}(\text{OH})_2$. Moreover, the $\text{Ca}(\text{OH})_2$ NPs displayed a lower absorption rate constant of ($K_a = 2.44 \text{ h}^{-1}$) compared to the free $\text{Ca}(\text{OH})_2$ ($K_a = 17.09 \text{ h}^{-1}$).

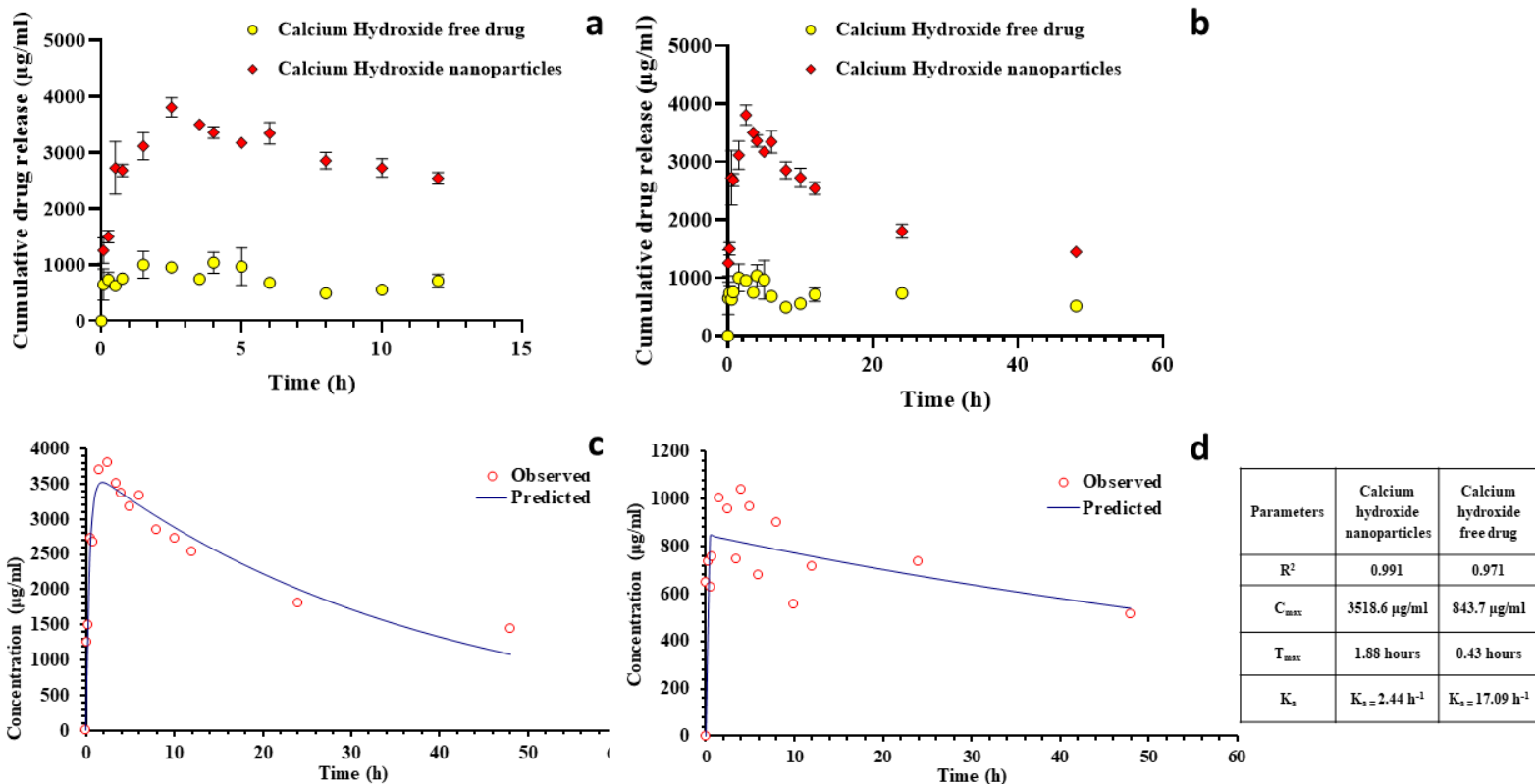


Figure 26 Drug release profile of the calcium hydroxide nanoparticles and the free calcium hydroxide. (a) Cumulative drug release of the calcium hydroxide nanoparticles and the free calcium hydroxide after the first 12 hours. (b) Cumulative drug release of the calcium hydroxide nanoparticles and the free calcium hydroxide after the 48 hours. (c) Drug release of the calcium hydroxide nanoparticles after 48 hours fitted to a one-compartmental model (blue line). (d) Drug release of the free calcium hydroxide after 48 hours fitted to a one-compartmental model (blue line).

7.1.9 Freeze dry of the nanoparticles

Different conditions were tested to determine the most suitable and fitting cryoprotectants for the NPs. A combination of different amount of cryoprotectants were added at different concentrations, these included Polyethylene glycol 3350, D-mannitol, and (2-Hydroxypropyl)- β -cyclodextrin. Ultimately, 18 different combinations of were tested (Table 9). Additionally, to increase the concentration of Ca(OH)_2 and enhance the antibacterial capacity of the Ca(OH)_2 /PLGA NPs obtaining a first burst effect, an extra additional amount of Ca(OH)_2 (0.6 mg/ml) was added to all these combinations. This resulted in increasing the overall concentration of Ca(OH)_2 to 2.3 mg/ml, as 1.7 mg/ml was encapsulated, and 0.6 mg/ml were added to outer layer with the cryoprotectants. All the formulations were tested at the same conditions (Table 1) utilizing the laboratory freeze dryer Lyomicron: Cylindric chamber configuration (Coolvacuum Technologies, Spain).

The NPs appearance after freeze drying procedure was observed (164) and documented (Table 9). When possible, samples were resuspended, by adding 1.5 ml of Milli-Q water and the sample was vortexed, after 1 hour the measurements for the NPs physicochemical parameters were performed. Out of the 18 formulations tested, the combination of 5 % of (2-Hydroxypropyl)- β -cyclodextrin and 15 % D-mannitol gave rise to the most stable outcome and the best appearance after freeze drying (Figure 27). Using this combination of the cryoprotectants, the NPs were able to keep all their parameters Z_{av} , PI, ZP and EE at the desired limits (Table 9). The experiment was repeated in sextuplicate by placing the formulations in different sections of the freeze dryer using the same conditions with all the results presented in table 10.

Table 9 Cryoprotectants assessed and physicochemical parameters of the resuspended freeze dried calcium hydroxide nanoparticles (HP β CD; (2-Hydroxypropyl)- β -cyclodextrin, PEG; Polyethylene glycol 3350).

% of Cryoprotects	Appearance after freeze drying	Average size (Z_{av}) (nm)	Polydispersity index (PI)	Zeta potential (mV)	Entrapment efficiency (%)
5% HP β CD	Broken cake	Unable to resuspend			
2.5% HP β CD	Lifted cake				
5% HP β CD + 15% Mannitol	Good cake	194.9 \pm 1.04	0.118 \pm 0.006	-9.75 \pm 0.36	22.86
5% HP β CD + 5% Mannitol	Lifted cake	Unable to resuspend			
5% HP β CD + 2.5% Mannitol	Collapsed cake				
15% Mannitol	Good cake with slight cracks	242.9 \pm 7.03	0.271 \pm 0.010	-1.34 \pm 0.93	-
5% Mannitol	Collapsed cake with skin formation	Unable to resuspend			
2.5% Mannitol	Lifted cake				
5% PEG	Boiled up				
15% PEG	Boiled up				
25% PEG	Boiled up				
5% PEG + 2.5% HP β CD	Broken cake with chipping				
5% PEG + 5% HP β CD	Collapsed cake				
15% PEG + 2.5% HP β CD	Collapsed cake with boiling				
15% PEG + 5% HP β CD	Broken cake with dusting				
25% PEG + 2.5% HP β CD	Broken cake with skin formation				
25% PEG + 5% HP β CD	Collapsed cake				
15% PEG + 15% Mannitol	Good cake with dusting and fog				

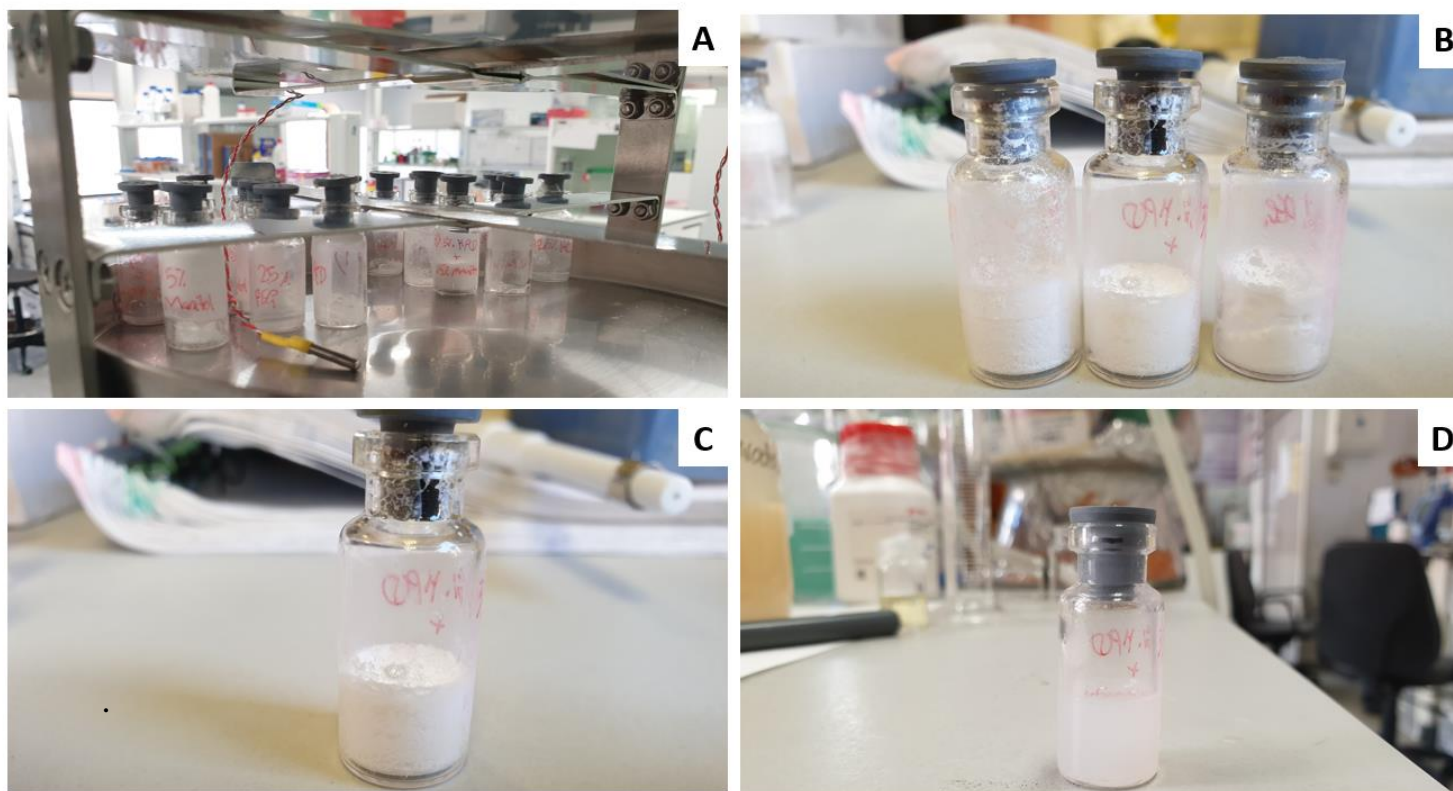


Figure 27 Freeze drying of the nanoparticles. (A) Combinations of cryoprotectants tested. (B) Potential suitable combination. (C) Combination of 5% of (2-Hydroxypropyl)- β -cyclodextrin and 15% D-mannitol before resuspension. (D) Combination of 5% of (2-Hydroxypropyl)- β -cyclodextrin and 15% D-mannitol after resuspension.

Table 10 Physicochemical parameters of the formulation with 5% HP β CD + 15% Mannitol repeated in sextuplicate HP β CD; (2-Hydroxypropyl)- β -cyclodextrin).

Sample	Average size (Z_{av}) (nm)	Polydispersity index (PI)	Zeta potential (mV)	Entrapment efficiency (%)
01	173.1 ± 1.70	0.088 ± 0.013	-7.25 ± 1.23	20.44
02	162.9 ± 0.46	0.107 ± 0.019	-10.32 ± 0.98	26.56
03	160.9 ± 0.77	0.126 ± 0.009	-8.87 ± 0.06	21.95
04	154.7 ± 1.55	0.127 ± 0.013	-7.54 ± 0.67	24.77
05	163.2 ± 0.49	0.129 ± 0.021	-9.56 ± 0.04	23.19
06	177.8 ± 0.62	0.092 ± 0.012	-10.78 ± 0.34	22.75

7.1.10 Sterilization assays

In order to determine if the sterilization process via γ radiation had any effect on the NPs, characteristics Z_{av} , PI, ZP and EE were evaluated before and after γ radiation. It was observed that there was no significant difference between before and after radiation (Table 11). And that it had no effect on the NPs features, in which they were all maintained within the desired limit of a Z_{av} of ≤ 200 nm, PI of ≤ 0.1 , ZP ≈ -10 mV and EE percentage as high as possible.

Table 11 Physicochemical parameters of the nanoparticles before and after sterilization via γ radiation

Sample	Average size (Z_{av}) (nm)	Polydispersity index (PI)	Zeta potential (ZP)	Entrapment efficiency (%)
Liquid sample before	185.3 ± 1.53	0.150 ± 0.018	-15.4 ± 0.28	22.07
Liquid sample after	175.2 ± 0.26	0.101 ± 0.013	-11.4 ± 0.17	23.58
Freeze dried sample before	164.9 ± 2.58	0.093 ± 0.014	-9.57 ± 1.23	26.98
Freeze dried sample after	196.9 ± 1.64	0.207 ± 0.012	-11.36 ± 0.23	25.14

7.1.11 Confocal laser scanning microscopy study

Both the rhodamine labelled $\text{Ca}(\text{OH})_2/\text{PLGA}$ NPs, and the free $\text{Ca}(\text{OH})_2$ mixed with rhodamine were examined under a Carl Zeiss LSM 880 spectral confocal microscope (Carl Zeiss AG, Germany) to measure the depth, area, percentage, MFI, and integrated density of the drug inside the dentinal tubules. The $\text{Ca}(\text{OH})_2/\text{PLGA}$ NPs displayed superior depth of penetration inside the dentinal tubules, even managing to reach the outer limits of the periphery of the root (Figure 28b & 29b) compared to their free drug counterpart, with a statistical significance difference ($p < 0.05$) and to the samples treated with the negative control of only sterile saline (Figure 30) (Table 12). Additionally, the $\text{Ca}(\text{OH})_2/\text{PLGA}$ NPs exhibited higher area of drug penetration and greater percentage of the total canal were covered compared to free $\text{Ca}(\text{OH})_2$, in which both were

statistically significant ($p < 0.05$). Furthermore, the $\text{Ca}(\text{OH})_2/\text{PLGA}$ NPs demonstrated higher MIF and integrated density numbers compared to the free drug which can indicate that a higher concentration of the NPs is present inside the tubules, even though only the integrated density was statistically significant ($p < 0.05$) (Table 12). This could be due to the fact that the integrated density measures the sum of the intensities of all the included pixels rather than taking the mean which can be misleading. Additionally, the MIF obtained in the negative control group (Table 12) that can indicate a presence of a constant intensity noise in the background regardless of the concentration of the drug.

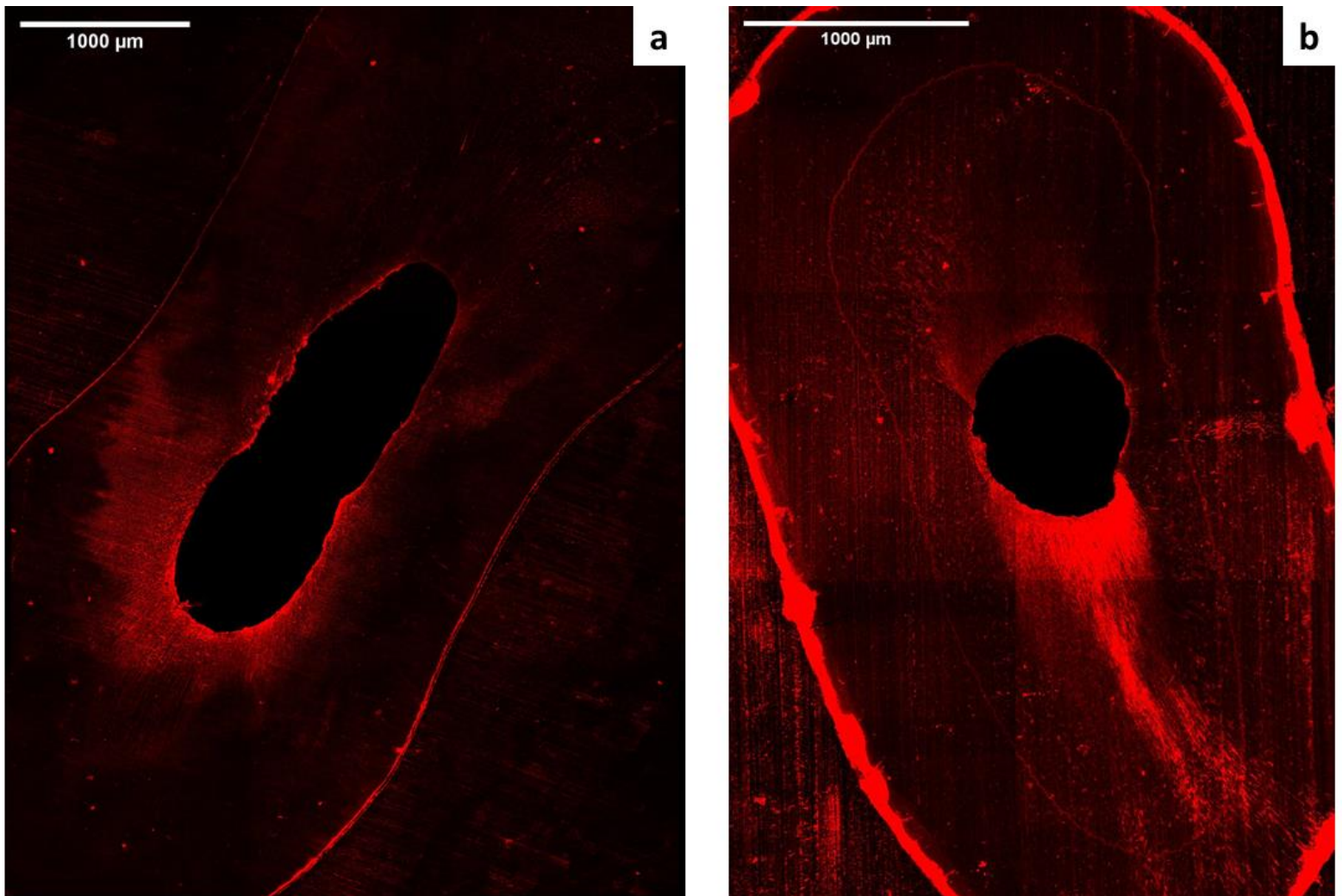


Figure 28 Depth of penetration of the nanoparticles and the free drug inside the dentinal tubules. (a) Depth of penetration of the free Calcium Hydroxide drug mixed with rhodamine inside the dentinal tubules. (b) Depth of penetration of the Calcium Hydroxide nanoparticles labelled with rhodamine inside the dentinal tubules.

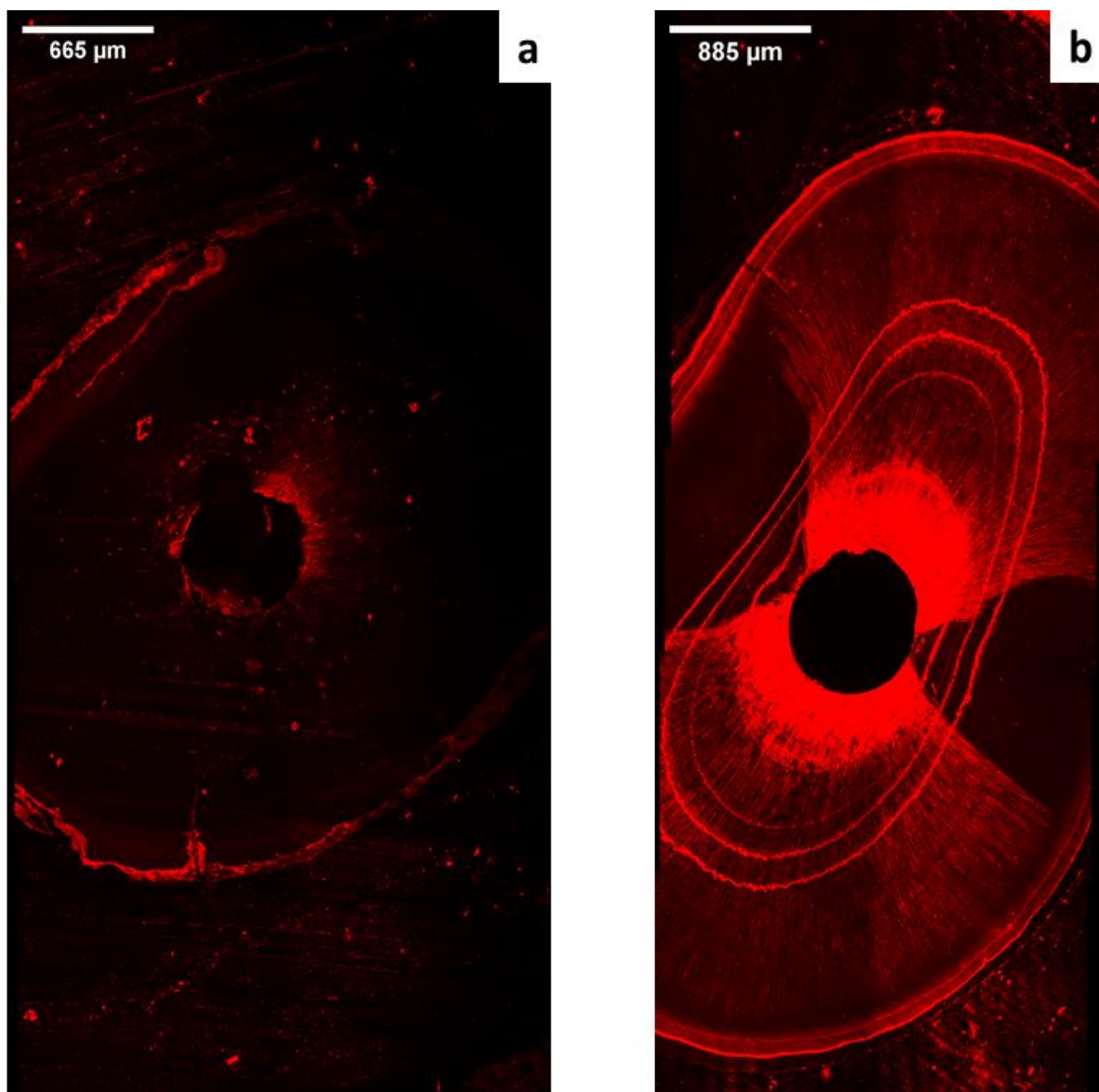


Figure 29 Depth of penetration of the nanoparticles and the free drug inside the dentinal tubules. (a) Depth of penetration of the free Calcium Hydroxide drug mixed with rhodamine inside the dentinal tubules. (b) Depth of penetration of the Calcium Hydroxide nanoparticles labelled with rhodamine inside the dentinal tubules.

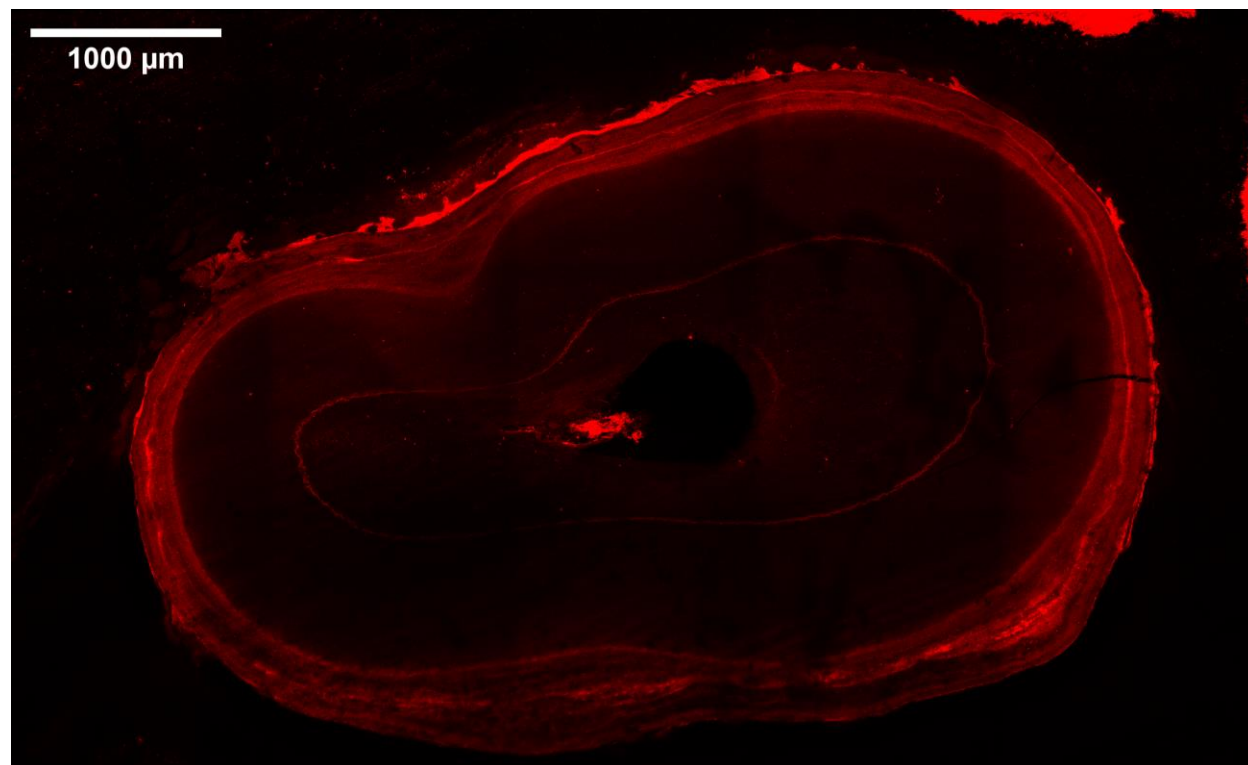


Figure 30 Confocal image of a control sample treated only with sterile saline.

Table 12 Comparison of the confocal results between the free drug and the calcium hydroxide nanoparticles.

Group	Parameter	Area (μm^2)	Penetration depth (μm)	Mean fluorescence intensity	Integrated density	Percentage (%)
Free calcium hydroxide drug (n=5)	Mean	1591533	728	23.06	47129594	15.12
	Minimum	622061	509	12.57	15103752	7.92
	Maximum	5095971	973	36.81	154139464	34.56
Calcium hydroxide nanoparticles (n=6)	Mean	4842195	1868	60.30	226667170	44.86
	Minimum	2986617	992	35.51	124171790	34.15
	Maximum	10002055	2611	179.00	355203532	77.25
Mann-Whitney U test (p value)		0.035	0.008	0.170	0.027	0.013
Sterile Saline (n=4)	Mean	-	-	47.10	512698479	-

7.1.12 Therapeutic efficacy: Antibacterial capacity

7.1.12.1 Agar diffusion test

After examination of the agar plates, it was noted that both Amoxicillin antibiotic 500 mg and Calcium Hydroxide (Ca(OH)₂/PLGA) NPs showed clear maximal zones of growth inhibition of *Porphyromonas gingivalis* bacterium around the filter papers (Figure 31). In comparison, there was minimal inhibition zones around both Calciur (VOCO, Germany) and Calcium hydroxide 98 % extra pure ACROS Organics™ (Fisher Scientific, USA) mixed with sterile saline. The negative control of BHI agar blank showed complete growth of the microorganism. Examining these results and the growth inhibition zones, the Ca(OH)₂ NPs displayed inhibition zones comparable to the ones obtained by the Amoxicillin antibiotic. However, due to the irregularity of the inhibition zones we were not able to measure the exact radius and hence statistical results were not possible to extract accurately. Nevertheless, just by examination under the naked eye it was evident that the inhibition zones produced by the Ca(OH)₂ NPs were far larger than those obtained by the Calciur (VOCO, Germany) which is the commercially used brand and Calcium hydroxide 98 % extra pure ACROS Organics™ (Fisher Scientific, USA) which the pure free drug. Even though, these are initial results, they are still very encouraging, and they demonstrate the antibacterial capacity of the Ca(OH)₂ NPs.

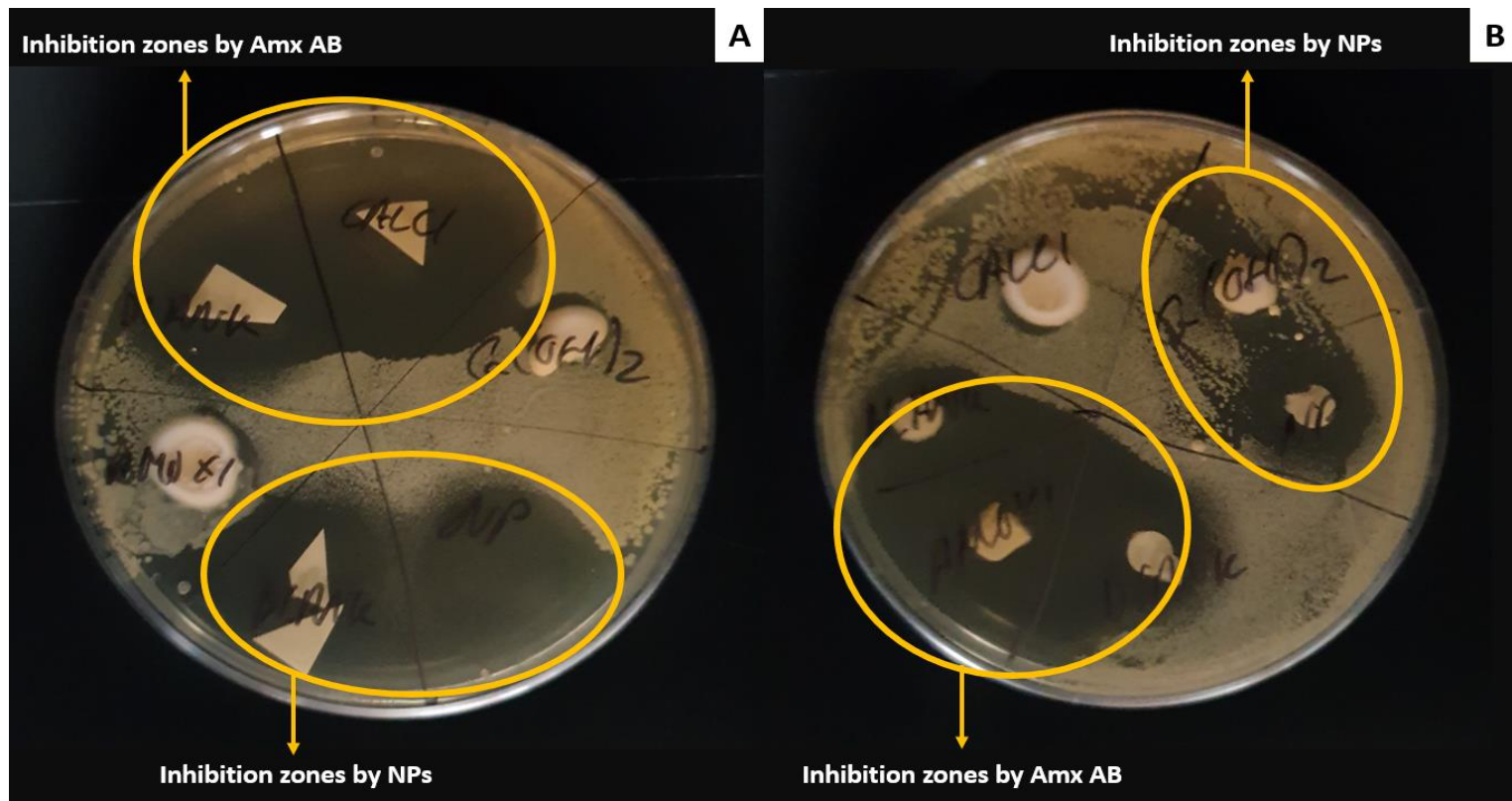


Figure 31 Two samples of agar plates harvesting *porphyromonas gingivalis* bacteria. (A) Agar plate displaying the growth inhibition zones around the Ca(OH)_2 NPs after incubation for 48 hours. (B) Agar plate displaying the growth inhibition zones around the Ca(OH)_2 NPs after incubation for 24 hours.

7.1.12.2 Minimal inhibitory concentration

After incubation for 24 hours, it was established that both the antibacterial $\text{Ca(OH)}_2/\text{PLGA}$ NPs and Calcium hydroxide 98 % extra pure ACROS Organics™ (Fisher Scientific, USA) mixed with Milli-Q water were able to inhibit the growth of the three bacterial strains *Porphyromonas gingivalis*, *Fusobacterium nucleatum* and *Enterococcus faecalis* at all the tested concentrations. Table 13 demonstrates the absorbance rates obtained after examining the sample using the spectrophotometer (BioTek Synergy™ HT, Vermont USA) at a wavelength of 600 nm. Analysing these absorbance rates indicates that all the tested samples displayed clear suspensions and no turbidity, which shows that there was no bacterial growth in those wells (154). However,

it is important to note, even though there were no statistically significant differences, the samples treated with the $\text{Ca(OH)}_2/\text{PLGA}$ NPs at the highest possible concentration (1:1 dilution) obtained the highest rates indicating less bacterial growth. Moreover, the ability of the $\text{Ca(OH)}_2/\text{PLGA}$ NPs to maintain their antibacterial capacity even at a dilution of 1:500 is very promising sign and further highlights its enhanced antibacterial proprieties.

Table 13 Absorbance rates observed using spectrophotometer in the samples after incubation for 24 hours.

Dilutions	1:1	1:2	1:5	1:10	1:20	1:50	1:100	1:200	1:500
Samples	Absorbance rate at 600nm								
NPs (PG) (1)	0.2273	0.1480	0.0965	0.0789	0.0758	0.0662	0.0590	0.0567	0.0528
NPs (PG) (2)	0.2101	0.1241	0.0973	0.0756	0.0694	0.0626	0.0522	0.0502	0.0505
NPs (PG) (3)	0.2034	0.1329	0.0985	0.0833	0.0730	0.0588	0.0530	0.0502	0.0503
Ca(OH)_2 (PG) (1)	0.0548	0.0536	0.0557	0.0524	0.0556	0.0549	0.0543	0.0528	0.0546
Ca(OH)_2 (PG) (2)	0.0587	0.0539	0.0516	0.0512	0.0534	0.0532	0.0500	0.0533	0.0518
Ca(OH)_2 (PG) (3)	0.0539	0.0468	0.0497	0.0486	0.0555	0.0512	0.0542	0.0522	0.0520
NPs (FN) (1)	0.2352	0.1583	0.1200	0.1051	0.1098	0.0804	0.0657	0.0541	0.0578
NPs (FN) (2)	0.1841	0.1308	0.0913	0.0838	0.0769	0.0682	0.0723	0.0614	0.0572
NPs (FN) (3)	0.1834	0.1163	0.0970	0.0800	0.0660	0.0588	0.0561	0.0614	0.0524
Ca(OH)_2 (FN) (1)	0.0532	0.0538	0.0605	0.0567	0.0583	0.0574	0.0523	0.0508	0.0544
Ca(OH)_2 (FN) (2)	0.0501	0.0693	0.0712	0.0666	0.0611	0.0584	0.0559	0.0526	0.0531
Ca(OH)_2 (FN) (3)	0.0509	0.0646	0.0607	0.0639	0.0581	0.0579	0.0566	0.0537	0.0556
NPs (EF) (1)	0.1077	0.0453	0.0526	0.0554	0.0529	0.0432	0.0444	0.0446	0.0416

NPs (EF) (2)	0.1003	0.0432	0.0502	0.0511	0.0488	0.0543	0.0476	0.0455	0.0435
NPs (EF) (3)	0.0639	0.0462	0.0462	0.0484	0.0481	0.0450	0.0458	0.0462	0.0447

NPs; Calcium Hydroxide nanoparticles, Ca(OH)₂; Free Calcium hydroxide drug. PG; Porphyromonas gingivalis, FN;

Fusobacterium nucleatum, EF; Enterococcus faecalis.

7.2 Results of the Clobetasol Propionate/PLGA nanoparticles

7.2.1 Preformulation studies

Z_{av} and PI of clobetasol propionate/PLGA NPs were determined by photon correlation spectroscopy (PCS) after a 1:10 dilution with a Zetasizer Nano ZS (Malvern Instruments, Malvern, UK) at 25 °C using disposable quartz cells and (Malvern Instruments). NPs surface charge, measured as ZP, was evaluated after a further dilution of the previous solution in 1000 μ l Milli-Q water and using laser-Doppler electrophoresis with M3 PALS system in Zetasizer Nano ZS. All the experiments were prepared by triplicate.

These measurements were performed on the clobetasol propionate/PLGA NPs prepared before the development of the factorial design in order to confirm that the preparation method works and yields to consistent results regarding Z_{av} , PI and ZP of the NPs. Target results were a Z_{av} of \leq 200 nm, PI of \leq 0.1 and ZP of \approx -25 mV. The results of the samples were all within the desired limit and are presented in Table 14.

Table 14 Physicochemical parameters of the preformulated samples

Sample	Average size (Z_{av}) (nm)	Polydispersity index (PI)	Zeta potential (ZP)
Sample 01	156.7 \pm 1.89	0.066 \pm 0.025	- 26.8 \pm 0.40
Sample 02	171.3 \pm 1.21	0.099 \pm 0.004	- 26.8 \pm 0.60
Sample 03	177.3 \pm 0.91	0.058 \pm 0.029	- 30.2 \pm 1.22

7.2.2 Entrapment efficiency measurement

7.2.2.1 Clobetasol propionate quantification method

Firstly as a clobetasol propionate standard solution was prepared for the development of an HPLC method for Clobetasol propionate measurement. In order to prepare the standard used, a 200 mL solution of 90:10 methanol:H₂O was firstly prepared and filtered using vacuum filtration. Then, a stock solution of clobetasol propionate of 1 mg/ml was elaborated. In order to do this, 10 mg of Clobetasol propionate were weighted directly in a 10 mL flask and dissolved with the previously prepared 90:10 methanol:H₂O solution. The flask was placed in an ultrasonic bath (Elma Digital Ultrasonic Cleaners[®]) until the drug was completely dissolved. The solution was then placed into a clean and dry vial and called STOCK 1; 1mg/ml Clobetasol propionate.

In order to facilitate the standard preparation, a STOCK 2 solution (0.5 mg/ml) was prepared from the previous one. In order to do this, a 2 mL flask was filled with 1 mL of the previous solution and the rest was filled with the previously prepared 90:10 methanol:H₂O solution up to 2 mL. The flask was then placed in an ultrasonic bath (Elma Digital Ultrasonic Cleaners[®]) in order to ensure complete dissolution. The solution was placed into a clean and dry vial. From these stocks, different standards preparations were carried out and their quantification was performed. Subsequently, the clobetasol quantification range was set from 1000 µg/ml until 0.25 µg/ml.

Clobetasol quantification method was confirmed to be reproducible obtaining a peak around 8 minutes (Figure 32) undertaking a chromatogram of 10 minutes.

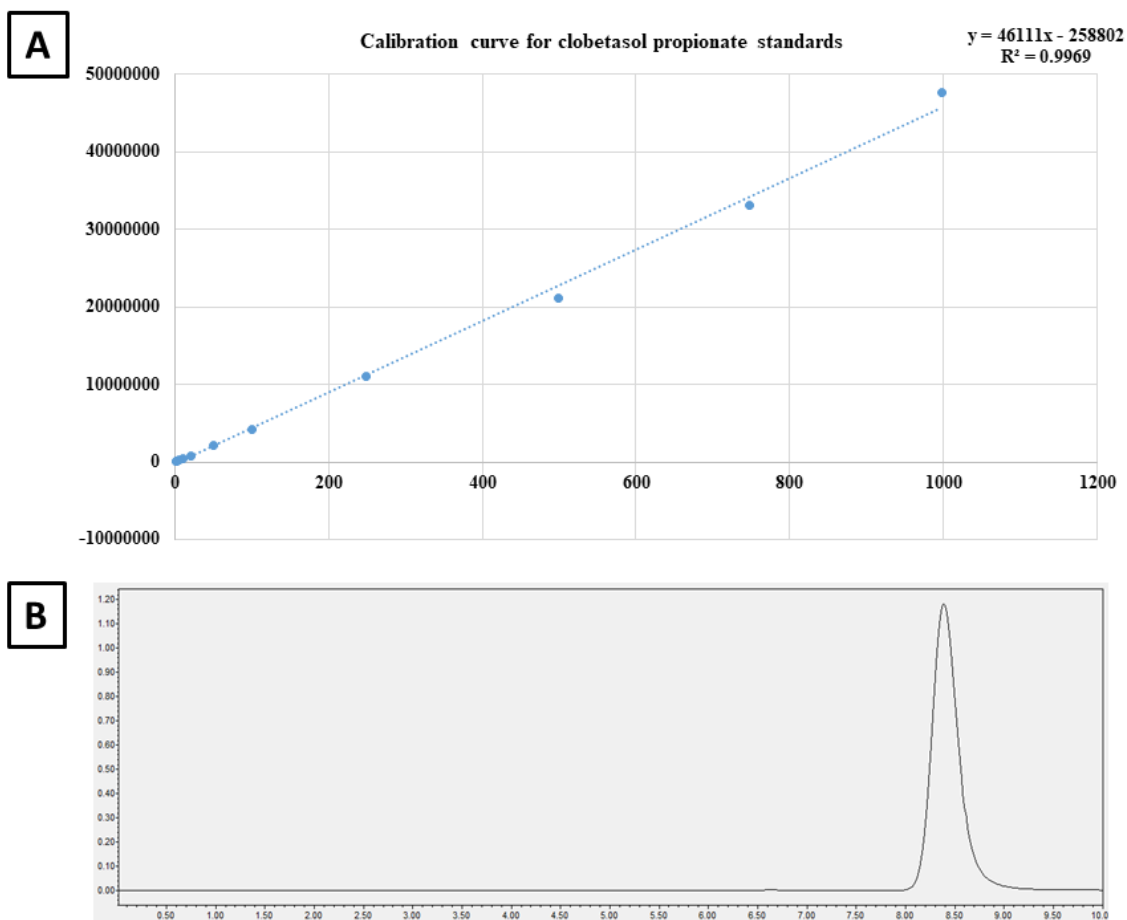


Figure 32 (A) Calibration curve for clobetasol propionate standards. (B) Peak achieved by clobetasol propionate standards.

7.2.2.2 Entrapment efficiency measurement using clobetasol quantification method

Regarding the EE preformulation studies (Table 15), examining the results, it was noticed that adding DMSO affected the quantification method obtaining incorrect peaks, hence it was discarded as a proper quantification method. Further examining the results, it was observed that diluting the NPs in 1:10 methanol presented the most trustworthy results of EE. Presenting the least amount of dilution that obtain the highest and consistent percentages of EE. Thus, it was selected as the proper quantification method using the HPLC.

Table 15 Results of different sample treatments for HPLC quantification **DMSO; Dimethyl sulfoxide, Meth; Methanol.**

Sample name	Sample area (mean)	Concentration (ug/ml)	Initial Concentration (ug/ml)	Undo dilution	Sample treatment	EE (%)
Pellet DMSO 1:2 Meth	19418200.84	415.50	1365	831.01	DIRECT EE	60.88
Supernatant 1:2 Meth	3985996.95	80.83	1365	161.66	INDIRECT EE	88.16
1:10 DMSO	31769528.17	683.36	1365	6833.67	The whole amount	-
1:10 DMSO / Meth	2775166.61	54.57	1365	5457.19	The whole amount	-
1:10 Meth	1125787.87	18.80	1365	188.02	INDIRECT EE	86.23
1:100 Meth	320073.76	1.32	1365	132.88	INDIRECT EE	90.27

7.2.3 Design of experiments (DoE) approach

Design of experiments (DoE) approach was used to optimize the formulation. Thus, a factorial design was applied, and a suitable formulation was obtained. According to the composite design matrix generated by Statgraphics Centurion XV software (StatPoint Technologies, Inc., Warrenton, VA, USA), a total of 26 experiments were required for the design. The studied experimental responses were the result of the individual influence and the interaction of the four independent variables which were the concentrations of Clobetasol, PLGA and Tween[®]80, and also pH values. These interactions were studied and analyzed to assess their effect against the dependent variables of Z_{av} , PI, ZP and EE. All the values of the matrix of the factorial design are presented in Table 16.

Table 16 Values of the matrix of a factorial design of concentration parameters and measured responses.

Formula	Clobetasol		PLGA		Tween®80		pH		Z _{av} (nm)	PI	ZP (mV)	EE (%)
	Coded level	mg/ml	Coded level	mg/ml	Coded level	mg/ml	Coded level	Level				
F1	0	1.5	-2	6.5	0	8.5	0	7.4	205.2 ± 4.59	0.113 ± 0.036	-28.5 ± 0.90	80.37
F2	0	1.5	0	8.5	0	8.5	-2	2.6	245.8 ± 1.02	0.150 ± 0.019	-22.9 ± 0.51	80.14
F3	-1	1	+1	9.5	+1	10	-1	5	174.3 ± 0.87	0.083 ± 0.012	-31.3 ± 0.20	70.62
F4	0	1.5	0	8.5	0	8.5	0	7.4	173.3 ± 1.55	0.068 ± 0.016	-38.4 ± 0.26	89.67
F5	+1	2	+1	9.5	-1	7	-1	5	162.0 ± 1.36	0.058 ± 0.007	-30.6 ± 0.20	93.28
F6	+1	2	+1	9.5	-1	7	+1	9.8	154.3 ± 1.85	0.077 ± 0.012	-36.6 ± 0.30	87.22
F7	0	1.5	0	8.5	+2	11.5	0	7.4	145.3 ± 1.04	0.098 ± 0.020	-31.8 ± 0.58	77.00
F8	+1	2	-1	7.5	-1	7	+1	9.8	155 ± 1.012	0.068 ± 0.013	-31.9 ± 0.40	91.64
F9	0	1.5	0	8.5	0	8.5	+2	12.2	112.9 ± 0.36	0.117 ± 0.013	-36.2 ± 1.52	87.46
F10	0	1.5	+2	10.5	0	8.5	0	7.4	159.7 ± 1.22	0.073 ± 0.002	-31.8 ± 0.74	85.04
F11	-1	1	+1	9.5	-1	7	+1	9.8	155.3 ± 0.40	0.081 ± 0.002	-33.8 ± 0.28	84.04
F12	+1	2	-1	7.5	+1	10	-1	5	157.2 ± 1.00	0.128 ± 0.012	-21.6 ± 0.66	88.64
F13	+1	2	+1	9.5	+1	10	-1	5	156.5 ± 0.52	0.097 ± 0.011	-30.0 ± 0.00	79.94
F14	+1	2	+1	9.5	+1	10	+1	9.8	140.1 ± 1.26	0.130 ± 0.002	-35.3 ± 0.60	96.82
F15	0	1.5	0	8.5	-2	5.5	0	7.4	146.4 ± 1.01	0.090 ± 0.008	-33.3 ± 1.07	88.21
F16	-1	1	-1	7.5	-1	7	+1	9.8	140.0 ± 1.45	0.109 ± 0.018	-35.7 ± 0.20	78.27
F17	-1	1	+1	9.5	-1	7	-1	5	158.6 ± 0.72	0.070 ± 0.020	-30.7 ± 0.35	67.76
F18	-1	1	-1	7.5	+1	10	+1	9.8	138.4 ± 0.75	0.112 ± 0.009	-36.4 ± 0.91	64.78
F19	-1	1	+1	9.5	+1	10	+1	9.8	137.7 ± 1.26	0.123 ± 0.013	-32.9 ± 0.72	82.05
F20	-2	0.5	0	8.5	0	8.5	0	7.4	148.7 ± 0.85	0.099 ± 0.010	-32.1 ± 1.37	15.91
F21	+1	2	-1	7.5	+1	10	+1	9.8	142.6 ± 1.13	0.102 ± 0.012	-35.3 ± 0.52	81.65
F22	+1	2	-1	7.5	-1	7	-1	5	147.1 ± 1.75	0.094 ± 0.019	-30.2 ± 0.15	89.70
F23	-1	1	-1	7.5	+1	10	-1	5	147.6 ± 0.66	0.091 ± 0.027	-27.3 ± 0.50	71.49
F24	+2	2.5	0	8.5	0	8.5	0	7.4	150.6 ± 1.18	0.097 ± 0.021	-33.0 ± 0.68	92.81
F25	-1	1	-1	7.5	-1	7	-1	5	151.1 ± 1.09	0.071 ± 0.030	-29.2 ± 0.50	69.22
F26	0	1.5	0	8.5	0	8.5	0	7.4	146.5 ± 0.45	0.120 ± 0.016	-33.6 ± 3.06	83.24

7.2.3.1 Independent variables analysis

7.2.3.1.1 Clobetasol propionate concentration

Examining the pareto's chart, it was noted the concentration of clobetasol had a significant effect on the EE percentages ($P < 0.05$). In these, the increase in the concentration of clobetasol causes an increase in the EE percentage (Figure 33). Furthermore, analyzing the surface response diagrams to examine any trends, it was noted that when PLGA concentration is fixed at 8.5 mg/ml and Tween[®]80 concentration is fixed at 8.5 mg/ml the EE percentage will increase gradually with the increase of the clobetasol concentration regardless of the pH value (Figure 34). Also, it was noted that when PLGA concentration is fixed at 8.5 mg/ml and Tween[®]80 concentration is fixed at 8.5 mg/ml, the Z_{av} will be maintained in the limit of 110-140 nm when maintaining a high value of pH of around 12 regardless of the clobetasol concentration (Figure 34). Finally, it was noted that when the PLGA concentration is fixed at 8.5 mg/ml and the pH value is fixed at 9 the PI will decrease to the desired limit of ≤ 0.1 when decreasing the Tween[®]80 concentration to around 9 mg/ml while maintaining a high clobetasol concentration of 2 mg/ml or higher (Figure 34). Attending the analysis to the influence of clobetasol, high concentrations of clobetasol will result in high EE percentages while the PI values will decrease to the desired limits, with little effect on other parameters like Z_{av} .

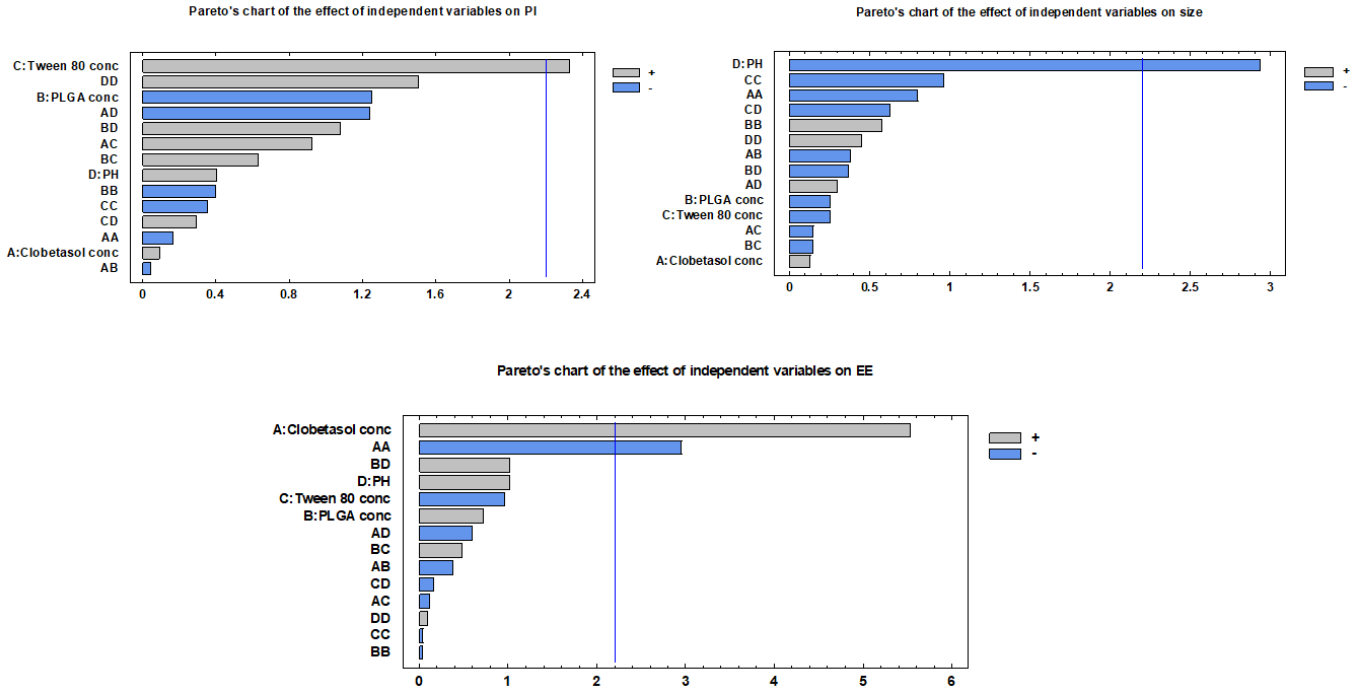


Figure 33 Pareto's charts of the effect of the independent variables.

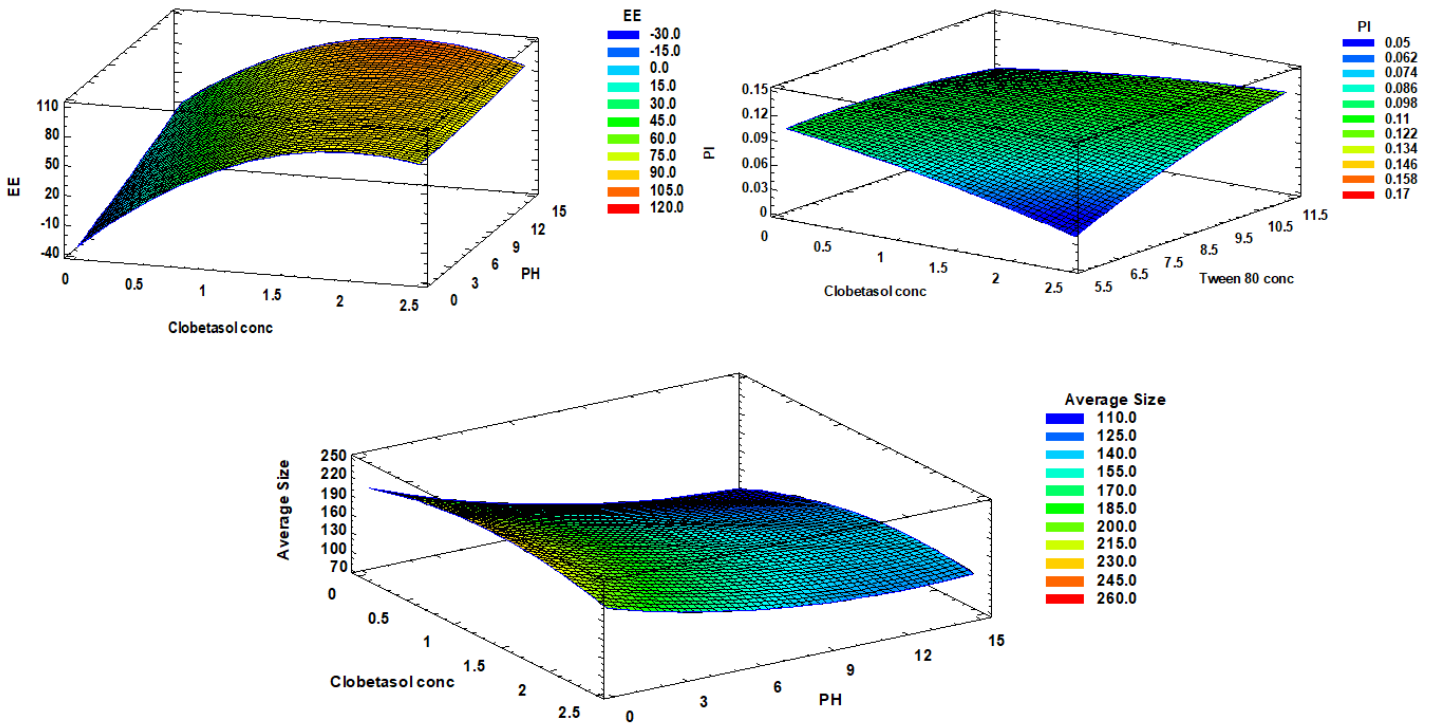


Figure 34 Surface response diagrams for Clobetasol concentration.

7.2.3.1.2 PLGA concentration

Examining the pareto's chart, it was noted the concentration of PLGA did not have a significant effect on any of the dependent variables (Figure 33). Furthermore, analyzing the surface response diagrams to examine any trends, it was noted that when clobetasol concentration is fixed at 2 mg/ml and the pH value is fixed at 9 the EE percentage will be fixed at around 90 % regardless of the PLGA or Tween[®]80 concentration (Figure 35). Also, it was noted that when clobetasol concentration is fixed at 2 mg/ml and Tween[®]80 concentration is fixed at 8.5 mg/ml, the Z_{av} will be maintained in the limit of 110-140 nm when maintaining a high value of pH of around 12, regardless of the PLGA concentration (Figure 35). Finally, it was noted that when the clobetasol concentration is fixed at 2 mg/ml and the pH value is fixed at 9 the PI will decrease to the desired limit below 0.1 when decreasing the Tween[®]80 concentration to around 9 mg/ml regardless of the PLGA concentration (Figure 35). Attending the analysis to the influence of PLGA, maintaining high concentrations seemed to have little influence on Z_{av} , PI values or EE percentages.

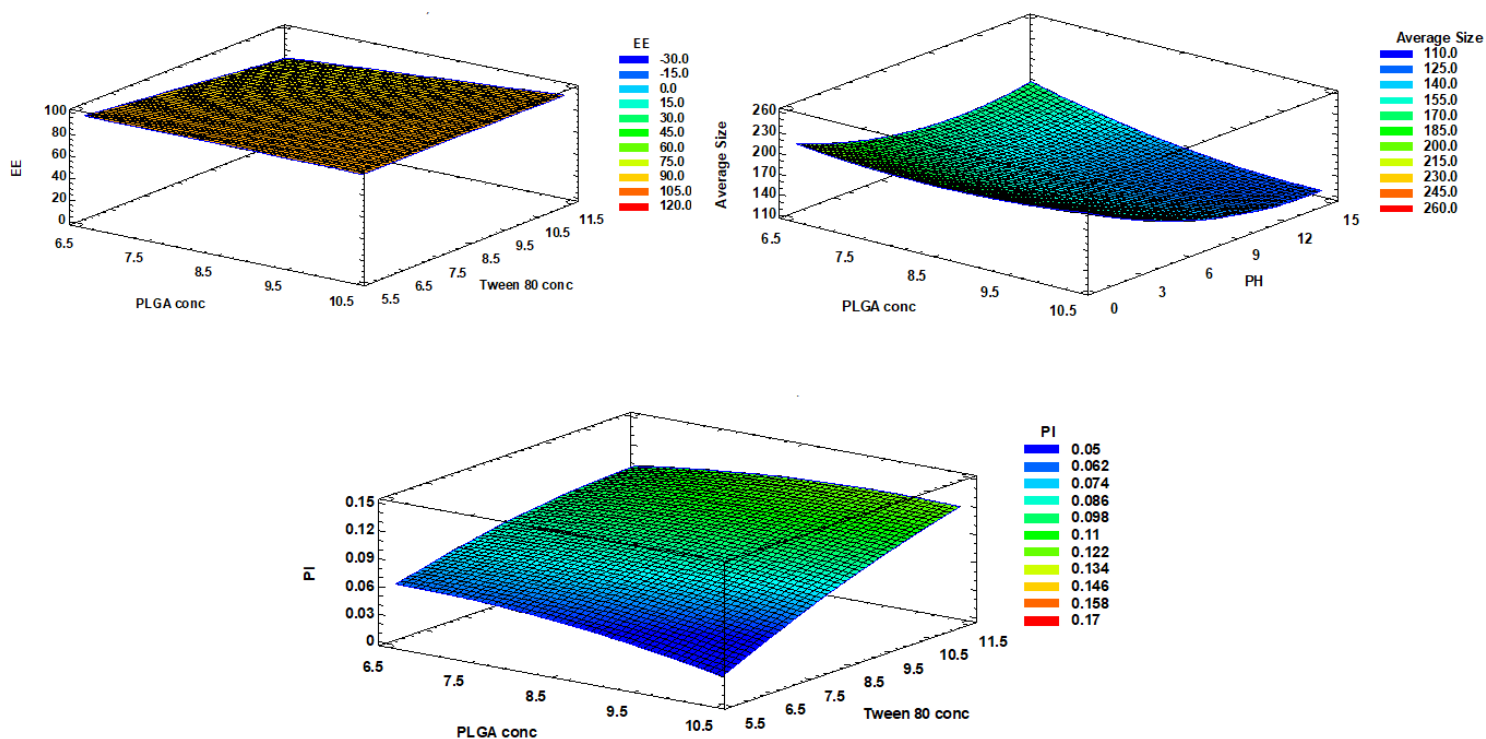


Figure 35 Surface response diagrams for PLGA concentration.

7.2.3.1.3 Tween[®]80 concentration

Examining the pareto's chart, it was noted the concentration of Tween[®]80 only had a significant effect on the PI values ($P < 0.05$). In which lower Tween[®]80 concentrations resulted in lower values of polydispersity index (Figure 33). Furthermore, analyzing the surface response diagrams to examine any trends, it was noted that when PLGA concentration is fixed at 8.5 mg/ml and the pH value is fixed at 9 the EE percentage will increase to around 90 % when maintaining a clobetasol concentration of 1.5 mg/ml or higher regardless of the Tween[®]80 concentration (Figure 36). Also, it was noted that when the clobetasol concentration is fixed at 1.5 mg/ml and the PLGA concentration is fixed at 8.5 mg/ml, the Z_{av} will decrease significantly until 110 nm when maintaining a high Tween[®]80 concentration of 11.5 mg/ml and a high pH value of around 12 (Figure 36). Finally, it was noted that when the clobetasol concentration is fixed at 1.5 mg/ml and the PLGA concentration is fixed at 8.5 mg/ml the PI will increase significantly to around 0.17 when increasing the Tween[®]80 concentration to around 10.5 mg/ml but only when maintaining a very low value of pH of around 1 or very high value of around 15 (Figure 36). In around a neutral pH value of 7, the PI will be the smallest of around 0.062 when maintaining a low concentration of Tween[®]80 of around 6 mg/ml. The PI will start increasing gradually when

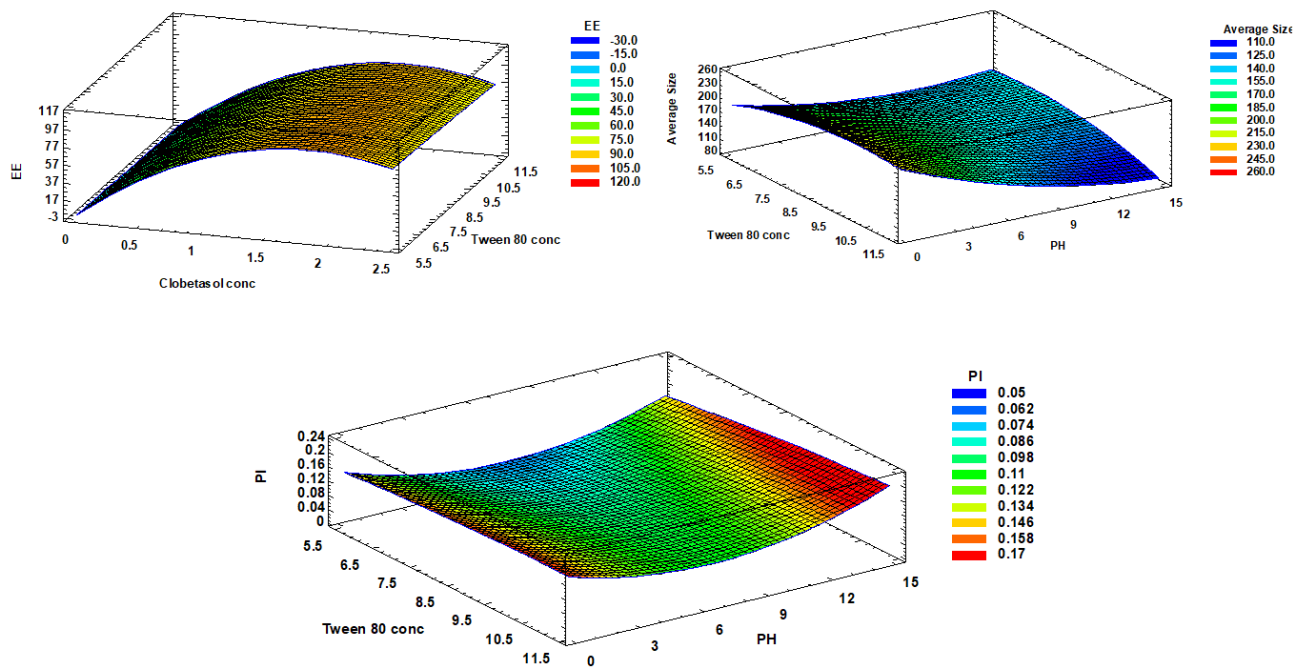


Figure 36 Surface response diagrams for Tween[®]80 concentration.

increasing the concentration of Tween[®]80 and increasing the value of pH to around 9 (Figure 36). Attending the analysis to the influence of Tween[®]80, high concentrations of Tween[®]80 will result in high PI values and low Z_{av} to around desirable limits, with little effect on other paraments like EE.

7.2.3.1.4 pH value

Examining the pareto's chart, it was noted the pH value only had a significant effect on the Z_{av} values ($P < 0.05$). In which higher basic pH levels resulted in the formulation of NPs with smaller average size. (Figure 33). Furthermore, analyzing the surface response diagrams to examine any trends. It was noted that when PLGA concentration is fixed at 8.5 mg/ml and Tween[®]80 concentration is fixed at 8.5 mg/ml the EE percentage will increase gradually with the increase of the clobetasol concentration regardless of the pH value (Figure 37). Also, it was noted that when clobetasol concentration is fixed at 2 mg/ml and Tween[®]80 concentration is fixed at 8.5 mg/ml, the Z_{av} will be maintained in the limit of 110-140 nm when maintaining a high value of pH of around 12 regardless of the PLGA concentration (Figure 37). Finally, it was noted that when

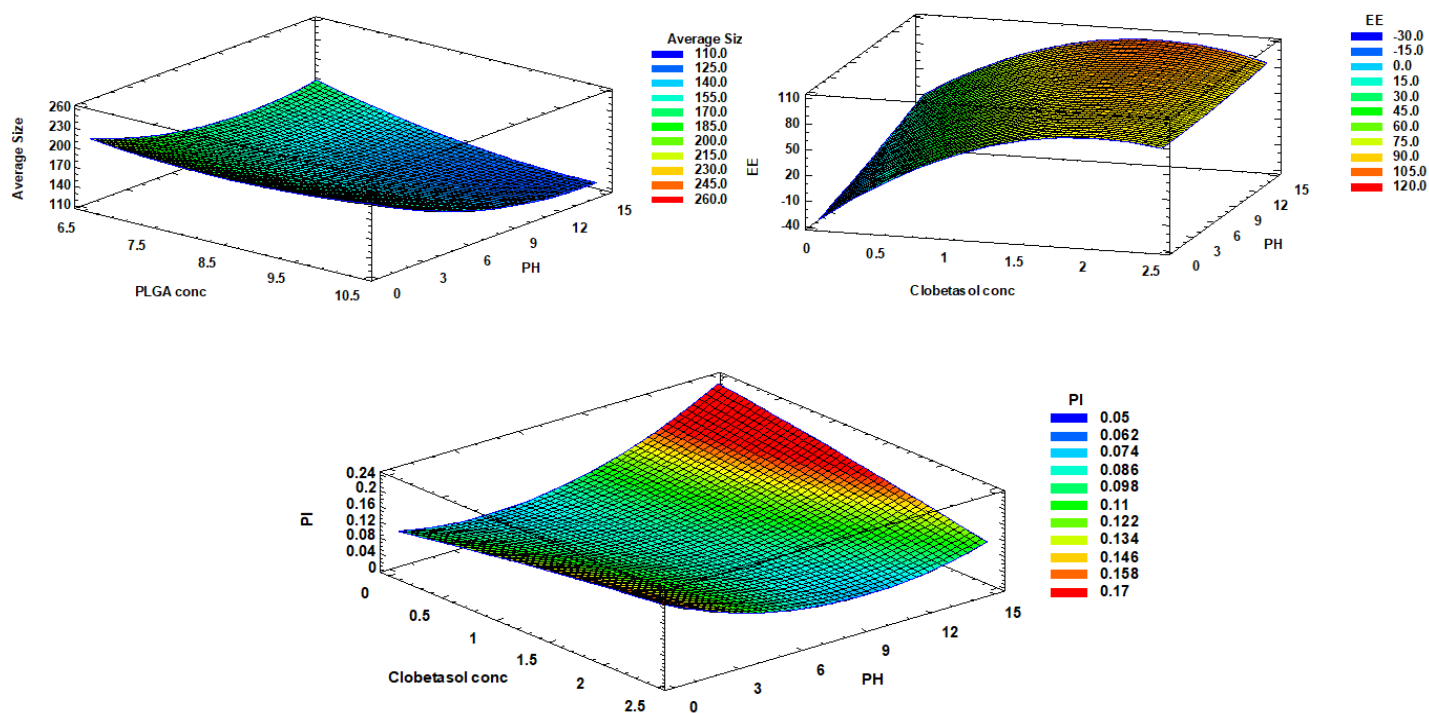


Figure 37 Surface response diagrams for pH values.

Results

PLGA concentration is fixed at 8.5 mg/ml and Tween[®]80 concentration is fixed at 8.5 mg/ml the PI will decrease to the desired limit of ≤ 0.1 when maintaining a pH value of around 6-8 and maintaining a low clobetasol concentration of 0.5 mg/ml. This desired PI value of below 0.1 was also maintained when increasing the pH value to around 9-12 while also increasing the clobetasol concentration to around 2.5 mg/ml (Figure 37). Attending the analysis to the influence of pH, high values of pH will result in low Z_{av} and PI values to around desirable limits, with little effect on other parameters like EE.

After analyzing all the surface response diagrams and examining all the possible trends and interactions, it was decided in order to achieve the desired characteristics of the NPs of a Z_{av} of ≤ 200 nm, PI of below 0.1, $ZP \approx -25$ mV and EE as high as possible, that we had to maintain a high clobetasol and Tween[®]80 concentrations with maintaining a pH value as high as possible. Accordingly, the optimal formulation should be as following, clobetasol concentration of 2 mg/ml, PLGA concentration of 9.5 mg/ml, Tween[®]80 concentration of 8 mg/ml and a pH value of 9.

7.2.4 Reproducibility of the optimized formulation

After using the Pareto's charts and the surface response diagrams to assess the different interactions between the variables and the effect they had. The final optimized formulation was made using a clobetasol concentration of 2 mg/ml, PLGA concentration of 9.5 mg/ml, Tween[®]80 concentration of 8 mg/ml and pH value of 9.

To confirm the reproducibility and effectiveness of the optimized formulation, three more samples were prepared according to the optimized formulation. Subsequently, the different dependent variables of Z_{av} , PI and ZP were assessed using Zetasizer Nano ZS (Malvern Instruments, Malvern, UK) after proper dilution of the sample as mentioned before. Finally, the EE of the samples were evaluated using an indirect method and the HPLC-UV/vis. All the results of these different variables are presented in Table 17. Samples were prepared by triplicate to confirm their reproducibility.

Table 17 Physicochemical characteristics of the optimized formulation

Sample	Clobetasol (mg/ml)	PLGA (mg/ml)	Twen®80 (mg/ml)	pH	Average size (Z_{av}) (nm)	Polydispersity index (PI)	Zeta potential (mV)	Entrapment efficiency (%)
1	2	9.5	8	9	158.6 ± 0.70	0.112 ± 0.004	-45.4 ± 7.58	93.03
2	2	9.5	8	9	157.9 ± 0.58	0.057 ± 0.020	-31.5 ± 0.17	91.33
2	2	9.5	8	9	160.0 ± 0.90	0.081 ± 0.007	-37.8 ± 0.96	92.71

7.2.5 Nanoparticles morphology studies

In regard to the visualization of the NPs using negative staining and TEM (Figure 38), the images were evaluated at different magnifications (Figure 38 a-d). Analysing the images, it can be observed that the optimized NPs displayed a fairly uniform spherical shape without any signs of aggregation or compaction at all examined magnifications.

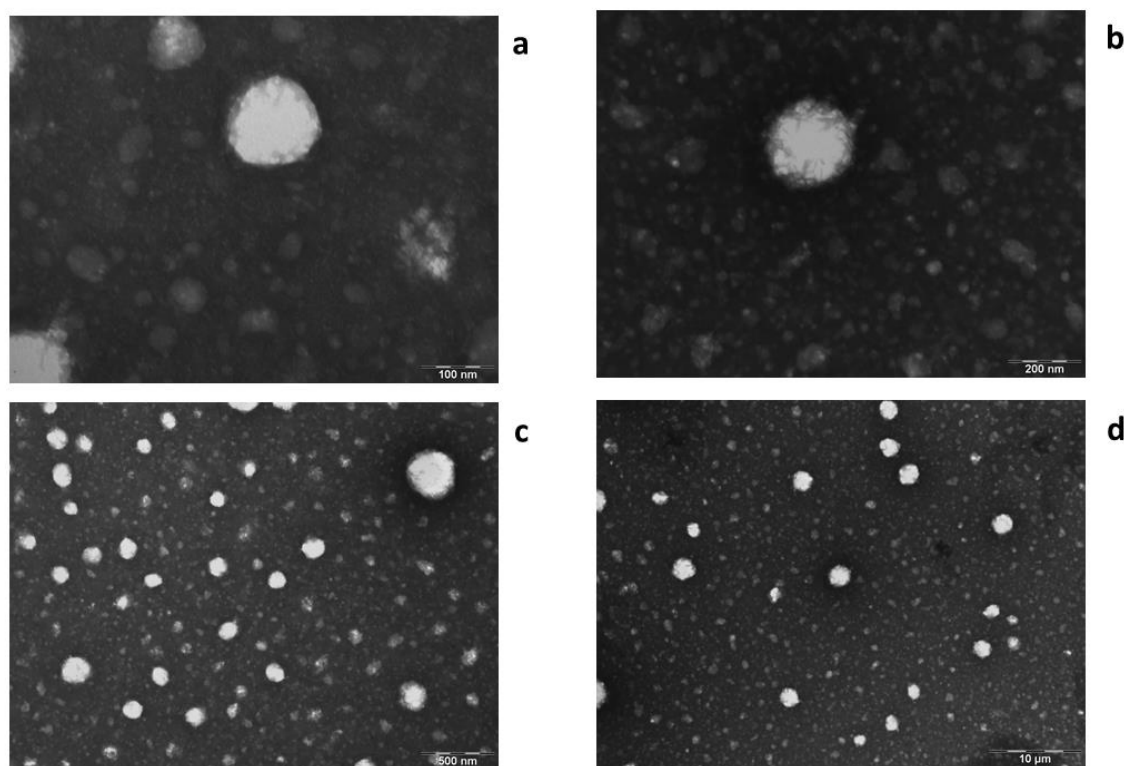


Figure 38 Transmission electron microscopy of clobetasol NPs. (a) Visualization of the clobetasol NPs at 100nm scale bar. (b) Visualization of the clobetasol NPs at 200 nm scale bar. (c) Visualization of the clobetasol NPs at 500nm scale bar. (d) Visualization of the clobetasol NPs at 10μm scale bar.

7.2.6 Nanoparticles characterization and interaction studies

Regarding the XRD (Figure 39) the powder free drug (clobetasol propionate) displayed a profile with different very prominent sharp crystalline peaks at $2\theta = 10^\circ$, 11.5° , 13° , 16° and 21° . Moreover, the polymer (PLGA) displayed an amorphous profile. Similarly, both the drug loaded, and empty NPs (clobetasol propionate/PLGA NPs) displayed an amorphous profile. However, the drug loaded NPs also displayed extremely small peaks corresponding to the clobetasol propionate. The small size of the peaks can indicate that this was only due to the drug encapsulated on the most external layers of the NPs.

FTIR analysis were performed to evaluate the formation of new covalent bonds between the NPs compounds (Figure 40). The free drug (clobetasol propionate) displayed multiple moderately sharp peak at around 1605 , 1660 and 1730 cm^{-1} . Furthermore, the polymer (PLGA) showed sharp peaks at 1090 and 1750 cm^{-1} and an intense band at 3300 cm^{-1} . Both the drug loaded, and empty NPs (clobetasol propionate/PLGA NPs) did not show the characteristic bands of clobetasol around 3640 cm^{-1} , which can indicate that the whole amount of drug is encapsulated inside the NPs. However, they displayed bands corresponding to the ones obtained by the polymer and at around 1750 cm^{-1} , plus an intense band at around 3300 cm^{-1} .

Evaluating the DSC profiles (Figure 41), we can notice that the free drug (clobetasol propionate) exhibited an endothermal peak corresponding to its melting transition at $199.12\text{ }^\circ\text{C}$, whilst the polymer (PLGA) exhibited a smaller peak at $53.01\text{ }^\circ\text{C}$. The drug loaded (clobetasol propionate/PLGA NPs) displayed melting temperatures (T_m) at $48.38\text{ }^\circ\text{C}$, whilst the empty NPs displayed a T_m at $53.00\text{ }^\circ\text{C}$, the slight difference in the T_m between the drug loaded NPs and the empty NPs, can be attributed to the presence of clobetasol inside the NPs.

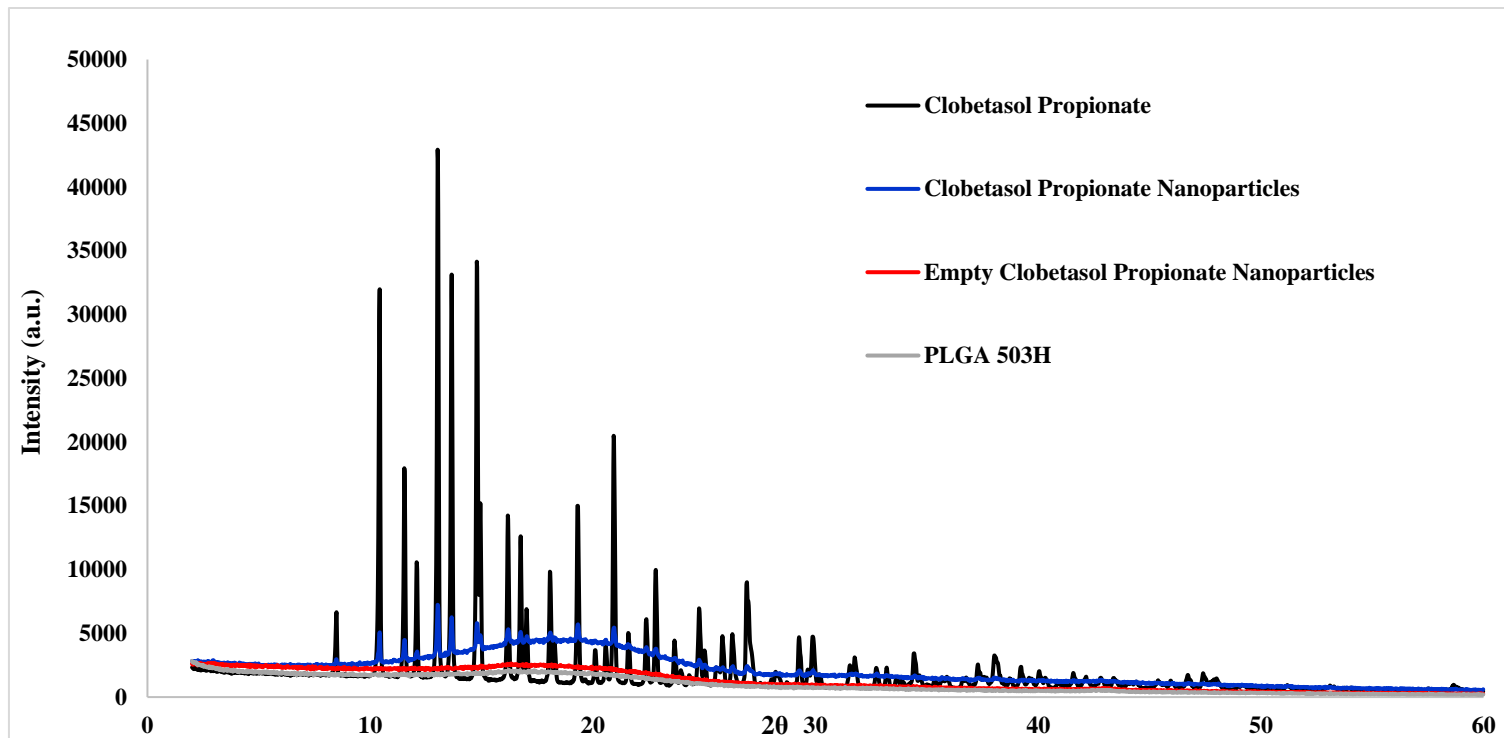


Figure 39 X-ray diffraction analysis of clobetasol propionate nanoparticles and free drug.

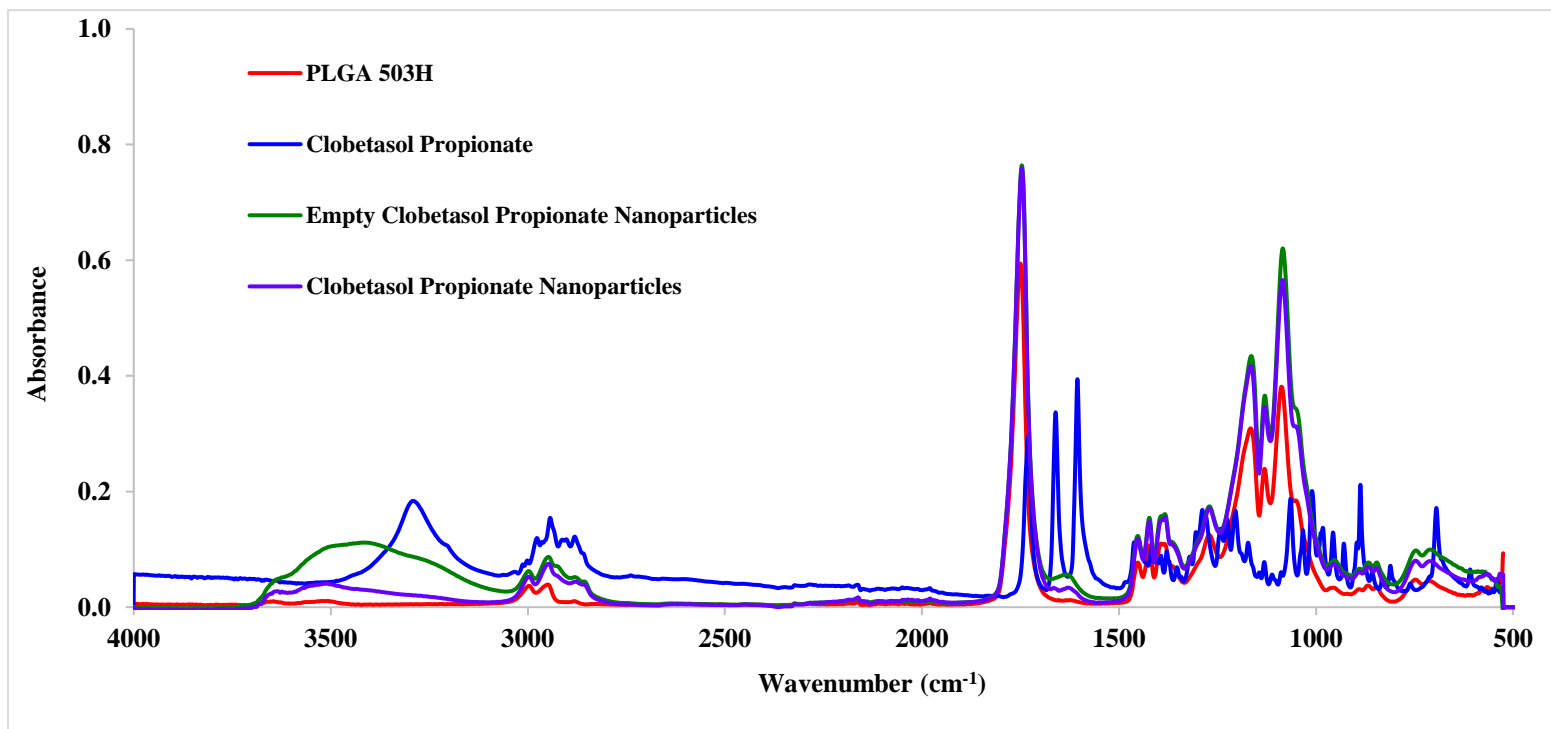


Figure 40 Fourier transformed infra-red analysis of clobetasol propionate nanoparticles and free drug.

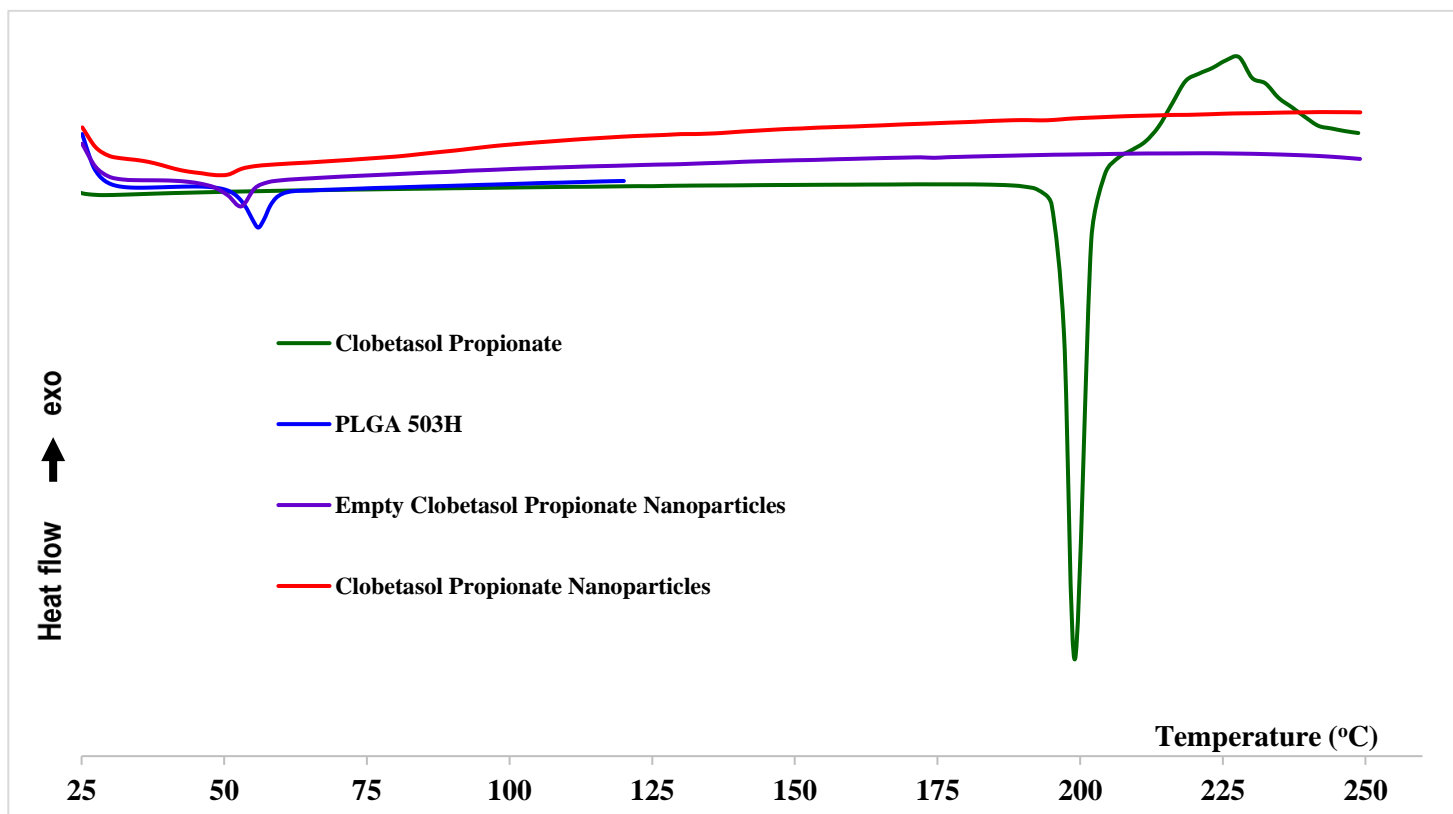


Figure 41 Differential scanning calorimetry analysis of clobetasol propionate nanoparticles and free drug.

7.2.7 Stability studies

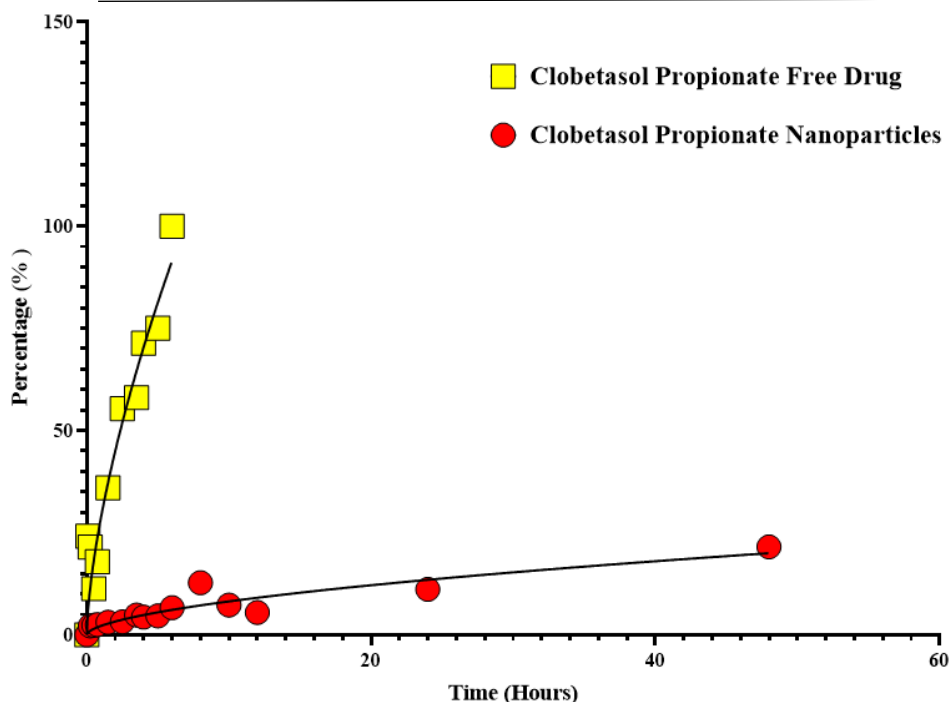
Stability of the developed clobetasol propionate/PLGA NPs at three different temperatures (4, 25 and 38 °C) was monitored. Samples stored at 4 and 25 °C remained visually unchanged during the whole 8 months of storage. In contrast, samples stored at 37 °C were completely transparent and unstable by the end of the 2nd month. Furthermore, it was noted that samples stored at 4°C kept all their parameters Z_{av} , PI and ZP within the desired limits for the whole experiment, being this the most suitable storage temperature. However, samples stored at 25 °C were able to keep only their Z_{av} till 8 months but the PI and ZP readings were unstable and beyond the desired limit in the 8th month. Finally, samples stored at 37°C had all their parameters beyond the desired limits by the end of the 2nd month. All the results of the samples stored at the three different temperatures are presented in Table 18.

Table 18 Physicochemical parameters of the samples stored at different temperatures.

Temperature	4 °C			25 °C			37 °C		
Parameter	Average size (Z_{av}) (nm)	Polydispersity index (PI)	Zeta potential (ZP)	Average size (Z_{av}) (nm)	Polydispersity index (PI)	Zeta potential (ZP)	Average size (Z_{av}) (nm)	Polydispersity index (PI)	Zeta potential (ZP)
Month 1	141 ± 1.60	0.095 ± 0.009	-29.7 ± 1.23	140.2 ± 1.26	0.059 ± 0.008	-23.4 ± 0.92	243 ± 0.35	0.246 ± 0.016	-3.23 ± 1.39
Month 2	145.4 ± 1.12	0.076 ± 0.012	-32.9 ± 0.20	121.4 ± 2.93	0.170 ± 0.029	-19.0 ± 0.77	The count rate is too low for the measurement		
Month 3	125.6 ± 0.35	0.079 ± 0.006	-26.8 ± 1.27	116.6 ± 1.35	0.070 ± 0.011	-15.3 ± 0.40	Sample clearly unstable to measure		
Month 4	123.7 ± 0.88	0.061 ± 0.008	-8.35 ± 0.79	131.5 ± 1.34	0.076 ± 0.010	-13.8 ± 0.30			
Month 8	136.8 ± 1.85	0.088 ± 0.024	-24.4 ± 0.41	134.4 ± 10.1	0.954 ± 0.048	0.66 ± 0.30			

7.2.8 *In vitro* drug release

Comparing the release profile of the clobetasol propionate free and the clobetasol propionate/PLGA NPs, adjusted to the Korsmeyer-Peppas drug release equation, it was noticed that the free drug exhibited a much faster release kinetics than the NPs, displaying a burst release during the first few hours (Figure 42). After 6 hours, 100 % of the free drug was completely released, in comparison to only 6 % from the NPs. In total, after 48 hours of observation only 21% of the NPs was released, thus meaning that longer times of release might be necessary. Despite this, release kinetics can be examined to predict clobetasol release at longer times.



Parameters	Clobetasol propionate nanoparticles	Clobetasol propionate free drug
$B_{max}(\%)$	29.05	99.19
$K_d(\text{hours})$	24.11	1.682
$Sy.x$	3.81	24.99

Figure 42 Cumulative drug release of the clobetasol propionate/PLGA nanoparticles and free clobetasol propionate by percentage after the first 48 hours adjusted by the Korsmeyer-Peppas model.

7.2.9 Freeze dry of the nanoparticles

Different conditions were tested to determine the most suitable and fitting cryoprotectants for the NPs. A combination of different amounts of the most commonly used cryoprotectants were added at different concentrations. These included D-mannitol, (2-Hydroxypropyl)- β -cyclodextrin and their combinations. Ultimately, 5 different combinations of cryoprotectants were tested (Table 19). All the formulations were assessed at the same conditions (Table 1) utilizing the laboratory freeze dryer Lyomicron: Cylindric chamber configuration (Coolvacuum Technologies, Spain).

The NPs appearance after freeze drying was observed (164) and documented (Table 19) and then suitable samples were resuspended, by adding 1.5 ml of Milli-Q water and the sample was vortexed, after 1 hour the measurements for the NPs physicochemical parameters were

performed. All of the 5 formulations seemed by the naked eye physically suitable after the lyophilization cycle. Unfortunately, after resuspension and examining their physical characteristics, none of the formulations meet the desired criteria for the NPs, displaying large sizes and high PI numbers (Table 19). Therefore, further experiments will be necessary in order to freeze dry the formulation using either different lyophilization conditions or a different combination of cryoprotectants.

Table 19 Cryoprotectants assessed and physicochemical parameters of the resuspended freeze dried clobetasol propionate nanoparticles. (HP β CD; (2-Hydroxypropyl)- β -cyclodextrin).

Formulation	Appearance after freeze drying	Average size (Z_{av}) (nm)	Polydispersity index (PI)
5% HP β CD + 15% Mannitol	Good cake with cracks	499.3 \pm 20.78	0.408 \pm 0.022
5% Mannitol	Good cake	923.4 \pm 5.53	0.830 \pm 0.189
10% Mannitol	Good cake with slight fogging	981.6 \pm 84.67	0.369 \pm 0.034
15% Mannitol	Good cake	919.6 \pm 255.3	0.523 \pm 0.180
5% HP β CD	Good cake with dusting	1246 \pm 277.9	0.592 \pm 0.099

7.2.10 Sterilization assays

Clobetasol NPs without freeze drying were sterilised using gamma radiation. In order to determine if the sterilization process via γ radiation had any effect on the NPs, characteristics like Z_{av} , PI, ZP and EE were evaluated before and after γ radiation. It was observed that there was no significance difference between before and after radiation (Table 20). And that it had no effect on the NPs features, in which they were all maintained within the desired limit of a Z_{av} of ≤ 200 nm, PI of ≤ 0.1 , ZP ≈ -10 mV and EE percentage as high as possible.

Table 20 Physicochemical parameters of the nanoparticles before and after sterilization via γ radiation

Sample	Average size (Z_{av}) (nm)	Polydispersity index (PI)	Zeta potential (ZP)	Entrapment efficiency (%)
Before sterilization	163.4 \pm 1.76	0.067 \pm 0.020	-23.4 \pm 0.58	93.73
After sterilization	166.6 \pm 1.15	0.067 \pm 0.021	-25.8 \pm 0.17	91.29

7.2.11 Confocal laser scanning microscopy test

Both the rhodamine labelled clobetasol propionate/PLGA NPs and the free clobetasol propionate drug mixed with rhodamine were examined under a Carl Zeiss LSM 880 spectral confocal microscope (Carl Zeiss AG, Germany) to measure the depth, area, percentage, MFI, and integrated density of the drug inside the dentinal tubules. The clobetasol propionate/PLGA NPs displayed superior depth of penetration inside the dentinal tubules, even managing to reach the outer limits of the periphery of the root (Figure 43b) compared to their free drug counterpart, with a statistical significance difference ($p < 0.05$) (Table 21). Additionally, clobetasol propionate/PLGA NPs exhibited higher area of drug penetration and greater percentage of the total canal were covered compared to the free clobetasol propionate, in which both were statistically significant ($p < 0.05$). Furthermore, the clobetasol propionate/PLGA NPs demonstrated higher MIF and integrated density numbers compared to the free clobetasol propionate drug which can indicate that a higher concentration of the NPs is present inside the tubules, even though there were not statistically significant ($p < 0.05$) (Table 21) which could be explained by the MIF and integrated density obtained in the negative control group (Table 21) that can indicate a presence of a constant intensity noise in the background regardless of the concentration of the drug.

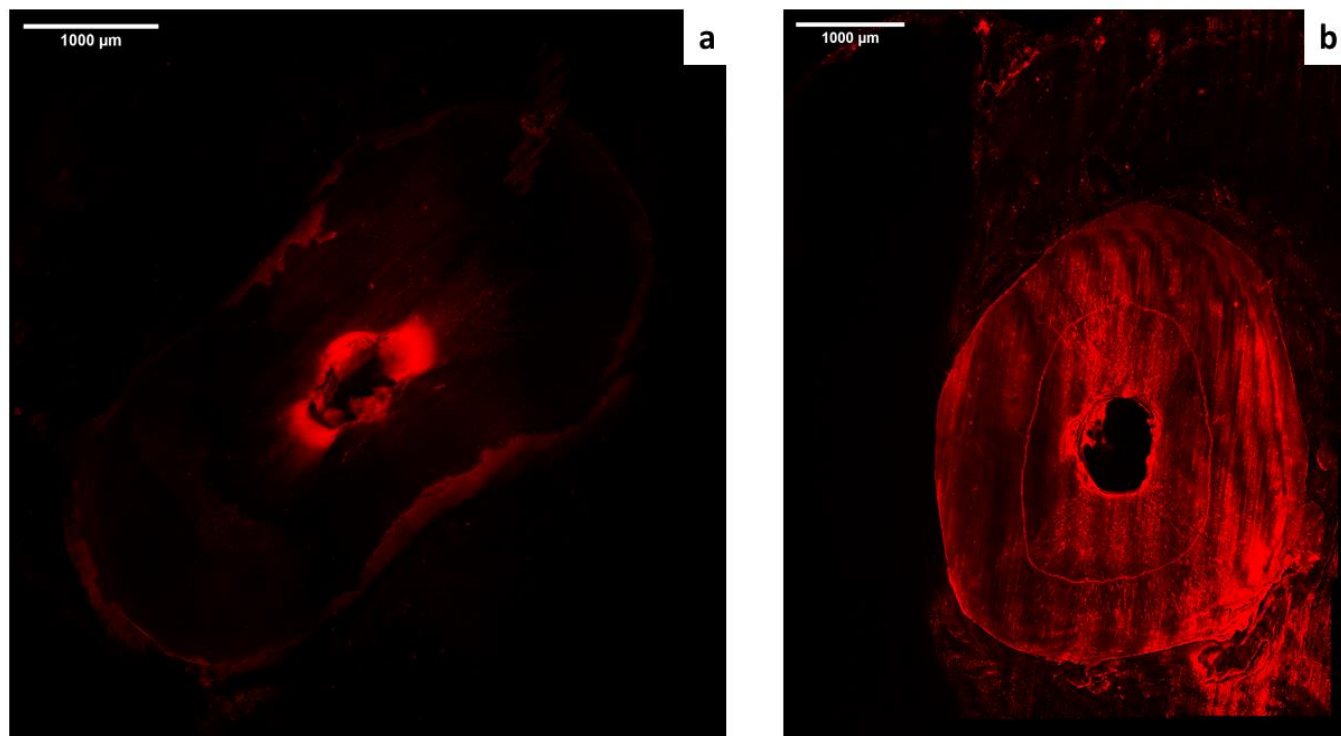


Figure 43 Depth of penetration of the nanoparticles and the free drug inside the dentinal tubules. (a) Depth of penetration of the free clobetasol propionate mixed with rhodamine inside the dentinal tubules. (b) Depth of penetration of the clobetasol propionate/PLGA nanoparticles labelled with rhodamine inside the dentinal tubules.

Table 21 Comparison of the confocal microscopy results between the free drug and the clobetasol propionate nanoparticles

Group	Parameter	Area (μm^2)	Penetration depth (μm)	Mean fluorescence intensity	Integrated density	Percentage (%)
Clobetasol propionate nanoparticles (n=3)	Mean	8121661	1678	61.63	456346050	58.90
Free clobetasol propionate drug (n=2)	Mean	839177	830	49.45	41495167	10.20
Two-sample t-test (p value)		0.005	0.010	0.332	0.061	0.002
Sterile Saline (n=4)	Mean	-	-	47.10	512698479	-

7.2.12 *In vitro* inflammatory response assessment of the Clobetasol Propionate/PLGA nanoparticles

7.2.12.1 Cytotoxicity assays: cell morphology and metabolic activity using alamarBlue®

Images obtained by the phase contrast microscopy exhibited that NPs at concentrations of 1 mg/ml, 0.5 mg/ml and 0.2 mg/ml did not allow for macrophages growth and displayed cytotoxic tendencies for both time periods at 24 and 48 hours (Figure 44). However, macrophage treated with NPs concentrations at 0.1 mg/ml, 0.05 mg/ml, 0.02 mg/ml and 0.01 mg/ml displayed normal growth and a rounded morphology at 24 and 48 hours (Figure 44). Furthermore, analyzing the metabolic activity using alamarBlue®, it can be noticed by the color change after adding the alamarBlue® in the well plates, as NPs concentrations of 1 mg/ml, 0.5 mg/ml and 0.2 mg/ml displayed a darker bluish color compared to the rest of the conditions which had a lighter purple color (Figure 45). Additionally, after adjusting the absorbance rates at 570 and 600 nm to the metabolic activity equation, we can observe that NPs concentrations at 0.05 mg/ml, 0.02 mg/ml and 0.01 were able to maintain metabolic activity percentages comparable to the 100 % obtained by the positive control group of TCP (Figure 46). However, NPs concentrations at 1 mg/ml, 0.5 mg/ml and 0.2 mg/ml reduced the metabolic activity significantly ($p < 0.05$) (Figure 46).

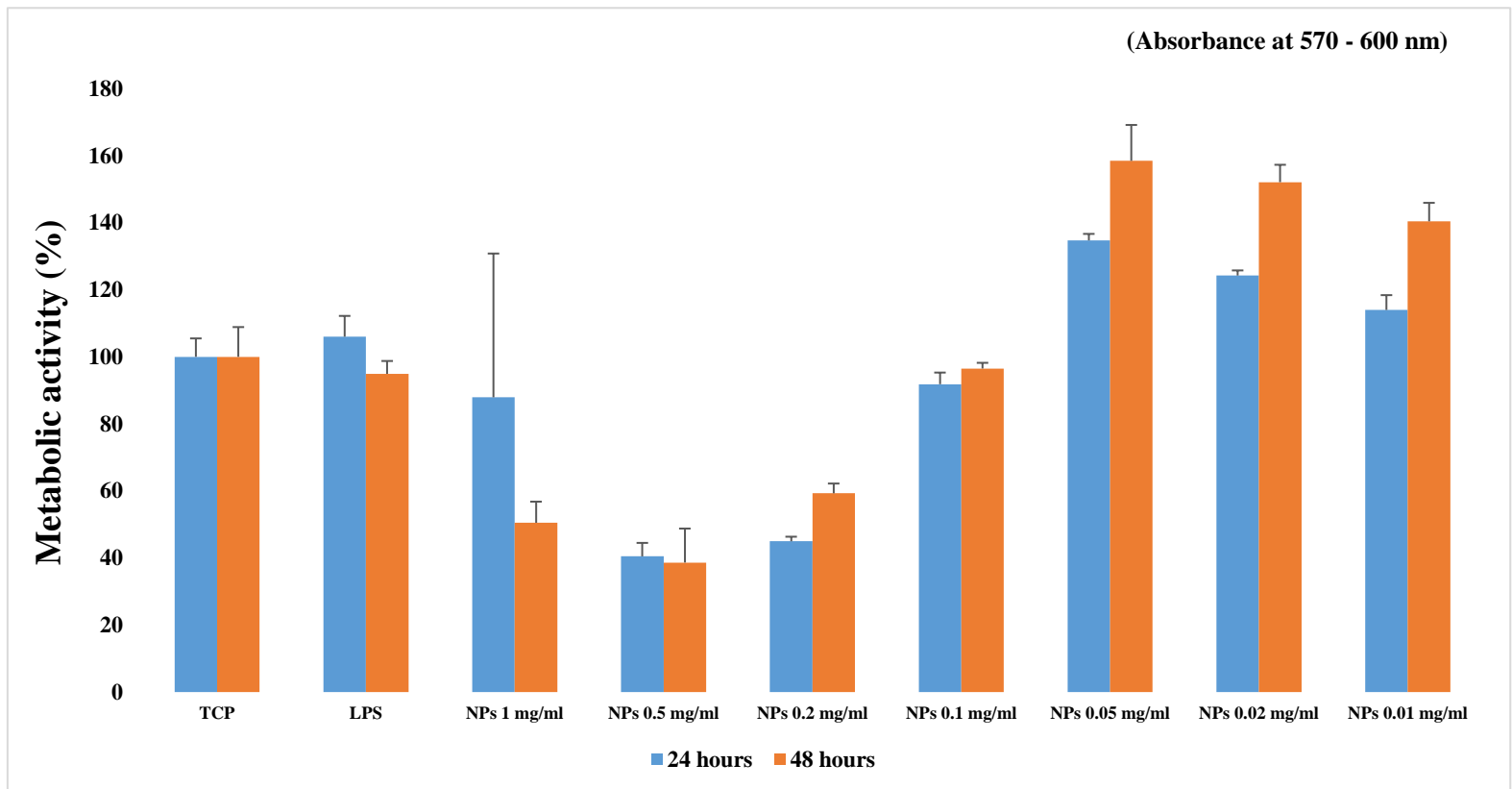


Figure 46 Metabolic activity of macrophages in response to tissue culture plastic (TCP), lipopolysaccharide (LPS) and clobetasol propionate/PLGA nanoparticles with different concentrations at different periods of 24 and 48 hours measured by alamarBlue® reduction with absorbance at 570 and 600 nm.

7.2.12.2 Enzyme-linked immunosorbent assays

Evaluating the inflammatory cytokines release, all NPs concentrations that displayed cytotoxic tendencies were discarded. IL-1 β and TNF- α cytokine release was examined against NPs concentrations of 0.1 mg/ml, 0.05 mg/ml, 0.02 mg/ml and 0.01 mg/ml, plus the controls. It was seen that TNF- α release was reduced considerably with NPs concentration of 0.1 mg/ml and 0.05 mg/ml compared to the LPS negative control ($p < 0.05$), displaying results similar and even less than the TCP positive control after 48 hours (Figure 47). However, examining the release of IL-1 β , it was observed that all the tested NPs concentrations resulted in the release of IL-1 β in amounts similar to the TCP positive control and lesser than the LPS negative control group ($p <$

0.05) (Figure 48). Finally, analyzing the inflammatory cytokines release of the LPS pretreated macrophages, it was noticed that NPs at all tested concentrations were not able to reduce the cytokines release of $TNF-\alpha$ (Figure 49) and $IL-1\beta$ (Figure 50) to limits below the amounts obtained by the LPS pretreated macrophages or the TCP positive control group

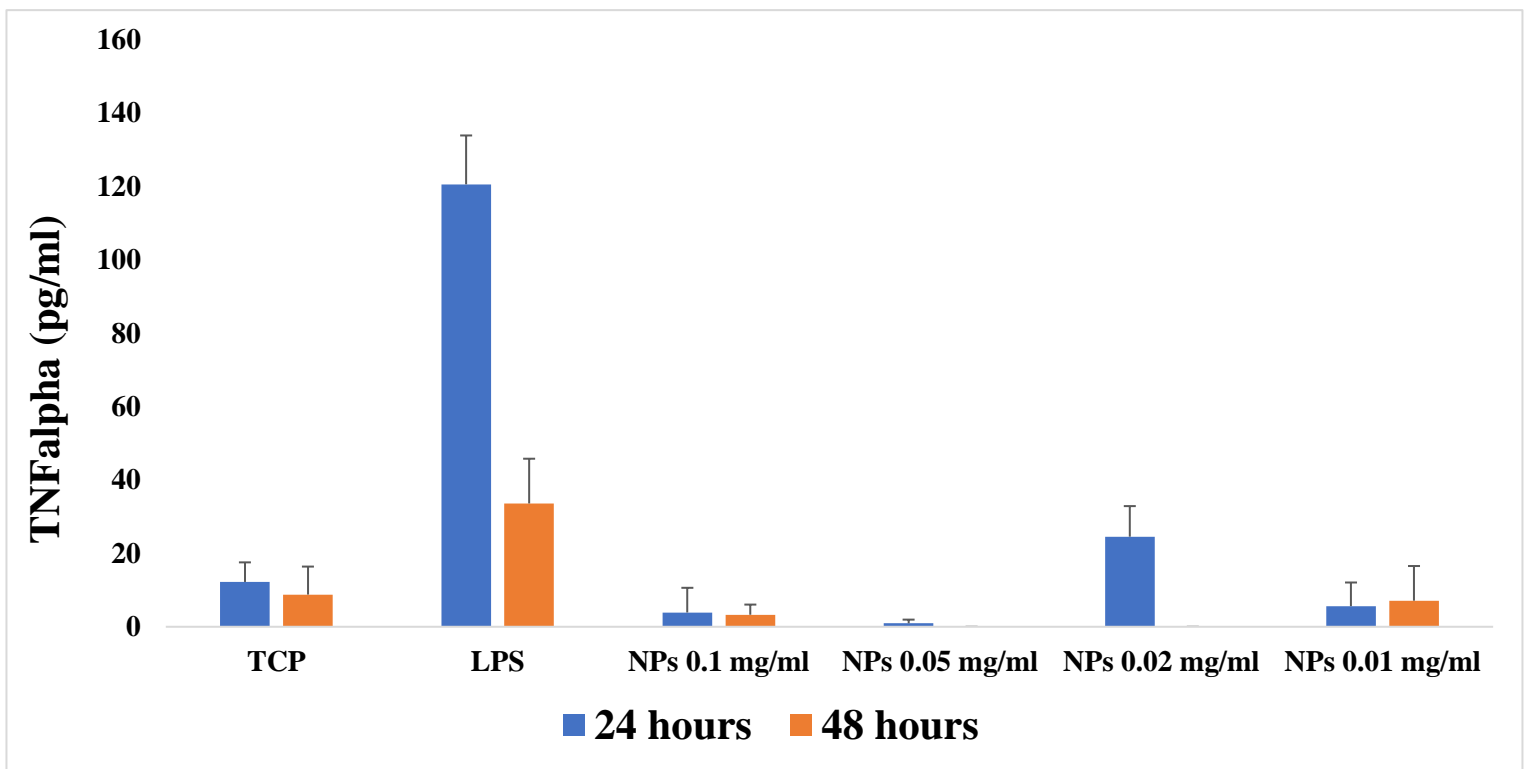


Figure 47 Inflammatory cytokines release of $TNF-\alpha$ from macrophages in response to tissue culture plastic (TCP), lipopolysaccharide (LPS) and clobetasol propionate/PLGA nanoparticles with different concentrations at different periods of 24 and 48 hours.

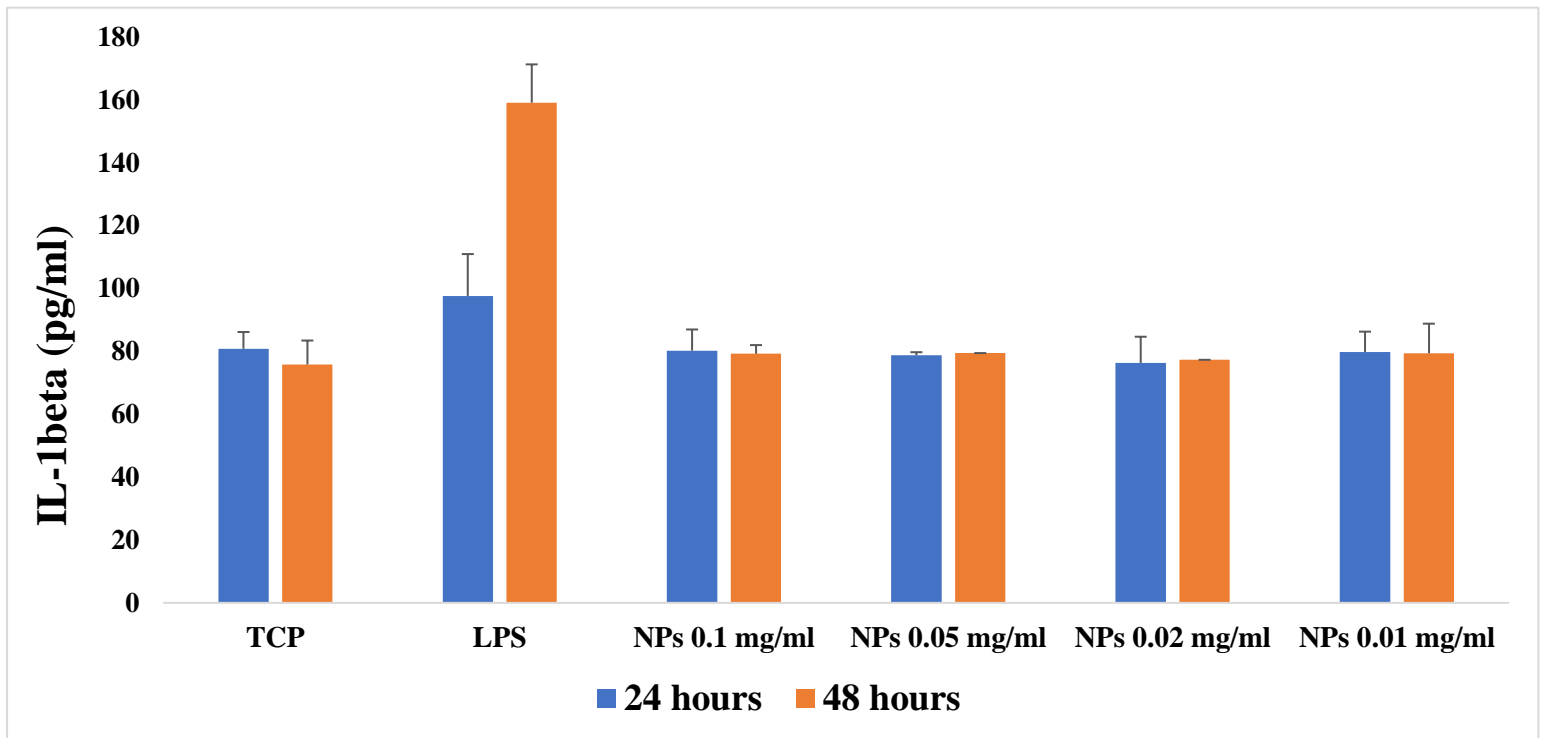


Figure 48 Inflammatory cytokines release of IL-1beta from macrophages in response to tissue culture plastic (TCP), lipopolysaccharide (LPS) and clobetasol propionate/PLGA nanoparticles with different concentrations at different periods of 24 and 48 hours..

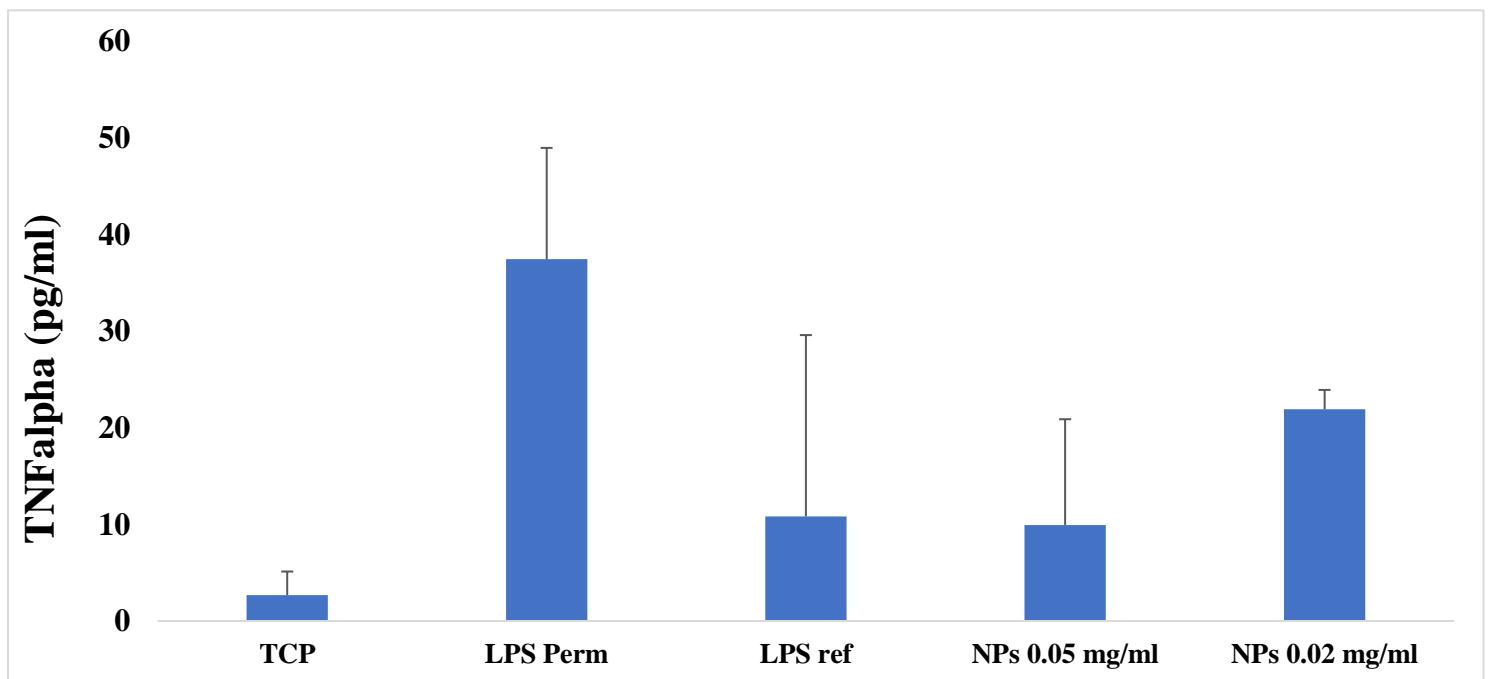


Figure 49 Inflammatory cytokines release of TNF- α from macrophages pretreated with lipopolysaccharide (LPS) in response to tissue culture plastic (TCP), lipopolysaccharide permanent (LPS Perm), lipopolysaccharide removed (LPS ref) and clobetasol propionate/PLGA nanoparticles with different concentrations at 48 hours

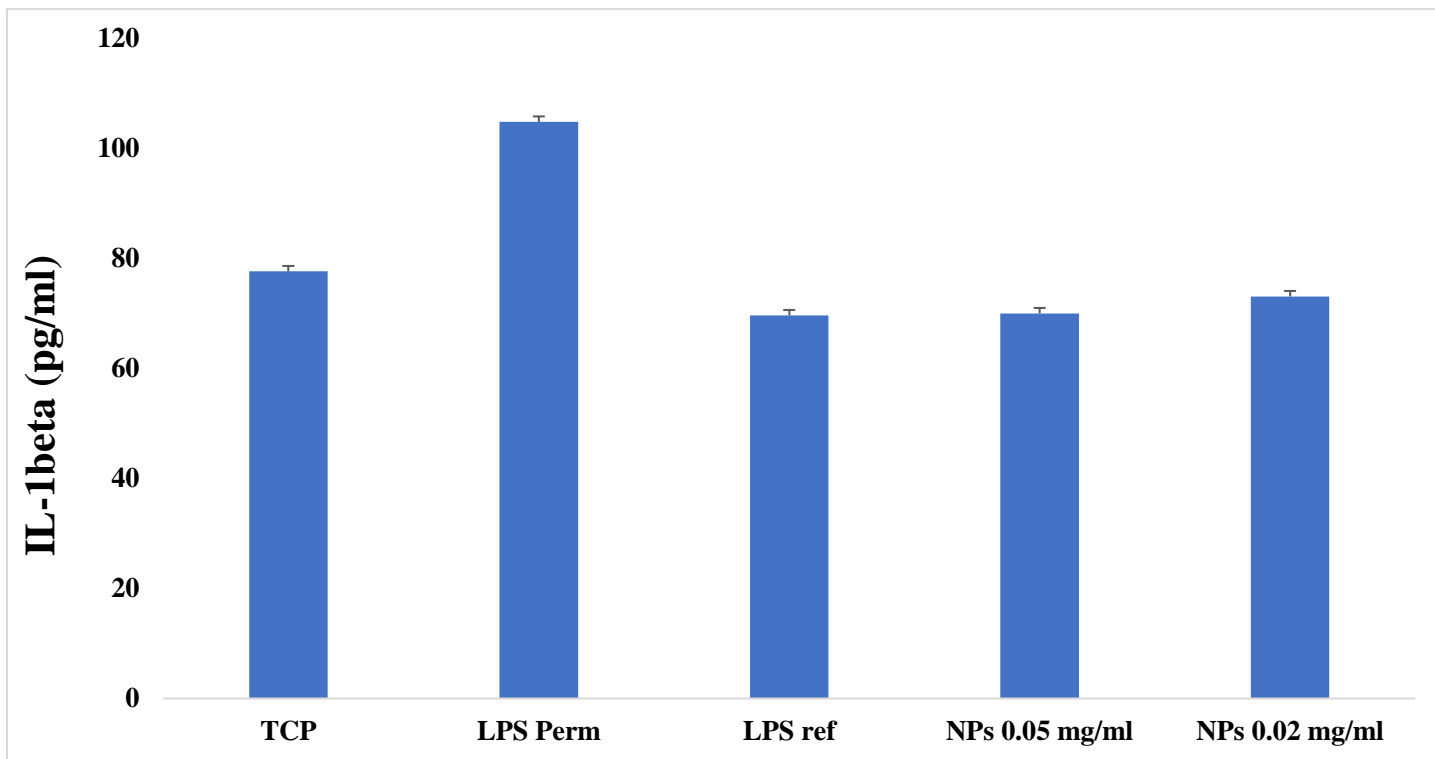


Figure 50 Inflammatory cytokines release of IL-1beta from macrophages pretreated with lipopolysaccharide (LPS) in response to tissue culture plastic (TCP), lipopolysaccharide permanent (LPS Perm), lipopolysaccharide removed (LPS ref) and clobetasol propionate/PLGA nanoparticles with different concentrations at 48 hours.

DISCUSSION

DISCUSSION

8. DISCUSSION

8.1 Discussion of the Calcium Hydroxide/PLGA nanoparticles

Ca(OH)₂ has been commonly used for decades as an intracanal medication in endodontics for its antibacterial qualities (4). Consequently, throughout the years many attempts have been made to overcome or improve any limitations encountered. Including the decreased antibacterial effect due to the buffer action of the dentin leading to the reduction of the drugs alkalinity (5). Additionally, the anatomical complexities of root canal systems can further demote and complicate the reachability of any conventional intracanal medication (128). Therefore, advances in drug delivery systems using nanotechnology had been envisioned to overcome these issues (11,122).

In the present study, Ca(OH)₂ loaded PLGA NPs were successfully optimized and characterized with aims to increase the antibacterial effect through controlled drug release and superior reach to areas of complicated root canal anatomy due to the smaller mean nanoscopic size. Ultimately, the characteristics of the NPs utilizing the optimized formula were $Z_{av} = 167.6 \pm 2.21$ nm, $PI = 0.11 \pm 0.024$, $ZP = -8.59 \pm 0.16$ mV. Considering that the size of a normal Ca(OH)₂ aggregates can reach to as big as 20 μ m (20000 nm) (165), the results obtained in regards of the Z_{av} of the NPs are very promising. Additionally, these findings are comparable to previous publications attempting to utilize the advantages of nanotechnology in developing an improved intracanal antibacterial medication. Kishen et al. and Shrestha et al. (124,166) utilized chitosan and zinc oxide NPs in elimination of bacterial biofilms. Javidi et al. (167) tested the effect of combining silver NPs and Ca(OH)₂ as a suspension on bacterial biofilm elimination. However, none of them actually loaded an antibacterial agent inside a nanostructured drug carrier. Pagonis et al. (168) produced PLGA NPs loaded with photosensitizer methylene blue with a mean size 100 to 250 nm and ZP of -31.87 mV, still details of the full optimization was not revealed including the PI and EE of the NPs. Furthermore, Farhadian et al. (169) obtained polymeric NPs by loading

Discussion

Ca(OH)₂ into chitosan with a mean size of 292 nm and PI of 0.32. Compared to the results obtained in this current study, we were able to produce NPs with smaller mean size and lower PI values, which indicate a more uniform, stable NPs (170). In the practice of polymer based NPs, PI values of ≤ 0.2 are most commonly deemed acceptable (11,170).

Further clarifying the rationale in adopting these desired characteristics for the NPs and deciding the optimal formulation. Since this medicament was intended to be used as an intracanal antibacterial agent. It was important that the NPs were of a small size below 200 nm. Since it has been shown that many of the bacterial species that cause root canal infection can enter and reside inside the dentinal tubules (171). Also, the root canal system with its intricate anatomy, usually includes isthmuses, accessory and lateral canals which can contain bacteria and their products (23). Accessibility to these bacterial species has always been challenging using standard antibacterial medication used in our current endodontic practice. However, we believe using NPs with a size below 200 nm can help overcome these problems, especially as we know the diameter of the dentinal tubules is around 2400 to 4280 nm depending on their depth (172). Presumably, using NPs with these small sizes can reach even further inside the dentinal tubules than standard antibacterial agents and help eliminate all the bacterial species and their byproducts that reside inside. Especially as one of the most fundamental principles for the action of Ca(OH)₂ against bacteria, is direct contact with them (4,86), therefore penetrating those tubules in which the bacteria resides is necessary.

Moreover, another important consideration that we intended to attain with the optimal formulation, was to maintain a pH value as high pH as possible. As it has been proven, the antibacterial activity of Ca(OH)₂ is achieved through the release of the highly oxidant free radicals hydroxyl ions (5,173). They act on the bacterial cells causing damage to the cytoplasmic membrane through protein denaturation plus causing damage to the DNA (4). Furthermore, a high basic pH has to be retained in order for the hydroxyl ions to sustain their antibacterial capacity (5). As the pH gradient of the cytoplasmic membrane is altered by the high concentration of hydroxyl ions, which causes protein denaturation by acting on the proteins of the membrane (5). Additionally, the integrity of the cytoplasmic membrane is altered by the high

pH of Ca(OH)_2 through chemical injury to the organic components and transport of nutrients (59). However, many studies have shown that this effect is distorted in clinical scenarios due to the buffering effect of dentine and the hydroxyapatite against alkaline substances like Ca(OH)_2 (72), which leads to severe decline in the antibacterial capacity of Ca(OH)_2 . Consequently, it was of the utmost importance that the pH value for the final optimized formula was calculated and accounted for in the optimization procedure. It could be assumed, that the developed optimized formulation of Ca(OH)_2 NPs that generates and maintains an environment with a high basic pH of 12 can overcome these adverse effects and sustain their antibacterial effects for longer periods.

Quantification of Ca(OH)_2 was performed using inductively coupled plasma optical emission spectroscopy (ICP-OES). This technique allows the determination of low concentrations of calcium in samples and it is highly regarded for its speed and accuracy (135). It uses the inductively coupled plasma to produce excited atoms and ions that emit electromagnetic radiation at wavelengths characteristic of a particular element. Subsequently, the intensity of these emissions are proportional to the concentrations of the calcium elements within the sample (135). Since the ICP-OES solely calculates the calcium concentration inside the samples, by applying Ca(OH)_2 standard solutions we were able to apply a recovery percentage for the measurement and quantify Ca(OH)_2 by converting calcium concentration. In this way, a reliable and reproducible method was applied for quantifying small concentrations of Ca(OH)_2 .

Different interaction studies were performed to characterize the NPs. TEM was used to visualize the NPs and confirm their shape and uniformity. Additionally, we performed XRD, FTIR and DSC to analyse the profiles of the NPs and the elements that were used in their production. Also, interactions between the different components were evaluated. When examining the profile of the Ca(OH)_2 NPs in XRD and DSC, it can be noticed that the peaks indicative of the Ca(OH)_2 drug were not detected, which suggest that the drug is encapsulated inside the NPs. Furthermore, it is important to note that for all the interaction studies, pure form of Ca(OH)_2 powder was used

and the not the dental commercial brand, this can be the reason that the drug presented as either poorly crystalline or amorphous, which is in agreement with previous studies (162,163,174).

Examining the drug release profile, the Ca(OH)_2 NPs released exhibited higher drug concentrations that remained stable in the steady state up to 48 hours compared to the free drug. The profile displayed an early burst in the first hours proceeding to maintain the release at these high concentrations for the remainder of the observation period. On the other hand, the free drug displayed a slight burst release in the initial 30 minutes with a constant release throughout of the remainder of the observation period at lower concentrations. This can be attributed to the degree of conversion of the drug, as Ca(OH)_2 has shown that it can go through chemical changes fairly easy when subjected to adverse environmental circumstances (5,175). In a study assessing the degree of Ca(OH)_2 conversion into non-active clinical species with different vehicles (176), it was found that Ca(OH)_2 was transformed severely with all tested vehicles. Examining the results after just 24 hours, it was found that out 47.5 mg only 1.4 - 2.2 mg were left unreacted and the rest converted to calcium carbonate (CaCO_3). These may have a significant effect, especially on the free drug that is not encapsulated and is subjected directly in bulk to the outer environment both *in vitro* and also in the *in vivo* clinical practice. Regarding the *in vitro* drug release studies, Ca(OH)_2 could lead to the formation of calcium phosphate species as well as hydroxyapatite crystals with a quick conversion rate that can take between 5 to 20 minutes (177–179). These forms may be undetectable in the present quantification method quantifying only the clinically active Ca(OH)_2 . It could be assumed, that due to this high conversion rate, in the first hour a proportional amount of the free Ca(OH)_2 has been chemically transformed to phosphate species, deeming them undetectable in our quantification method. On the other hand, since Ca(OH)_2 NPs were encapsulated and protected from the outer environment, they displayed a much lesser degree of conversion after 48 hours. This may also explain the well documented shortcomings of the conventional Ca(OH)_2 in bacterial elimination in endodontics. As it has been reported, in order for the Ca(OH)_2 to be effective as an antibacterial intracanal medication, high concentrations of hydroxyl ions needs to be released with direct contact with the bacteria (4). Unfortunately, this is not attained clinically, in a systematic review by Sathorn *et al.* (2007), the antibacterial efficiency of Ca(OH)_2 was assessed in clinical trials, in which they concluded that

Ca(OH)₂ had limited effectiveness in eliminating bacteria from human root canal when assessed by culture techniques. This is due to the buffering effect that is exerted by the dentine and hydroxyapatite clinically, in which the alkalinity of Ca(OH)₂ is reduced, resulting in decreased antibacterial potential and subsequently diminished diffusion of the hydroxyl ions (72,84,85). Nevertheless, even though the Ca(OH)₂ NPs displayed a prolonged steady drug release at high concentrations, further experiments are required with longer observations periods to evaluate release profile and to examine for how long these concentrations can be maintained.

According to the results of the confocal laser scanning microscopy, it was shown that the Ca(OH)₂ NPs had much better penetration inside the dentinal tubules when compared to the free Ca(OH)₂ drug. Confocal microscopy was used to evaluate the penetration due to its ability in allowing for a standard, reproducible, three dimensional image without the need for any previous preparation that can affect the integrity of the sample (180). Additionally, rhodamine was chosen as the fluorescent agent to visualise the penetration inside the tubules, as this low concentration of rhodamine has been proven to not affect or alter the physical properties of Ca(OH)₂ (181). Furthermore, the potential clinical significance of these results cannot be underestimated. As it has been explained earlier, the ability of the antibacterial agent to penetrate inside the dentinal tubules is of the utmost importance in accessing and eliminating the bacterial species that reside there (171). According to our results, we have tangible proof that utilizing the Ca(OH)₂ NPs will yield significantly better results compared to the conventional free Ca(OH)₂ drug in regards to penetration inside the dentinal tubules, reaching even to the limits of the root periphery. The penetration numbers of the free Ca(OH)₂ obtained in the present study are slightly less comparable to previous studies that examined the penetration of Ca(OH)₂ mixed with rhodamine inside dentinal tubules (182). This could be explained by the difference in methodology, as the process of determining the exact level of penetration could be subjective as it depends on the human intuition and interpretation that could be different from one individual to the other. Moreover, examining the results of the mean fluorescent intensity in the present study, Ca(OH)₂ NPs displayed significantly higher mean fluorescent intensity when compared to the free drug, which indicate that larger volumes of the NPs were present inside the tubules. This can be attributed to the considerably smaller size of the NPs of ≤ 200 nm compared to the diameter of

Discussion

the dentinal tubules which is around 2400 to 4280 nm (172). It could be assumed, that since the Ca(OH)_2 NPs present better ability to penetrate further inside the dentinal tubules and they were present in significantly larger volumes than the free Ca(OH)_2 drug, their ability in eliminating bacterial species there will be enhanced substantially due to their superior reachability.

Furthermore, the antibacterial efficiency of the $\text{Ca(OH)}_2/\text{PLGA}$ NPs was tested using different *in vitro* experiments. The agar diffusion test was used to compare the antibacterial performance in terms of inducing growth inhibition zones in the agar plate of the $\text{Ca(OH)}_2/\text{PLGA}$ NPs against free Ca(OH)_2 . In addition, antibiotics and sterile saline were used as positive and negative control groups. After examination of the agar plates, it was noted that the $\text{Ca(OH)}_2/\text{PLGA}$ NPs showed clear maximal zones of growth inhibition around the filter papers comparable only to the positive group of antibiotics. In comparison, there was minimal to non-existent inhibition zones around traditional Ca(OH)_2 in the form of the free powder drug and the commercial product. These results are in agreement with previous studies (19,74,183,184), in which the inefficiency of traditional Ca(OH)_2 using the agar diffusion test is well documented. This could be due to the buffer substances that within culture media, which decreases the pH levels to values deemed insufficient to produce any antibacterial properties (4,184). The fact that the NPs were able to overcome these circumstances and develop prominent growth inhibition zones is a major advantage and a sign that they have the ability to maintain high pH values thus their antibacterial properties even in adverse conditions. Additionally, the MIC of the NPs was compared to the traditional Ca(OH)_2 in regards to inhibiting bacterial growth for 3 bacterial species. It was noted that after 24 hours of incubation both the NPs and the traditional Ca(OH)_2 were able to inhibit bacterial growth at all tested concentrations. The results obtained in the current study are comparable to previous studies (124–127,185), in which the antibacterial efficacy of different types of NPs, ranging from metallic origin like silver to bioactive glass and chitosan NPs were validated and proven to be an effective antibacterial agent even against the more resistant bacterial biofilms. It is important to note, that additional experiments are required to further evaluate the antibacterial competency of the $\text{Ca(OH)}_2/\text{PLGA}$ NPs especially against the more resistant and resilient bacterial biofilms.

8.2 Discussion of the Clobetasol Propionate/PLGA nanoparticles

As stated earlier, avulsed teeth with extended extra oral time present an extremely poor prognosis. In fact the final outcome of replacement resorption is considered as a forgone conclusion and all our available treatment measures are towards trying to prolong the survival of the avulsed tooth as long as possible (100). There is no treatment available that will prevent or reverse the resorptive process that occurs for avulsed teeth with extended extra oral time (93). Fortunately, recent animal studies presented promising results utilizing Clobetasol propionate as an anti-inflammatory intracanal medication (10). Clobetasol is a potent corticosteroid that has anti-inflammatory and antiresorptive properties acting by releasing a group of proteins known as Lipocortin that inhibit the production of Phospholipase A2 which is a precursor to Arachidonic acid and many inflammatory mediators (105). As mentioned before, biodegradable NPs present a specialized drug delivery system that offers many advantages compared to conventional drug delivery (11). Mainly, it provides prolonged drug release with target specificity and less side effects compared to conventional drug delivery systems (133). We believe the combination of the anti-inflammatory and antiresorptive properties of clobetasol propionate and the controlled target specific prolonged drug release of the biodegradable NPs can result in the production of a novel anti-inflammatory intracanal medication that can provide the solution to the dilemma of replacement resorption of avulsed teeth with extended extra oral time.

The NPs were prepared using a method according to the chemical characteristics of the encapsulated drug. The solvent-displacement method is a well-known procedure in order to entrap hydrophobic compounds such as clobetasol propionate. As described before, the organic solvent used was acetone due to its relative safety compared with other solvents and it was evaporated under reduced pressure (186). In the present study, clobetasol propionate loaded PLGA NPs were successfully optimized and characterized with aims to increase the anti-inflammatory effect through controlled drug release and superior reach to areas of complicated root canal anatomy due to the smaller mean nanoscopic size. Ultimately, the characteristics of the NPs utilizing the optimized formula were Z_{av} below 200 nm, PI value below 0.1 corresponding to a monodisperse system with a highly negative ZP indicating a good short term

Discussion

stability and high EE percentages which were superior to 90%. These findings are comparable to previous publications (142,187,188) attempting to utilize the advantages of nanotechnology in developing an improved drug release of clobetasol propionate.

The design of the experiment (DoE) approach was utilized so, a factorial design was applied, in order to obtain a suitable formulation. Furthermore, independent variables were analyzed, and their interactions were studied in order to determine their influence on the physicochemical parameters of the NPs. This was all performed in order to determine the optimal formulation that can guarantee the best and desirable results for the NPs physicochemical characteristics. Examining the Pareto's charts and the surface response diagrams we could detect certain trends. It was noted the high EE (%) could be achieved by maintaining a high clobetasol propionate concentration of around 2 mg/ml. Also, that maintaining a high basic pH of around 9 resulted in a decrease in the NPs Z_{av} to the desired limit of ≤ 200 nm. Finally, it was noted that the higher concentrations of Tween®80 resulted in higher values of PI. Putting all this into consideration the optimal formulation that can achieve all the suitable physicochemical parameters was clobetasol propionate concentration of 2 mg/ml, PLGA concentration of 9.5 mg/ml, Tween®80 concentration of 8 mg/ml and a pH value of 9. In order to confirm the validity and the reproducibility of this formulation. Three further samples were prepared following the optimal formulation and then the NPs physicochemical parameters were examined. Results obtained confirm that all the dependent variables were within the desirable limit and most importantly achieving a high EE and ensuring that most of the drug is actually encapsulated inside the nanoparticles.

Further clarifying the rationale in adopting these desired characteristics for the NPs and deciding the optimal formulation. Given that this medicament was intended to be used as an intracanal anti-inflammatory agent, it was of the utmost importance that the NPs were of a small size below 200 nm. As explained earlier, in cases of avulsed teeth with more than 60 minutes extra oral dry time, ankylosis or replacement resorption occurs due to the extended damage to the outer root surface which causes an inflammatory resorptive stimulus in that area (8). For that reason, it is important that the anti-inflammatory NPs will be able to penetrate inside the dentinal tubules and reach to the periphery of the root surface to stop and halt this inflammatory process. Considering

the diameter of the dentinal tubules which is around 2400 to 4280 nm depending on their depth (172), it's safe to assume that the anti-inflammatory NPs with much smaller size of ≤ 200 nm will be able to penetrate inside the dentinal tubules easily. This was confirmed by the confocal studies, in which rhodamine labelled clobetasol propionate/PLGA NPs and the free clobetasol propionate drug mixed with rhodamine were examined to measure the depth and area of penetration of the drug inside is the dentinal tubules. The clobetasol propionate/PLGA NPs displayed superior depth and area of penetration inside the dentinal tubules, even managing to reach the outer limits of the periphery of the root compared to their free drug counterpart, with a statistical significance difference.

Different interaction studies were performed to characterize the NPs. TEM was used to visualize the NPs and confirm their shape and uniformity, in which they displayed a fairly spherical structure. Additionally, we performed XRD, FTIR and DSC to analyse the profiles of the NPs and the elements that were used in their production. Also, interactions between the different components were evaluated. When examining the profile of the clobetasol propionate/PLGA NPs in FTIR and DSC, it can be noticed that the peaks indicative of the clobetasol propionate drug were not detected, which suggest that the drug is encapsulated inside the NPs. However, examining the XRD profile of the drug loaded NPs, small peaks corresponding to the clobetasol propionate drug were detected which can be due to the drug present on the most external layers of the NPs since penetration depth of XRD achieves the firsts layers inside the NPs core. Furthermore, stability of the developed clobetasol propionate/PLGA NPs at different temperatures (4, 25 and 37 °C) was monitored up to 8 months examining the NPs characteristics. In which, samples stored at 4°C kept all their parameters Z_{av} , PI and ZP and within the desired limits. In contrast, samples stored at 37 °C were completely transparent and unstable by the end of the 2nd month. This is in agreement with other publications utilizing polymeric nanostructured systems (134,136,138), which can be attributed to the degradation process of the polymer.

Comparing the drug release profile of the clobetasol propionate free and the clobetasol propionate/PLGA NPs, it was noticed that the free drug exhibited a much faster release kinetics than the NPs, displaying a burst release and after only 6 hours 100 % of the free drug was

Discussion

completely released. In comparison, only 6 % of clobetasol from the NPs was released at this timepoint. Additionally, clobetasol NPs best fit was Korsmeyer-Peppas, which is in accordance with other authors studying PLGA NPs (134,148,189). These results can have significant potential, as this sustained prolonged drug release that is presented by the NPs system can help overturing and overcoming the inflammatory process presented by the dry avulsed tooth. Also, it is worth noting that in total after 48 hours of observation only 21% of the NPs was released, meaning that the anti-inflammatory effect presented by the NPs is guaranteed to be long-lasting further helping in plummeting the inflammatory process.

Moreover, it was important to examine the biocompatibility of the NPs hence they will be used in direct contact with vital tissues. Hence, cytotoxicity assays were performed on the clobetasol propionate/PLGA NPs examining their effect on macrophages with different concentrations. These were examined in regard to cell morphology and metabolic activity using alamarBlue[®]. In which NPs concentrations at below 0.1 mg/ml allowed for normal growth of macrophage with a rounded morphology at 24 and 48 hours, deeming them safe to use with vital tissues. Furthermore, the anti-inflammatory capacity of the clobetasol propionate/PLGA NPs were examined, in which ELISA assays were used to evaluate the inflammatory cytokines release of TNF- α and IL-1 β , both are released by the macrophages in response to an inflammation due to trauma or infection, after exposure to the NPs that presented biocompatible concentrations. In which the anti-inflammatory capacity of the NPs was observed as the releases of TNF- α was reduced considerably with NPs concentration of 0.1 mg/ml and 0.05 mg/ml compared to the LPS negative control, displaying results similar and even less than the TCP positive control after 48 hours. However, examining the release of IL-1 β , it was observed that all the tested NPs concentrations resulted in the release of IL-1 β in amounts similar to the TCP positive control and lesser than the LPS negative control group, this could be due to the IL-1 β as it has been reported that its difficult to control and regulate properly (190,191). Moreover, analyzing the results of the second experiment, we can notice that the inflammatory cytokines release of IL-1 β and TNF- α from the LPS pretreated macrophages, was not reduced with the NPs at all tested concertation to limits below the amounts obtained by the LPS pretreated macrophages or the TCP positive control group after 48 hours. This could be explained by the drug release profile of the clobetasol

propionate/PLGA NPs, as we observed in our drug release experiment, only 21 % of the drug was released after 48 hours, which could be deemed insufficient to induce a proper anti-inflammatory response in such short time and little amount of the drug released. It could be advised that the experiment is repeated with an observation period longer than 48 hours which, to allow to adequate amount of the drug to be released that could induce as proper anti-inflammatory reaction, since in the drug release experiment only 21 % of the drug encapsulated in the NPs was released after 48 hours and. In addition, it is important to note that NPs did not developed or induce an inflammatory response whatsoever, so it may be safe to assume that they are not pro-inflammatory.

Even though we were able to optimize and characterize a proper formulation for clobetasol propionate/PLGA NPs, further future studies are still required in order to for it to be utilized in a clinical condition and to achieve its goal as an anti-inflammatory intracanal medication in halting the inflammatory resorptive reaction in cases of avulsed teeth with extended extra oral time. In which, the therapeutic effect of the NPs has to be evaluated on extracted teeth in laboratory conditions and finally moving to animal studies to examine the true anti-inflammatory effect of the NPs.

CONCLUSIONS

CONCLUSIONS

9. CONCLUSIONS

In the present thesis, biodegradable PLGA nanoparticles were prepared to be used as an intracanal antibacterial and anti-inflammatory medicament. All the alternative hypotheses were accepted expect for hypothesis number 7.

- 1) Using the solvent displacement method, Ca(OH)_2 loaded PLGA NPs were successfully optimized and formulated with aims to increase the antibacterial effect through controlled drug release and superior reach to areas of complicated root canal anatomy due to the nanoscopic size. The characteristics of the NPs utilizing the optimized formula showed a PI value lower than 0.2 and an average size below 200 nm along with a highly negative ZP and maximum EE percentage.
- 2) Using the solvent displacement method, clobetasol propionate loaded PLGA NPs were successfully optimized and formulated to be used as an intracanal anti-inflammatory medication in cases of avulsed teeth with extended extra oral time. The characteristics of the NPs utilizing the optimized formula was Z_{av} below 200 nm, PI value below 0.1, highly negative ZP and high EE percentages which were superior to 90 %.
- 3) For both the Ca(OH)_2 /PLGA and the clobetasol propionate/PLGA NPs, the characterization of the NPs was performed, and the spherical morphology was confirmed using TEM and different interaction studies were carried including XRD, FTIR and DSC to examine the profile of the NPs. No interactions were confirmed, and the drug appeared to be encapsulated inside the NPs.
- 4) Examining the drug release profile for the Ca(OH)_2 /PLGA NPs, the Ca(OH)_2 NPs exhibited a prolonged and steady release with higher concentrations than free Ca(OH)_2 drug that remained stable up to 48 hours.
- 5) Examining the drug release profile for the clobetasol propionate/PLGA NPs, the NPs exhibited a prolonged and steady release with only around 21% of the encapsulated drug released after 48 hours, in comparison the free drug that was completely released after just 6 hours.

- 6) For the freeze drying of the $\text{Ca(OH)}_2/\text{PLGA}$ NPs, the combination of 5% of (2-Hydroxypropyl)- β -cyclodextrin and 15% D-mannitol gave rise to the most stable outcome and the best appearance after lyophilization. Unfortunately, for the clobetasol propionate/PLGA NPs, we were not able to achieve a suitable combination.
- 7) Evaluating the pH values of the antibacterial Calcium Hydroxide ($\text{Ca(OH)}_2/\text{PLGA}$) NPs during the first week after their preparation, it was able to maintain a consistent high basic pH till after 1 week from its preparation.
- 8) Cytotoxicity assays were performed on the clobetasol propionate/PLGA NPs, in which NP concentrations at 0.1 mg/ml, 0.05 mg/ml, 0.02 mg/ml and 0.01 mg/ml allowed for normal growth of macrophage with a rounded morphology at 24 and 48 hours, deeming them safe to use with vital tissues.
- 9) The antibacterial efficiency of the $\text{Ca(OH)}_2/\text{PLGA}$ NPs was tested using different *in vitro* experiments. Using the agar diffusion test, it was noted that the NPs showed clear maximal zones of growth inhibition around the filter papers comparable only to the positive group of antibiotics. Additionally, the MIC of the NPs was measured in regards to inhibiting bacterial growth for 3 bacterial species. It was noted that after 24 hours of incubation the NPs were able to inhibit bacterial growth at all tested concentrations.
- 10) The anti-inflammatory capacity of the clobetasol propionate/PLGA NPs were examined, in which ELISA assays were used to evaluate the inflammatory cytokines release of the macrophages in response to the NPs, the releases of $\text{TNF-}\alpha$ was reduced considerably to almost undetectable amounts with NPs compared to the LPS negative control, displaying results similar and even less than the TCP positive control after 48 hours. However, resulted in the release of $\text{IL-1}\beta$ in higher amounts which were similar to the TCP positive control and lesser than the LPS negative control group. Additionally, the inflammatory cytokines release of $\text{IL-1}\beta$ and $\text{TNF-}\alpha$ from the LPS pretreated macrophages, was not reduced with the NPs at all tested concentration to limits below the amounts obtained by the LPS pretreated macrophages or the TCP positive control group after 48 hours. Further testing with longer observation periods are required.
- 11) Using the confocal laser scanning microscopy, it was shown that both the $\text{Ca(OH)}_2/\text{PLGA}$ and the clobetasol propionate/PLGA NPs had a better depth and area of

penetration inside the dentinal tubules when compared to the free drug. Plus, the NPs displayed higher values MFI and integrated density compared to the free drug.

9.1 Future perspectives

Even though, we were able to successfully optimize and characterize two (Ca(OH)₂/PLGA and clobetasol propionate/PLGA) NPs and demonstrate their advantages and their therapeutic antibacterial and intracanal anti-inflammatory efficacy to be used as a an endodontic intracanal medicament, additional experiments are needed. In order for the developed NPs to be utilized in our daily clinical practice, further laboratory and clinical studies need to be carried out. For the Ca(OH)₂/PLGA NPs their antibacterial efficacy needs to be examined on extracted teeth and against the more resilient bacterial biofilms, before moving to blinded randomized clinical trials comparing their effect against the commercially available Ca(OH)₂. As for the clobetasol propionate/PLGA NPs their anti-inflammatory efficacy capacity needs to be examined in animal studies before examining them in clinical conditions and performing *in vivo* studies to prove their therapeutic efficacy.

REFERENCES

REFERENCES

10. REFERENCES

- 1 Sjögren Ulf, Hägglund Björn, Sundqvist Göran, Wing Kenneth. Factors affecting the long-term results of endodontic treatment. *J Endod* 1990;16:498–504.
- 2 Hulsmann Michael, Peters Ove A., Dummer Paul M.H. Mechanical preparation of root canals: shaping goals, techniques and means. *Endod Top* 2005;10:30–76.
- 3 Siqueira José F. Endodontic infections: Concepts, paradigms, and perspectives. *Oral Surg Oral Med Oral Pathol Oral Radiol Endod* 2002;94:281–93.
- 4 Siqueira J. F., Lopes H. P. Mechanisms of antimicrobial activity of calcium hydroxide: A critical review. *Int Endod J* 1999:361–9.
- 5 Mohammadi Z., Dummer P. M.H. Properties and applications of calcium hydroxide in endodontics and dental traumatology. *Int Endod J* 2011:697–730.
- 6 Ng Y. L., Mann V., Rahbaran S., Lewsey J., Gulabivala K. Outcome of primary root canal treatment: Systematic review of the literature - Part 1. Effects of study characteristics on probability of success. *Int Endod J* 2007:921–39.
- 7 Ashraf Fouad Authors F, Abbott Paul V, Tsilingaridis Georgios, et al. International Association of Dental Traumatology Guidelines for the Management of Traumatic Dental Injuries: 2. Avulsion of Permanent Teeth. *Dent Traumatol* 2020;36:331–42.
- 8 Trope Martin. Clinical management of the avulsed tooth: Present strategies and future directions. *Dent Traumatol* 2002:1–11.
- 9 Chen H., Teixeira F. B., Ritter A. L., Levin L., Trope M. The effect of intracanal anti-inflammatory medicaments on external root resorption of replanted dog teeth after extended extra-oral dry time. *Dent Traumatol* 2008;24:74–8.
- 10 Kirakozova Anna, Teixeira Fabricio B., Curran Alice E., Gu Fang, Tawil Peter Z., Trope Martin. Effect of Intracanal Corticosteroids on Healing of Replanted Dog Teeth after Extended Dry Times. *J Endod* 2009;35:663–7.

References

- 11 Bhatia Saurabh, Bhatia Saurabh. Nanotechnology and Its Drug Delivery Applications. *Nat. Polym. Drug Deliv. Syst.* Springer International Publishing; 2016. Chapter 1. 1–32.
- 12 Kishen Anil, Shrestha Annie. Nanoparticles for endodontic disinfection. *Nanotechnol. Endod. Curr. Potential Clin. Appl.* Springer International Publishing; 2015. Chapter 4. 97–120.
- 13 Endodontic treatment statistics. American Association of Endodontists. Available at: <http://www.aae.org/about-aae/news-room/endodontic-treatment-statistics> 2006.
- 14 Ng Y. L., Mann V., Gulabivala K. A prospective study of the factors affecting outcomes of nonsurgical root canal treatment: Part 1: Periapical health. *Int Endod J* 2011;44:583–609.
- 15 Salehrabi Robert, Rotstein Ilan. Endodontic treatment outcomes in a large patient population in the USA: An epidemiological study. *J Endod* 2004;30:846–50.
- 16 Ng Y. L., Mann V., Gulabivala K. A prospective study of the factors affecting outcomes of non-surgical root canal treatment: Part 2: Tooth survival. *Int Endod J* 2011;44:610–25.
- 17 Chen Shih Chung, Chueh Ling Huey, Kate Hsiao Chuhsing, Tsai Miao Yu, Ho Shih Chang, Chiang Chun Pin. An Epidemiologic Study of Tooth Retention After Nonsurgical Endodontic Treatment in a Large Population in Taiwan. *J Endod* 2007;33:226–9.
- 18 Kojima Koko, Inamoto Kyoko, Nagamatsu Kumiko, et al. Success rate of endodontic treatment of teeth with vital and nonvital pulps. a meta-analysis. *Oral Surg Oral Med Oral Pathol Oral Radiol Endod* 2004;97:95–9.
- 19 Siqueira J. F., de Uzeda M. Intracanal medicaments: evaluation of the antibacterial effects of chlorhexidine, metronidazole, and calcium hydroxide associated with three vehicles. *J Endod* 1997;23:167–9.
- 20 Sedgley Christine. Seltzer and Bender’s Dental Pulp, 2nd ed. *J Endod* 2012;38:708.
- 21 Kakehashi S., Stanley H. R., Fitzgerald R. J. The effects of surgical exposures of dental pulps in germ-free and conventional laboratory rats. *Oral Surgery, Oral Med Oral Pathol* 1965;20:340–9.

- 22 Trope Martin, Bergenholtz Gunnar. Microbiological basis for endodontic treatment: can a maximal outcome be achieved in one visit? *Endod Top* 2002;1:40–53.
- 23 Ricucci Domenico, Siqueira José F. Biofilms and apical periodontitis: Study of prevalence and association with clinical and histopathologic findings. *J Endod* 2010;36:1277–88.
- 24 Nair P. N.R., Henry Stéphane, Cano Victor, Vera Jorge. Microbial status of apical root canal system of human mandibular first molars with primary apical periodontitis after “one-visit” endodontic treatment. *Oral Surgery, Oral Med Oral Pathol Oral Radiol Endodontology* 2005;99:231–52.
- 25 Vera Jorge, Siqueira José F., Ricucci Domenico, et al. One- versus two-visit endodontic treatment of teeth with apical periodontitis: A histobacteriologic study. *J Endod* 2012;38:1040–52.
- 26 Pashley D. H. Dentin-predentin complex and its permeability: physiologic overview. *J Dent Res* 1985;64:613–20.
- 27 Garberoglio R., Brännström M. Scanning electron microscopic investigation of human dentinal tubules. *Arch Oral Biol* 1976;21:355–62.
- 28 Nagaoka Shigetaka, Miyazaki Youichi, Liu Hong Jih, Iwamoto Yuko, Kitano Motoo, Kawagoe Masataka. Bacterial invasion into dentinal tubules of human vital and nonvital teeth. *J Endod* 1995;21:70–3.
- 29 Nair P. N.Ramachandran, Sjögren Ulf, Krey Gunthild, Kahnberg Karl Erik, Sundqvist Göran. Intraradicular bacteria and fungi in root-filled, asymptomatic human teeth with therapy-resistant periapical lesions: A long-term light and electron microscopic follow-up study. *J Endod* 1990;16:580–8.
- 30 Lin Louis M., Skribner Joseph E., Gaengler Peter. Factors associated with endodontic treatment failures. *J Endod* 1992;18:625–7.
- 31 Siqueira J. F. Aetiology of root canal treatment failure: Why well-treated teeth can fail. *Int Endod J* 2001;1–10.
- 32 Narayanan LLakshmi, Vaishnavi C. Endodontic microbiology. *J Conserv Dent*

- 2010;13:233.
- 33 Lawrence Jeffrey G. Common themes in the genome strategies of pathogens. *Curr Opin Genet Dev* 2005:584–8.
- 34 Henderson B., Wilson M. Commensal communism and the oral cavity. *J Dent Res* 1998:1674–83.
- 35 Costerton J. W., Lewandowski Z., DeBeer D., Caldwell D., Korber D., James G. Biofilms, the customized microniche. *J Bacteriol* 1994:2137–42.
- 36 Costerton J. W., Stewart Philip S., Greenberg E. P. Bacterial biofilms: A common cause of persistent infections. *Science* (80-) 1999:1318–22.
- 37 Siqueira José F., Rôças Isabela N. Present status and future directions in endodontic microbiology. *Endod Top* 2014;30:3–22.
- 38 Sjögren U., Figdor D., Spångberg I., Sundqvist G. The antimicrobial effect of calcium hydroxide as a short-term intracanal dressing. *Int Endod J* 1991;24:119–25.
- 39 Haapasalo M., Ørstavik D. In vitro Infection and Disinfection of Dentinal Tubules. *J Dent Res* 1987;66:1375–9.
- 40 Safavi Kamran E., Spngberg Larz S.W., Langeland Kaare. Root canal dentinal tubule disinfection. *J Endod* 1990;16:207–10.
- 41 Siqueira José F., De Uzeda Milton. Disinfection by calcium hydroxide pastes of dentinal tubules infected with two obligate and one facultative anaerobic bacteria. *J Endod* 1996;22:674–6.
- 42 Heling I., Steinberg D., Kenig S., Gavrilovich I., Sela M. N., Friedman M. Efficacy of a sustained-release device containing chlorhexidine and Ca(OH)₂ in preventing secondary infection of dentinal tubules. *Int Endod J* 1992;25:20–4.
- 43 Wang Zhejun, Shen Ya, Haapasalo Markus. Effectiveness of endodontic disinfecting solutions against young and old *Enterococcus faecalis* biofilms in dentin canals. *J Endod* 2012;38:1376–9.
- 44 J Nygren. Radgivare Angaende Basta Sattet Att Varda Ah Bevara Tandernas Fuskhet. *Osv*

- Stock 1838.
- 45 BW Hermann. Calciumhydroxyd als mittel zurn behandel und füllen vonxahnwurzelkanälen. [Thesis]. Univ Würzbg 1920:50.
- 46 BW Hermann. Dentinobliteration der Wurzelkanalen nach Behandlung mit Kalzium. Zahnarztl Rundsch 1930;21:888–99.
- 47 BW Hermann. Der desinfektorische Wert des Calxyl. Zahnarztl Rundsch 1935;44:1929–34.
- 48 BW Hermann. Biologische Wurzelbehandlung. Frankfurt Arn Main W Kramer 1936.
- 49 Zander H.A. Reaction of the Pulp to Calcium Hydroxide. J Dent Res 1939;18:373–9.
- 50 Teuscher GW Zander HA. A preliminary report on pulpotomy. Northwest Univ Bull 1938;39:4.
- 51 Byström Anders, Claesson Rolf, Sundqvist Göran. The antibacterial effect of camphorated paramonochlorophenol, camphorated phenol and calcium hydroxide in the treatment of infected root canals. Dent Traumatol 1985;1:170–5.
- 52 Byström A., Sunvqvist G. The antibacterial action of sodium hypochlorite and EDTA in 60 cases of endodontic therapy. Int Endod J 1985;18:35–40.
- 53 Sjögren U., Figdor D., Spångberg I., Sundqvist G. The antimicrobial effect of calcium hydroxide as a short-term intracanal dressing. Int Endod J 1991;24:119–25.
- 54 Ørstavik D., Kerekes K., Molven O. Effects of extensive apical reaming and calcium hydroxide dressing on bacterial infection during treatment of apical periodontitis: a pilot study. Int Endod J 1991;24:1–7.
- 55 GH Garcia. Bosquejo historico sobre Endodoncia. Rev Esp Endod 1983;1:123–33.
- 56 Alliet P Vande Voorde H. Le role de l’hydroxyde de calcium en Endodontie. Rev Belge Med Dent 1988;43:24–39.
- 57 Fava L. R.G., Saunders W. P. Calcium hydroxide pastes: Classification and clinical indications. Int Endod J 1999:257–82.

References

- 58 Lopes Helio Pereira, Costa Filho Arlindo dos Santos da, Jones Júnior Joel. O emprego do hidróxido de cálcio associado ao azeite de oliva. RGO (Porto Alegre) 1986:306–13.
- 59 Estrela Carlos, Pimenta Fabiana Cristina, Ito Izabel Yoko, Bammann Lili Luschke. Antimicrobial evaluation of calcium hydroxide in infected dentinal tubules. J Endod 1999;25:416–8.
- 60 Imlay James A., Linn Stuart. DNA damage and oxygen radical toxicity. Sci Sci 1988;240:1302–9.
- 61 Halliwell Barry. Oxidants and human disease: some new concepts. FASEB J 1987;1:358–64.
- 62 Cotran RS, Kumar V Collins T. *Robbins Pathologic Basis of Disease*. 6th ed. Philadelphia, USA: W. B. Saunders; 1999. Chapter 1. 23-56.
- 63 Pacios María Gabriela, de la Casa María Luisa, de Bulacio María los Angeles, López María Elena. Influence of different vehicles on the pH of calcium hydroxide pastes. J Oral Sci 2004;46:107–11.
- 64 Alaçam Tayfun, Oguz Yoldaş H., Gülen Orhan. Dentin penetration of 2 calcium hydroxide combinations. Oral Surg Oral Med Oral Pathol Oral Radiol Endod 1998;86:469–72.
- 65 LRG Fava. Pastas de hidroxido de calcio. Consideracoes sobre seu emprego clinico em Endodontia. Rev Paul Odontol 1991;13:36–43.
- 66 Byström Anders, Claesson Rolf, Sundqvist Göran. The antibacterial effect of camphorated paramonochlorophenol, camphorated phenol and calcium hydroxide in the treatment of infected root canals. Dent Traumatol 1985;1:170–5.
- 67 Han G. Y., Park S. H., Yoon Tai Cheol. Antimicrobial activity of Ca(OH)₂ containing pastes with enterococcus faecalis in vitro. J Endod 2001;27:328–32.
- 68 Estrela Carlos. Two methods to evaluate the antimicrobial action of calcium hydroxide paste. J Endod 2001;27:720–3.
- 69 Shuping George B., Ørstavik Dag, Sigurdsson Asgeir, Trope Martin. Reduction of

- intracanal bacteria using nickel-titanium rotary instrumentation and various medications. *J Endod* 2000;26:751–5.
- 70 Liewehr Frederick R. Antimicrobial activity of several calcium hydroxide preparations in root canal dentin. *J Endod* 2001;27:765–7.
- 71 Stevens Roy H., Grossman Louis I. Evaluation of the antimicrobial potential of calcium hydroxide as an intracanal medicament. *J Endod* 1983;9:372–4.
- 72 Portenier Isabelle, Haapasalo H., Rye A., Waltimo T., Ørstavik D., Haapasalo M. Inactivation of root canal medicaments by dentine, hydroxylapatite and bovine serum albumin. *Int Endod J* 2001;34:184–8.
- 73 Adorno Carlos G, Yoshioka Takatomo, Suda Hideaki. The Effect of Root Preparation Technique and Instrumentation Length on the Development of Apical Root Cracks. *J Endod* 2009;35:389–92.
- 74 DiFiore Peter M., Peters Donald D., Setterstrom Jean A., Lorton Lewis. The antibacterial effects of calcium hydroxide apexification pastes on *Streptococcus sanguis*. *Oral Surgery, Oral Med Oral Pathol* 1983;55:91–4.
- 75 Siqueira José F., Lopes Hélio P., De Uzeda Milton. Recontamination of coronally unsealed root canals medicated with camphorated paramonochlorophenol or calcium hydroxide pastes after saliva challenge. *J Endod* 1998;24:11–4.
- 76 Safavi Kamran E., Spngberg Larz S.W., Langeland Kaare. Root canal dentinal tubule disinfection. *J Endod* 1990;16:207–10.
- 77 Haapasalo M., Ørstavik D. In vitro Infection and Disinfection of Dentinal Tubules. *J Dent Res* 1987;66:1375–9.
- 78 Waltimo Tuomas, Trope Martin, Haapasalo Markus, Ørstavik Dag. Clinical efficacy of treatment procedures in endodontic infection control and one year follow-up of periapical healing. *J Endod* 2005;31:863–6.
- 79 Weiger R., De Lucena J., Decker H. E., Löst C. Vitality status of microorganisms in infected human root dentine. *Int Endod J* 2002;35:166–71.

References

- 80 Ørstavik Dag, Haapasalo Markus. Disinfection by endodontic irrigants and dressings of experimentally infected dentinal tubules. *Dent Traumatol* 1990;6:142–9.
- 81 Zand Vahid, Mokhtari Hadi, Hasani Aila, Jabbari Golchin. Comparison of the Penetration Depth of Conventional and Nano-Particle Calcium Hydroxide into Dentinal Tubules. *IEJ Iran Endod J* 2017;12:366–70.
- 82 Berkiten Mustafa, Okar Imer, Berkiten Rahmiye. In Vitro study of the penetration of *Streptococcus sanguis* and *Prevotella intermedia* strains into human dentinal tubules. *J Endod* 2000;26:236–9.
- 83 Taschieri Silvio, Del Fabbro Massimo, Samaranayake Lakshman, Chang Jeffrey W.W., Corbella Stefano. Microbial invasion of dentinal tubules: a literature review and a new perspective. *J Investig Clin Dent* 2014;5:163–70.
- 84 Wang J. -D, Hume W. R. Diffusion of hydrogen ion and hydroxyl ion from various sources through dentine. *Int Endod J* 1988;21:17–26.
- 85 Nerwich Alan, Figdor David, Messer Harold H. pH changes in root dentin over a 4-week period following root canal dressing with calcium hydroxide. *J Endod* 1993;19:302–6.
- 86 Sathorn C., Parashos P., Messer H. Antibacterial efficacy of calcium hydroxide intracanal dressing: A systematic review and meta-analysis. *Int Endod J* 2007;2–10.
- 87 Kargul Betul, Welbury Richard. An audit of the time to initial treatment in avulsion injuries. *Dent Traumatol* 2009;25:123–5.
- 88 Pohl Yango, Wahl Gerhard, Filippi Andreas, Kirschner Horst. Results after replantation of avulsed permanent teeth. III. Tooth loss and survival analysis. *Dent Traumatol* 2005;21:102–10.
- 89 Glendor Ulf, Halling Arne, Andersson Lars, Eilert-Petersson Elsvig. Incidence of traumatic tooth injuries in children and adolescents in the county of Västmanland, Sweden. *Swed Dent J* 1996;20:15–28.
- 90 Andreasen JO, Andreasen FM. *Textbook and Color Atlas of Traumatic Injuries to the Teeth, 4th Edition*, 4th ed. Oxford, UK: Wiley- Blackwell; 2103. Chapter 4. 56-78.

- 91 Hammarström Lars, Pierce Angela, Blomlöf Leif, Feiglin Barry, Lindskog Sven. Tooth avulsion and replantation — A review. *Dent Traumatol* 1986;2:1–8.
- 92 Rincon J. C., Young W. G., Bartold P. M. The epithelial cell rests of Malassez - A role in periodontal regeneration? *J Periodontal Res* 2006;245–52.
- 93 Trope Martin. Root Resorption due to Dental Trauma. *Endod Top* 2002;1:79–100.
- 94 Lindskog Sven, Blomlof Leif, Hammarstrom Lars. Repair of periodontal tissues In vivo and in vitro. *J Clin Periodontol* 1983;10:188–205.
- 95 Andreasen J. O. The effect of pulp extirpation or root canal treatment on periodontal healing after replantation of permanent incisors in monkeys. *J Endod* 1981;7:245–52.
- 96 Andreasen J. O., Borum M. K., Jacobsen H. L., Andreasen F. M. Replantation of 400 avulsed permanent incisors. 4. Factors related to periodontal ligament healing. *Dent Traumatol* 1995;11:76–89.
- 97 Andreasen J. O., Hjørting-Hansen E. Replantation of teeth. I. Radiographic and clinical study of 110 human teeth replanted after accidental loss. *Acta Odontol Scand* 1966;24:263–86.
- 98 Chappuis Vivianne, Von Arx Thomas. Replantation of 45 avulsed permanent teeth: A 1-year follow-up study. *Dent Traumatol* 2005;21:289–96.
- 99 Tzigkounakis Vasileios, Merglová Vlasta, Hecová Hana, Netolický Jan. Retrospective clinical study of 90 avulsed permanent teeth in 58 children. *Dent Traumatol* 2008;24:598–602.
- 100 Andersson Lars, Andreasen Jens O., Day Peter, et al. Guidelines for the management of traumatic dental injuries: 2. avulsion of permanent teeth. *Pediatr Dent* 2017;412–9.
- 101 Andersson Lars, Andreasen Jens O., Day Peter, et al. International Association of Dental Traumatology guidelines for the management of traumatic dental injuries: 2. Avulsion of permanent teeth. *Dent Traumatol* 2012;28:88–96.
- 102 Trope M. Root resorption of dental and traumatic origin: classification based on etiology. *Pract Periodontics Aesthet Dent* 1998;10:515–22.

References

- 103 Tronstad Leif. Root resorption — etiology, terminology and clinical manifestations. *Dent Traumatol* 1988;241–52.
- 104 Malmgren Barbro, Malmgren Olle. Rate of infraposition of reimplanted ankylosed incisors related to age and growth in children and adolescents. *Dent Traumatol* 2002;18:28–36.
- 105 Pels Ragna, Sterry Wolfram, Lademann Jürgen. Clobetasol propionate - Where, when, why? *Drugs of Today* 2008;547–57.
- 106 Yasir Muhammad, Sonthalia Sidharth. *Corticosteroid Adverse Effects*. StatPearls Publishing; 2019.
- 107 Martin Charles R. Welcome to nanomedicine. *Nanomedicine* 2006;5.
- 108 Bouwmeester H, Dekkers S, Noordam M, et al. *Health impact of nanotechnologies in food production This report is a co-production of RIKILT and RIVM*. RIKILT Institute of Food Safety; 2007.
- 109 Butler M., Boyle J. J., Powell J. J., Playford R. J., Ghosh S. Dietary microparticles implicated in Crohn’s disease can impair macrophage phagocytic activity and act as adjuvants in the presence of bacterial stimuli. *Inflamm Res* 2007;56:353–61.
- 110 Chaudhry Qasim, Scotter Michael, Blackburn James, et al. Applications and implications of nanotechnologies for the food sector. *Food Addit Contam - Part A Chem Anal Control Expo Risk Assess* 2008:241–58.
- 111 Boisseau Patrick, Loubaton Bertrand. Nanomedicine, nanotechnology in medicine. *Comptes Rendus Phys* 2011:620–36.
- 112 Sprintz Michael, Tasciotti Ennio, Allegri Massimo, Grattoni Alessandro, Driver Larry C., Ferrari Mauro. Nanomedicine: Ushering in a new era of pain management. *Eur J Pain Suppl* 2011;5:317–22.
- 113 Satalkar Priya, Elger Bernice Simone, Shaw David M. Defining Nano, Nanotechnology and Nanomedicine: Why Should It Matter? *Sci Eng Ethics* 2016;22:1255–76.
- 114 LaVan David A., McGuire Terry, Langer Robert. Small-scale systems for in vivo drug

- delivery. *Nat Biotechnol* 2003;1184–91.
- 115 Schmalz Gottfried, Hickel Reinhard, van Landuyt Kirsten L., Reichl Franz Xaver. Nanoparticles in dentistry. *Dent Mater* 2017;1298–314.
- 116 Priyadarsini Subhashree, Mukherjee Sumit, Mishra Monalisa. Nanoparticles used in dentistry: A review. *J Oral Biol Craniofacial Res* 2018;58–67.
- 117 Besinis Alexandros, De Peralta Tracy, Tredwin Christopher J., Handy Richard D. Review of nanomaterials in dentistry: Interactions with the oral microenvironment, clinical applications, hazards, and benefits. *ACS Nano* 2015;2255–89.
- 118 Galler K. M., D’Souza R. N., Hartgerink J. D., Schmalz G. Scaffolds for dental pulp tissue engineering. *Adv Dent Res* 2011;333–9.
- 119 Freitas Robert A. Molecular robots and other high-tech possibilities. *J Am Dent Assoc* 2000;131:1559–65.
- 120 Aeran Himanshu, Kumar Varun, Uniyal Shashank, Tanwer Pooja. Nanodentistry: Is just a fiction or future. *J Oral Biol Craniofacial Res* 2015;207–11.
- 121 Raura Natasha, Garg Anirudh, Arora Arpit, Roma M. Nanoparticle technology and its implications in endodontics: a review. *Biomater Res* 2020;21.
- 122 Shrestha Annie, Kishen Anil. Antibacterial Nanoparticles in Endodontics: A Review. *J Endod* 2016;1417–26.
- 123 Saafan Ali, Zaazou Mohamed H., Sallam Marwa K., Mosallam Osama, El Danaf Heba A. Assessment of Photodynamic Therapy and Nanoparticles Effects on Caries Models. *Open Access Maced J Med Sci* 2018;6:1289–95.
- 124 Kishen Anil, Shi Zhilong, Shrestha Annie, Neoh Koon Gee. An Investigation on the Antibacterial and Antibiofilm Efficacy of Cationic Nanoparticulates for Root Canal Disinfection. *J Endod* 2008;34:1515–20.
- 125 Shrestha Annie, Zhilong Shi, Gee Neoh Koon, Kishen Anil. Nanoparticulates for antibiofilm treatment and effect of aging on its antibacterial activity. *J Endod* 2010;36:1030–5.

- 126 Fan Wei, Wu Daming, Ma Tengjiao, Fan Bing. Ag-loaded mesoporous bioactive glasses against *Enterococcus faecalis* biofilm in root canal of human teeth. *Dent Mater J* 2015;34:54–60.
- 127 Wu Daming, Fan Wei, Kishen Anil, Gutmann James L., Fan Bing. Evaluation of the antibacterial efficacy of silver nanoparticles against *Enterococcus faecalis* biofilm. *J Endod* 2014;40:285–90.
- 128 Kishen Anil. Advanced therapeutic options for endodontic biofilms. *Endod Top* 2010;22:99–123.
- 129 Suffredini G., East J. E., Levy Lucien M. New applications of nanotechnology for neuroimaging. *Am J Neuroradiol* 2014:1246–53.
- 130 Virlan Maria Justina Roxana, Miricescu Daniela, Totan Alexandra, et al. Current uses of poly(lactic-co-glycolic acid) in the dental field: A comprehensive review. *J Chem* 2015.
- 131 Danhier Fabienne, Ansorena Eduardo, Silva Joana M., Coco Régis, Le Breton Aude, Prétat Véronique. PLGA-based nanoparticles: An overview of biomedical applications. *J Control Release* 2012:505–22.
- 132 Anderson James M., Shive Matthew S. Biodegradation and biocompatibility of PLA and PLGA microspheres. *Adv Drug Deliv Rev* 2012:72–82.
- 133 Astete Carlos E., Sabliov Cristina M. Synthesis and characterization of PLGA nanoparticles. *J Biomater Sci Polym Ed* 2006:247–89.
- 134 Sánchez-López Elena, Ettcheto Miren, Egea Maria Antonia, et al. New potential strategies for Alzheimer's disease prevention: pegylated biodegradable dexibuprofen nanospheres administration to APP^{swe}/PS1^{dE9}. *Nanomedicine Nanotechnology, Biol Med* 2017;13:1171–82.
- 135 Hou Xiandeng, Jones Bradley T. Inductively Coupled Plasma-Optical Emission Spectrometry. *Encycl. Anal. Chem.*, vol. 3. Chichester, UK: John Wiley & Sons, Ltd; 2008. Chapter 2. 24–33.
- 136 Sánchez-López E., Egea M. A., Cano A., et al. PEGylated PLGA nanospheres optimized

- by design of experiments for ocular administration of dexibuprofen-in vitro, ex vivo and in vivo characterization. *Colloids Surfaces B Biointerfaces* 2016;145:241–50.
- 137 Vega Estefanía, Egea M. Antònia, Garduño-Ramírez M. Luisa, et al. Flurbiprofen PLGA-PEG nanospheres: Role of hydroxy- β -cyclodextrin on ex vivo human skin permeation and in vivo topical anti-inflammatory efficacy. *Colloids Surfaces B Biointerfaces* 2013;110:339–46.
- 138 Abrego Guadalupe, Alvarado Helen L., Egea Maria A., Gonzalez-Mira Elizabeth, Calpena Ana C., Garcia Maria L. Design of nanosuspensions and freeze-dried PLGA nanoparticles as a novel approach for ophthalmic delivery of pranoprofen. *J Pharm Sci* 2014;103:3153–64.
- 139 Andreani Tatiana, Miziara Leonardo, Lorenzón Esteban N., et al. Effect of mucoadhesive polymers on the in vitro performance of insulin-loaded silica nanoparticles: Interactions with mucin and biomembrane models. *Eur J Pharm Biopharm* 2015;93:118–26.
- 140 Fangueiro Joana F., Andreani Tatiana, Egea Maria A., et al. Design of cationic lipid nanoparticles for ocular delivery: Development, characterization and cytotoxicity. *Int J Pharm* 2014;461:64–73.
- 141 Khachani M, Hamidi A El, Halim M, Arsalane S. Non-isothermal kinetic and thermodynamic studies of the dehydroxylation process of synthetic calcium hydroxide Ca(OH) 2. *J Mater Environ Sci* 2014;5:615–24.
- 142 Badıllı Ulya, Şen Tangül, Tarımcı Nilüfer. Microparticulate based topical delivery system of clobetasol propionate. *AAPS PharmSciTech* 2011;12:949–57.
- 143 Mohan Dixit C., Suresh Akhil, Mukundan Shilpa, Gupta Swati, Viswanad Vidya. Development and in vitro evaluation of nanolipid carriers of clobetasol propionate and pramoxine hydrochloride for topical delivery. *Int J Appl Pharm* 2018;10:28–36.
- 144 Sha W., O'Neill E. A., Guo Z. Differential scanning calorimetry study of ordinary Portland cement. *Cem Concr Res* 1999;29:1487–9.
- 145 Zhang Yong, Huo Meirong, Zhou Jianping, Xie Shaofei. PKSolver: An add-in program

- for pharmacokinetic and pharmacodynamic data analysis in Microsoft Excel. *Comput Methods Programs Biomed* 2010;99:306–14.
- 146 Ramos Yacasi Gladys Rosario, Calpena Campmany Ana Cristina, Egea Gras María Antonia, Espina García Marta, García López María Luisa. Freeze drying optimization of polymeric nanoparticles for ocular flurbiprofen delivery: effect of protectant agents and critical process parameters on long-term stability. *Drug Dev Ind Pharm* 2017;43:637–51.
- 147 Ramos Yacasi Gladys Rosario, García López María Luisa, Espina García Marta, Parra Coca Alexander, Calpena Campmany Ana Cristina. Influence of freeze-drying and γ -irradiation in preclinical studies of flurbiprofen polymeric nanoparticles for ocular delivery using d-(+)-trehalose and polyethylene glycol. *Int J Nanomedicine* 2016;11:4093–106.
- 148 Gonzalez-Pizarro Roberto, Parrotta Graziella, Vera Rodrigo, et al. Ocular penetration of fluorometholone-loaded PEG-PLGA nanoparticles functionalized with cell-penetrating peptides. *Nanomedicine* 2019;14:3089–104.
- 149 Pérez Alfayate Ruth. Ensayo aleatorizado “in vitro” sobre la capacidad de obturación de tres sistemas con vástago en conductos curvos 2016.
- 150 Alghamdi Faisal, Shakir Marwa. The Influence of *Enterococcus faecalis* as a Dental Root Canal Pathogen on Endodontic Treatment: A Systematic Review. *Cureus* 2020;12.
- 151 Chávez De Paz Villanueva Luis Eduardo. *Fusobacterium nucleatum* in endodontic flare-ups. *Oral Surg Oral Med Oral Pathol Oral Radiol Endod* 2002;93:179–83.
- 152 Tomazinho Luiz Fernando, Avila-Campos Mario J. Detection of *Porphyromonas gingivalis*, *Porphyromonas endodontalis*, *Prevotella intermedia*, and *Prevotella nigrescens* in chronic endodontic infection. *Oral Surgery, Oral Med Oral Pathol Oral Radiol Endodontology* 2007;103:285–8.
- 153 *M02-A12 Performance Standards for Antimicrobial Disk Susceptibility Tests; Approved Standard-Twelfth Edition*. 2015.
- 154 *M07-A10 Methods for Dilution Antimicrobial Susceptibility Tests for Bacteria That Grow Aerobically; Approved Standard-Tenth Edition*. 2015.

- 155 Siqueira José F., Rôças Isabela N., Silva Marlei G. Prevalence and Clonal Analysis of *Porphyromonas gingivalis* in Primary Endodontic Infections. *J Endod* 2008;34:1332–6.
- 156 Gomes B. P. F. A., Jacinto R. C., Pinheiro E. T., et al. *Porphyromonas gingivalis*, *Porphyromonas endodontalis*, *Prevotella intermedia* and *Prevotella nigrescens* in endodontic lesions detected by culture and by PCR. *Oral Microbiol Immunol* 2005;20:211–5.
- 157 Rôças Isabela N., Siqueira José F., Santos Kátia R.N., Coelho Ana M.A. “Red complex” (*Bacteroides forsythus*, *Porphyromonas gingivalis*, and *Treponema denticola*) in endodontic infections: A molecular approach. *Oral Surg Oral Med Oral Pathol Oral Radiol Endod* 2001;91:468–71.
- 158 Holt Stanley C., Ebersole Jeffrey L. *Porphyromonas gingivalis*, *Treponema denticola*, and *Tannerella forsythia*: The “red complex”, a prototype polybacterial pathogenic consortium in periodontitis. *Periodontol 2000* 2005;72–122.
- 159 Balouiri Mounyr, Sadiki Moulay, Ibsouda Saad Koraichi. Methods for in vitro evaluating antimicrobial activity : A review \$. *J Pharm Anal* 2016;6:71–9.
- 160 Delgado Luis M., Fuller Kieran, Zeugolis Dimitrios I. Collagen Cross-Linking: Biophysical, Biochemical, and Biological Response Analysis. *Tissue Eng - Part A* 2017;23:1064–77.
- 161 Delgado Luis M., Shologu Naledi, Fuller Kieran, Zeugolis Dimitrios I. Acetic acid and pepsin result in high yield, high purity and low macrophage response collagen for biomedical applications. *Biomed Mater* 2017;12.
- 162 Midgley H. G. The determination of calcium hydroxide in set Portland cements. *Cem Concr Res* 1979;9:77–82.
- 163 Milestone N. B. Hydration of Tricalcium Silicate in the Presence of Lignosulfonates, Glucose, and Sodium Gluconate. *J Am Ceram Soc* 1979;62:321–4.
- 164 Patel Sajal Manubhai, Nail Steven L., Pikal Michael J., et al. Lyophilized Drug Product Cake Appearance: What Is Acceptable? *J Pharm Sci* 2017:1706–21.

- 165 Komabayashi Takashi, D'souza Rena N., Dechow Paul C., Safavi Kamran E., Spångberg Larz S.W. Particle Size and Shape of Calcium Hydroxide. *J Endod* 2009;35:284–7.
- 166 Shrestha Annie, Zhilong Shi, Gee Neoh Koon, Kishen Anil. Nanoparticulates for antibiofilm treatment and effect of aging on its antibacterial activity. *J Endod* 2010;36:1030–5.
- 167 Javidi Maryam, Afkhami Farzaneh, Zarei Mina, Ghazvini Kiarash, Rajabi Omid. Efficacy of a combined nanoparticulate/calcium hydroxide root canal medication on elimination of *Enterococcus faecalis*. *Aust Endod J* 2014;40:61–5.
- 168 Pagonis Tom C, Chen Judy, Fontana Carla Raquel, et al. Nanoparticle-based endodontic antimicrobial photodynamic therapy. *J Endod* 2010;36:322.
- 169 Farhadian Negin, Godiny Mostafa, Moradi Sajad, Hemati Azandaryani Abbas, Shahlaei Mohsen. Chitosan/gelatin as a new nano-carrier system for calcium hydroxide delivery in endodontic applications: Development, characterization and process optimization. *Mater Sci Eng C* 2018;92:540–6.
- 170 Danaei M., Dehghankhold M., Ataei S., et al. Impact of particle size and polydispersity index on the clinical applications of lipidic nanocarrier systems. *Pharmaceutics* 2018.
- 171 Love Robert M. Invasion of dentinal tubules by root canal bacteria. *Endod Top* 2004;9:52–65.
- 172 Lenzi Tathiane L., Guglielmi Camila De Almeida B., Arana-Chavez Victor E., Raggio Daniela P. Tubule density and diameter in coronal dentin from primary and permanent human teeth. *Microsc Microanal* 2013;19:1445–9.
- 173 Siqueira José F. Endodontics Strategies to Treat Infected Root Canals. *Journal Of The California Dental Association*. 2001.
- 174 Rodriguez-Navarro Carlos, Burgos-Cara Alejandro, Lorenzo Fulvio Di, Ruiz-Agudo Encarnacion, Elert Kerstin. Nonclassical Crystallization of Calcium Hydroxide via Amorphous Precursors and the Role of Additives. *Cryst Growth Des* 2020;20:4418–32.
- 175 Estrela C., Pesce H. F. Chemical analysis of the formation of calcium carbonate and its

- influence on calcium hydroxide pastes in connective tissue of the dog--Part II. *Braz Dent J* 1997;8:49–53.
- 176 Gupta Shailendra. An in vitro Study of Diffusibility and Degradation of Three Calcium Hydroxide Pastes. *Int J Clin Pediatr Dent* 2011;4:15–23.
- 177 Tziafas Dimitrios, Economides Nikolaos. Formation of crystals on the surface of calcium hydroxide-containing materials in vitro. *J Endod* 1999;25:539–42.
- 178 Kapolos John, Koutsoukos Petros G. Formation of calcium phosphates in aqueous solutions in the presence of carbonate ions. *Langmuir* 1999;15:6557–62.
- 179 Chaikina Marina V., Bulina Natalia V., Vinokurova Olga B., Prosanov Igor Yu, Dudina Dina V. Interaction of calcium phosphates with calcium oxide or calcium hydroxide during the “soft” mechanochemical synthesis of hydroxyapatite. *Ceram Int* 2019;45:16927–33.
- 180 Van Meerbeek Bart, Vargas Marcos, Inoue Satoshi, et al. Microscopy investigations. Techniques, results, limitations. *Am J Dent* 2000;13:3D-18D.
- 181 Patel D. V., Sherriff M., Ford T. R.P., Watson T. F., Mannocci F. The penetration of RealSeal primer and Tubliseal into root canal dentinal tubules: A confocal microscopic study. *Int Endod J* 2007;40:67–71.
- 182 Deniz Sungur Derya, Aksel Hacer, Purali Nuhan. Effect of a Low Surface Tension Vehicle on the Dentinal Tubule Penetration of Calcium Hydroxide and Triple Antibiotic Paste. *J Endod* 2017;43:452–5.
- 183 Abdulkader A., Duguid R., Saunders E. M. The antimicrobial activity of endodontic sealers to anaerobic bacteria. *Int Endod J* 1996;29:280–3.
- 184 Siqueira José F., Gonçalves Reginaldo Bruno. Antibacterial activities of root canal sealers against selected anaerobic bacteria. *J Endod* 1996;22:79–80.
- 185 del Carpio-Perochena Aldo, Kishen Anil, Felitti Rafael, et al. Antibacterial Properties of Chitosan Nanoparticles and Propolis Associated with Calcium Hydroxide against Single- and Multispecies Biofilms: An In Vitro and In Situ Study. *J Endod* 2017;43:1332–6.

References

- 186 Pinto Reis Catarina, Neufeld Ronald J., Ribeiro António J., Veiga Francisco. Nanoencapsulation I. Methods for preparation of drug-loaded polymeric nanoparticles. *Nanomedicine Nanotechnology, Biol Med* 2006;8–21.
- 187 Fontana M. C., Coradini K., Guterres S. S., Pohlmann A. R., Beck R. C.R. Nanoencapsulation as a way to control the release and to increase the photostability of clobetasol propionate: Influence of the nanostructured system. *J Biomed Nanotechnol* 2009;5:254–63.
- 188 Campisi G., Giandalia G., De Caro V., Di Liberto C., Aricò P., Giannola L. I. A new delivery system of clobetasol-17-propionate (lipid-loaded microspheres 0.025%) compared with a conventional formulation (lipophilic ointment in a hydrophilic phase 0.025%) in topical treatment of atrophic/erosive oral lichen planus. A Phase IV, randomized, observer-blinded, parallel group clinical trial. *Br J Dermatol* 2004;150:984–90.
- 189 Sánchez-López Elena, Ettcheto Miren, Egea Maria Antonia, et al. Memantine loaded PLGA PEGylated nanoparticles for Alzheimer’s disease: In vitro and in vivo characterization. *J Nanobiotechnology* 2018;16:32.
- 190 Lopez-Castejon Gloria, Brough David. Understanding the mechanism of IL-1 β secretion. *Cytokine Growth Factor Rev* 2011:189–95.
- 191 Madej Mariusz P., Töpfer Elfi, Boraschi Diana, Italiani Paola. Different regulation of interleukin-1 production and activity in monocytes and macrophages: Innate memory as an endogenous mechanism of IL-1 inhibition. *Front Pharmacol* 2017;8.
- 192 Rutzke Michael A. Atomic absorption, inductively coupled plasma optical emission spectroscopy, and infrared spectroscopy. *Encycl. Earth Sci. Ser.* Springer Netherlands; 2018. Chapter 3. 76–83.

LIST OF FIGURES AND TABLES

11. LIST OF FIGURES AND TABLES

11.1 List of figures

FIGURE 1 DYNAMICS OF THE PULPAL RESPONSE TO MICROBIAL ASSULT (A) RESPONSE FROM CARIES EXPOSURE (B) PULP INFLAMMATION (C) PULPAL NECROSIS (D) APICAL PERIODONTITIS FORMATION .	42
FIGURE 2 SCANNING ELECTRON MICROSCOPE IMAGE OF DENTINAL TUBULES CROSS SECTIONAL VIEW WITH $\times 2000$ MAGNIFICATION (COURTESY OF DR JUAN GONZALO OLIVIERI FERNÁNDEZ).	43
FIGURE 3 DYNAMICS OF TOOTH AVULSION INJURY.	49
FIGURE 4 PREAPICAL RADIOGRAPHS DISPLAYING A CASE OF REPLACEMENT RESORPTION AFTER AN AVULSED TOOTH WITH EXTENDED DRY EXTRA ORAL TIME WAS REIMPLANTED. (A) TOOTH IMMEDIATELY AFTER REIMPLANTATION. (B) TOOTH AT FOLLOW UP APPOINTMENT DISPLAYING SIGNS OF REPLACEMENT RESORPTION AROUND THE ROOT. (COURTESY OF DR JOSÉ ANTONIO GONZÁLEZ SÁNCHEZ).	51
FIGURE 5 PROGRESSION OF EXTERNAL INFLAMMATORY ROOT RESORPTION FOR AN AVULSED TOOTH AFTER REIMPLANTATION.	52
FIGURE 6 MAIN BIOCHEMICAL PATHWAYS OF ARACHIDONIC ACID.	55
FIGURE 7 DIFFERENT TYPES OF NPs CLASSIFIED IN ACCORDANCE TO THEIR STRUCTURAL CONFIGURATION.	57
FIGURE 8 DIFFERENT TYPES OF DENTAL APPLICATIONS FOR NPs.	58
FIGURE 9 POLYMERIC BIODEGRADABLE NANOPARTICLES. (A) NANOCAPSULES. (B) NANOSPHERES (129).	59
FIGURE 10 SCHEME SHOWING THE STEPS AND THE EXPERIMENTS THAT WERE CARRIED OUT.	73
FIGURE 11 SOLVENT DISPLACEMENT METHOD.	75
FIGURE 12 INDUCTIVELY COUPLED PLASMA OPTICAL EMISSION SPECTROSCOPY.	76
FIGURE 13 SCHEME EXPLAINING THE STEP FOR CALCULATING THE CONCENTRATION OF CALCIUM HYDROXIDE IN THE SAMPLES.	78
FIGURE 14 TEETH SECTIONING USING DIAMOND SECTION MACHINE.	86
FIGURE 15 SCHEME EXPLAINING THE AGAR DIFFUSION TEST.	88
FIGURE 16 SCHEME SHOWING BROTH MICRODILUTION FOR ANTIBACTERIAL TESTING AS RECOMMENDED BY CLSI PROTOCOL (167).	89
FIGURE 17 PARETO'S CHARTS OF THE EFFECT OF THE INDEPENDENT VARIABLES.	100
FIGURE 18 SURFACE RESPONSE DIAGRAMS FOR CALCIUM HYDROXIDE CONCENTRATION.	100
FIGURE 19 SURFACE RESPONSE DIAGRAMS FOR PLGA CONCENTRATION.	101
FIGURE 20 SURFACE RESPONSE DIAGRAMS FOR LUTROL CONCENTRATION.	102
FIGURE 21 SURFACE RESPONSE DIAGRAMS FOR PH VALUES.	103

- FIGURE 22** TRANSMISSION ELECTRON MICROSCOPY OF CALCIUM HYDROXIDE NANOPARTICLES. (A) VISUALIZATION OF THE CALCIUM HYDROXIDE NANOPARTICLES AT 100NM SCALE BAR. (B) MEASUREMENT OF THE SIZE OF THE CALCIUM HYDROXIDE NANOPARTICLE WITH DIMENSIONS OF 141.91 NM X 143.85 NM AT 100NM SCALE BAR. (C) VISUALIZATION OF THE CALCIUM HYDROXIDE NANOPARTICLES AT 200NM SCALE BAR. (D) VISUALIZATION OF THE CALCIUM HYDROXIDE NANOPARTICLES AT 5MM SCALE BAR. 105
- FIGURE 23** X-RAY DIFFRACTION ANALYSIS OF CALCIUM HYDROXIDE NANOPARTICLES NANOPARTICLES AND FREE DRUG. 107
- FIGURE 24** FOURIER TRANSFORMED INFRA-RED ANALYSIS OF CALCIUM HYDROXIDE NANOPARTICLES NANOPARTICLES AND FREE DRUG. 107
- FIGURE 25** DIFFERENTIAL SCANNING CALORIMETRY ANALYSIS OF CALCIUM HYDROXIDE NANOPARTICLES NANOPARTICLES AND FREE DRUG. 108
- FIGURE 26** DRUG RELEASE PROFILE OF THE CALCIUM HYDROXIDE NANOPARTICLES AND THE FREE CALCIUM HYDROXIDE. (A) CUMULATIVE DRUG RELEASE OF THE CALCIUM HYDROXIDE NANOPARTICLES AND THE FREE CALCIUM HYDROXIDE AFTER THE FIRST 12 HOURS. (B) CUMULATIVE DRUG RELEASE OF THE CALCIUM HYDROXIDE NANOPARTICLES AND THE FREE CALCIUM HYDROXIDE AFTER THE 48 HOURS. (C) DRUG RELEASE OF THE CALCIUM HYDROXIDE NANOPARTICLES AFTER 48 HOURS FITTED TO A ONE-COMPARTMENTAL MODEL (BLUE LINE). (D) DRUG RELEASE OF THE FREE CALCIUM HYDROXIDE AFTER 48 HOURS FITTED TO A ONE-COMPARTMENTAL MODEL (BLUE LINE). 110
- FIGURE 27** FREEZE DRYING OF THE NANOPARTICLES. (A) COMBINATIONS OF CRYOPROTECTANTS TESTED. (B) POTENTIAL SUITABLE COMBINATION. (C) COMBINATION OF 5% OF (2-HYDROXYPROPYL)-B-CYCLODEXTRIN AND 15% D-MANNITOL BEFORE RESUSPENSION. (D) COMBINATION OF 5% OF (2-HYDROXYPROPYL)-B-CYCLODEXTRIN AND 15% D-MANNITOL AFTER RESUSPENSION. 113
- FIGURE 28** DEPTH OF PENETRATION OF THE NANOPARTICLES AND THE FREE DRUG INSIDE THE DENTINAL TUBULES. (A) DEPTH OF PENETRATION OF THE FREE CALCIUM HYDROXIDE DRUG MIXED WITH RHODAMINE INSIDE THE DENTINAL TUBULES. (B) DEPTH OF PENETRATION OF THE CALCIUM HYDROXIDE NANOPARTICLES LABELLED WITH RHODAMINE INSIDE THE DENTINAL TUBULES. 115
- FIGURE 29** DEPTH OF PENETRATION OF THE NANOPARTICLES AND THE FREE DRUG INSIDE THE DENTINAL TUBULES. (A) DEPTH OF PENETRATION OF THE FREE CALCIUM HYDROXIDE DRUG MIXED WITH RHODAMINE INSIDE THE DENTINAL TUBULES. (B) DEPTH OF PENETRATION OF THE CALCIUM HYDROXIDE NANOPARTICLES LABELLED WITH RHODAMINE INSIDE THE DENTINAL TUBULES. 116
- FIGURE 30** CONFOCAL IMAGE OF A CONTROL SAMPLE TREATED ONLY WITH STERILE SALINE. 117
- FIGURE 31** TWO SAMPLES OF AGAR PLATES HARVESTING PORPHYROMONAS GINGIVALIS BACTERIA. (A) AGAR PLATE DISPLAYING THE GROWTH INHIBITION ZONES AROUND THE $\text{Ca}(\text{OH})_2$ NPS AFTER INCUBATION FOR 48 HOURS. (B) AGAR PLATE DISPLAYING THE GROWTH INHIBITION ZONES AROUND THE $\text{Ca}(\text{OH})_2$ NPS AFTER INCUBATION FOR 24 HOURS. 119
- FIGURE 32** (A) CALIBRATION CURVE FOR CLOBETASOL PROPIONATE STANDARDS. (B) PEAK ACHIEVED BY CLOBETASOL PROPIONATE STANDARDS. 124

FIGURE 33 PARETO'S CHARTS OF THE EFFECT OF THE INDEPENDENT VARIABLES.	128
FIGURE 34 SURFACE RESPONSE DIAGRAMS FOR CLOBETASOL CONCENTRATION.	128
FIGURE 35 SURFACE RESPONSE DIAGRAMS FOR PLGA CONCENTRATION.	129
FIGURE 36 SURFACE RESPONSE DIAGRAMS FOR TWEEN [®] 80 CONCENTRATION.	130
FIGURE 37 SURFACE RESPONSE DIAGRAMS FOR PH VALUES.	131
FIGURE 38 TRANSMISSION ELECTRON MICROSCOPY OF CLOBETASOL NPs. (A) VISUALIZATION OF THE CLOBETASOL NPs AT 100NM SCALE BAR. (B) VISUALIZATION OF THE CLOBETASOL NPs AT 200 NM SCALE BAR. (C) VISUALIZATION OF THE CLOBETASOL NPs AT 500NM SCALE BAR. (D) VISUALIZATION OF THE CLOBETASOL NPs AT 10MM SCALE BAR.	133
FIGURE 39 X-RAY DIFFRACTION ANALYSIS OF CLOBETASOL PROPIONATE NANOPARTICLES AND FREE DRUG.	135
FIGURE 40 FOURIER TRANSFORMED INFRA-RED ANALYSIS OF CLOBETASOL PROPIONATE NANOPARTICLES AND FREE DRUG.	135
FIGURE 41 DIFFERENTIAL SCANNING CALORIMETRY ANALYSIS OF CLOBETASOL PROPIONATE NANOPARTICLES AND FREE DRUG.	136
FIGURE 42 CUMULATIVE DRUG RELEASE OF THE CLOBETASOL PROPIONATE/PLGA NANOPARTICLES AND FREE CLOBETASOL PROPIONATE BY PERCENTAGE AFTER THE FIRST 48 HOURS ADJUSTED BY THE KORSMEYER-PEPPAS MODEL.	138
FIGURE 43 DEPTH OF PENETRATION OF THE NANOPARTICLES AND THE FREE DRUG INSIDE THE DENTINAL TUBULES. (A) DEPTH OF PENETRATION OF THE FREE CLOBETASOL PROPIONATE MIXED WITH RHODAMINE INSIDE THE DENTINAL TUBULES. (B) DEPTH OF PENETRATION OF THE CLOBETASOL PROPIONATE/PLGA NANOPARTICLES LABELLED WITH RHODAMINE INSIDE THE DENTINAL TUBULES.	141
FIGURE 44 CELL METABOLIC ACTIVITY OF MACROPHAGES EXPRESSED IN TERMS OF COLOR CHANGE DUE TO REDUCTION OF ALAMARBLUE [®] IN RESPONSE TO TISSUE CULTURE PLASTIC (TCP), LIPOPOLYSACCHARIDE (LPS) AND CLOBETASOL PROPIONATE/PLGA NANOPARTICLES WITH DIFFERENT CONCENTRATIONS AT DIFFERENT PERIODS OF 24 AND 48 HOURS.	143
FIGURE 45 MICROSCOPIC IMAGE REPRESENTING THE MACROPHAGES RESPONSE TO TISSUE CULTURE PLASTIC (TCP), LIPOPOLYSACCHARIDE (LPS) AND CLOBETASOL PROPIONATE/PLGA NANOPARTICLES WITH DIFFERENT CONCENTRATIONS AT DIFFERENT PERIODS OF 24 AND 48 HOURS.	143
FIGURE 46 METABOLIC ACTIVITY OF MACROPHAGES IN RESPONSE TO TISSUE CULTURE PLASTIC (TCP), LIPOPOLYSACCHARIDE (LPS) AND CLOBETASOL PROPIONATE/PLGA NANOPARTICLES WITH DIFFERENT CONCENTRATIONS AT DIFFERENT PERIODS OF 24 AND 48 HOURS MEASURED BY ALAMARBLUE [®] REDUCTION WITH ABSORBANCE AT 570 AND 600 NM.	144
FIGURE 47 INFLAMMATORY CYTOKINES RELEASE OF TNF-A FROM MACROPHAGES IN RESPONSE TO TISSUE CULTURE PLASTIC (TCP), LIPOPOLYSACCHARIDE (LPS) AND CLOBETASOL PROPIONATE/PLGA NANOPARTICLES WITH DIFFERENT CONCENTRATIONS AT DIFFERENT PERIODS OF 24 AND 48 HOURS.	145

- FIGURE 48** INFLAMMATORY CYTOKINES RELEASE OF IL-1BETA FROM MACROPHAGES IN RESPONSE TO TISSUE CULTURE PLASTIC (TCP), LIPOPOLYSACCHARIDE (LPS) AND CLOBETASOL PROPIONATE/PLGA NANOPARTICLES WITH DIFFERENT CONCENTRATIONS AT DIFFERENT PERIODS OF 24 AND 48 HOURS.. 146
- FIGURE 49** INFLAMMATORY CYTOKINES RELEASE OF TNF-A FROM MACROPHAGES PRETREATED WITH LIPOPOLYSACCHARIDE (LPS) IN RESPONSE TO TISSUE CULTURE PLASTIC (TCP), LIPOPOLYSACCHARIDE PERMANENT (LPS PERM), LIPOPOLYSACCHARIDE REMOVED (LPS REF) AND CLOBETASOL PROPIONATE/PLGA NANOPARTICLES WITH DIFFERENT CONCENTRATIONS AT 48 HOURS 146
- FIGURE 50** INFLAMMATORY CYTOKINES RELEASE OF IL-1BETA FROM MACROPHAGES PRETREATED WITH LIPOPOLYSACCHARIDE (LPS) IN RESPONSE TO TISSUE CULTURE PLASTIC (TCP), LIPOPOLYSACCHARIDE PERMANENT (LPS PERM), LIPOPOLYSACCHARIDE REMOVED (LPS REF) AND CLOBETASOL PROPIONATE/PLGA NANOPARTICLES WITH DIFFERENT CONCENTRATIONS AT 48 HOURS. 147

11.2 List of tables

TABLE 1 CONDITIONS UTILIZED FOR FREEZE-DRYING.	83
TABLE 2 DISTRIBUTION OF THE SAMPLES USED FOR THE CONFOCAL LASER SCANNING MICROSCOPY TEST.	85
TABLE 3 CONCENTRATIONS USED FOR THE PREPARED SAMPLES	95
TABLE 4 PHYSICOCHEMICAL PARAMETERS OF THE PREFORMULATED SAMPLES	96
TABLE 5 CALCULATING THE RATIO OF CALCIUM CONCENTRATION	96
TABLE 6 VALUES OF THE MATRIX OF A FACTORIAL DESIGN OF CONCENTRATION PARAMETERS AND MEASURED RESPONSE.	98
TABLE 7 PHYSICOCHEMICAL PARAMETERS OF Ca(OH) ₂ NPs OPTIMIZED FORMULATION	104
TABLE 8 PHYSICOCHEMICAL PARAMETERS OF THE SAMPLES STORED AT DIFFERENT TEMPERATURES	109
TABLE 9 CRYOPROTECTANTS ASSESSED AND PHYSICOCHEMICAL PARAMETERS OF THE RESUSPENDED FREEZE DRIED CALCIUM HYDROXIDE NANOPARTICLES (HPBCD; (2-HYDROXYPROPYL)-B-CYCLODEXTRIN, PEG; POLYETHYLENE GLYCOL 3350).	112
TABLE 10 PHYSICOCHEMICAL PARAMETERS OF THE FORMULATION WITH 5% HPBCD + 15% MANNITOL REPEATED IN SEXTUPPLICATE HPBCD; (2-HYDROXYPROPYL)-B-CYCLODEXTRIN).	113
TABLE 11 PHYSICOCHEMICAL PARAMETERS OF THE NANOPARTICLES BEFORE AND AFTER STERILIZATION VIA Γ RADIATION	114
TABLE 12 COMPARISON OF THE CONFOCAL RESULTS BETWEEN THE FREE DRUG AND THE CALCIUM HYDROXIDE NANOPARTICLES.	117
TABLE 13 ABSORBANCE RATES OBSERVED USING SPECTROPHOTOMETER IN THE SAMPLES AFTER INCUBATION FOR 24 HOURS.	120
TABLE 14 PHYSICOCHEMICAL PARAMETERS OF THE PREFORMULATED SAMPLES	122
TABLE 15 RESULTS OF DIFFERENT SAMPLE TREATMENTS FOR HPLC QUANTIFICATION DMSO; DIMETHYL SULFOXIDE, METH; METHANOL .	125
TABLE 16 VALUES OF THE MATRIX OF A FACTORIAL DESIGN OF CONCENTRATION PARAMETERS AND MEASURED RESPONSES.	126
TABLE 17 PHYSICOCHEMICAL CHARACTERISTICS OF THE OPTIMIZED FORMULATION	133
TABLE 18 PHYSICOCHEMICAL PARAMETERS OF THE SAMPLES STORED AT DIFFERENT TEMPERATURES.	137
TABLE 19 CRYOPROTECTANTS ASSESSED AND PHYSICOCHEMICAL PARAMETERS OF THE RESUSPENDED FREEZE DRIED CLOBETASOL PROPIONATE NANOPARTICLES. (HPBCD; (2-HYDROXYPROPYL)-B-CYCLODEXTRIN).	139
TABLE 20 PHYSICOCHEMICAL PARAMETERS OF THE NANOPARTICLES BEFORE AND AFTER STERILIZATION VIA Γ RADIATION	140
TABLE 21 COMPARISON OF THE CONFOCAL MICROSCOPY RESULTS BETWEEN THE FREE DRUG AND THE CLOBETASOL PROPIONATE NANOPARTICLES	141

ANNEXES

ANNEXES

12. ANNEXES

12.1 Annexes I: approval letter of the PhD project

<p>Universitat Internacional de Catalunya</p>	<p>Campus Barcelona Immaculada, 22 08017 Barcelona, Spain T. +34 932 541 800 www.uic.es</p>	
---	---	---

**ESCUELA DE DOCTORADO
PROGRAMA DE DOCTORADO EN CIENCIAS DE LA SALUD**

Aprobación del Plan de Investigación por la Comisión Académica del Doctorado

Apreciados doctorando y directores,

Por la presente les comunicamos que la Comisión Académica del Doctorado en Ciencias de la Salud ha aprobado el siguiente plan de investigación:

Doctorando	FIRAS HUSSEIN ELMSMARI
Título	Nanoparticles: the next step in endodontic medicaments
Dirección de tesis	Dra. José Antonio González Sánchez Dra. Elena Sánchez López
Línea de investigación	Investigación básica y aplicada en odontología
Dedicación	A tiempo parcial (5 años)
1ª matrícula	2018-2019
Curso depósito de la tesis	2022-2023

Cualquier modificación que afecte al plan de investigación en relación a la dirección de tesis o a la temporalidad del programa deberá solicitarse previa instancia a la CAD.

Atentamente,





Universitat Internacional
de Catalunya
Escola de Doctorat

Sònia Soriano
Secretaria Escuela de Doctorado

Barcelona, 6 de septiembre de 2019

12.2 Annexes II: approval letter of Ethic committee

Universitat Internacional
de Catalunya

Comitè d'Ètica
de Recerca



APROVACIÓ PROJECTE PEL CER/ APROBACIÓN PROYECTO POR EL CER

Codi de l'estudi / Código del estudio: END-ELB-2020-01
 Versió del protocol / Versión del protocolo: 1.0
 Data de la versió / Fecha de la versión: 20/12/19

Sant Cugat del Vallès, 23 de gener de 2020

Doctorando: Firas Hussein Elmsmari
 Director de Tesi: José Antonio González Sánchez
 Codirectora: Elena Sánchez López

Títol de l'estudi / Título del estudio: Nanoparticles: the next step in endodontic medicaments

Benvolgut/da,

Valorat el projecte presentat, el CER de la Universitat Internacional de Catalunya, considera que, el contingut de la investigació, no implica cap inconvenient relacionat amb la dignitat humana, tracte ètic per als animals ni atempta contra el medi ambient, ni té implicacions econòmiques ni conflicte d'interessos, no s'han valorat els aspectes metodològics sense implicacions ètiques del projecte de recerca, degut a que tal anàlisis correspon a d'altres instàncies

Per aquests motius, el Comitè d'Ètica de Recerca, **RESOLT FAVORABLEMENT**, emetre aquest **CERTIFICAT D'APROVACIÓ**, per que pugui ser presentat a les instàncies que així ho requereixin.

Em permeto recordar-li que, si en el procés d'execució es produís algun canvi significatiu en els seus plantejaments, hauria de ser sotmès novament a la revisió i aprovació del CER.

Atentament,

Apreciado/a,

Valorado el proyecto presentado, el CER de la Universidad Internacional de Catalunya, considera que, el contenido de la investigación, no implica ningún inconveniente relacionado con la dignidad humana, trato ético para los animales, ni atenta contra el medio ambiente, ni tiene implicaciones económicas ni conflicto de intereses, pero no se han valorado aspectos metodológicos sin implicaciones éticas del proyecto de investigación, debido a que tal análisis corresponde a otras instancias.

Por estos motivos, el Comité d'Ètica de Recerca, RESUELVE FAVORABLEMENTE, emitir este CERTIFICADO DE APROBACIÓN, para que pueda ser presentado a las instancias que así lo requieran.

Me permito recordarle que, si el proceso de ejecución se produjera algún cambio significativo en sus planteamientos, debería ser sometido nuevamente a la revisión y aprobación del CER.

Atentamente,



Dr. Josep Maria Guardiola
President CER-UIC

12.3 Annexes III: patent application for Calcium Hydroxide/PLGA nanoparticles



Acknowledgement of receipt

We hereby acknowledge receipt of your request for grant of a European patent as follows:

Submission number	300368471	
Application number	EP20382504.7	
File No. to be used for priority declarations	EP20382504	
Date of receipt	11 June 2020	
Your reference	19-9661 EP	
Applicant	UNIVERSITAT INTERNACIONAL DE CATALUNYA, FUNDACIÓ PRIVADA	
Country	ES	
Title	COMPOSITION COMPRISING NANOPARTICLES, METHOD FOR THE PREPARATION OF A COMPOSITION COMPRISING NANOPARTICLES AND USES OF THE COMPOSITION FOR DENTAL TREATMENT	
Documents submitted	package-data.xml application-body.xml SPECNONEPO.pdf19-9661_ENCAPSULACIÓN NANOPARTICULAS_MEMORIA_ES_V07.pdf (13 p.) SPECTRANEPO-1.pdf19-9661-EP_ENCAPSULACIÓN NANOPARTICULAS_MEMORIA_EN_V07.pdf (11 p.) f1002-1.pdf (2 p.)	ep-request.xml ep-request.pdf (5 p.) OLF-ARCHIVE.zip\19-9661_ENCAPSULACIÓN NANOPARTICULAS_MEMORIA_ES_V07.zip OTHER-1.pdfAdditional representative Juncosa-Gislon.pdf (1 p.)
Submitted by	CN=Margalida Segui-Quetglas 67791	
Method of submission	Online	
Date and time receipt generated	11 June 2020, 08:59:37 (CEST)	
Official Digest of Submission	C1:0C:78:7B:FD:D7:4F:D7:E4:EC:A6:13:D1:94:82:A5:C5:7A:B4:BF	

/Madrid, Oficina Receptora/

12.4 Annexes IV: study of the patentability of the Clobetasol/PLGA nanoparticles



Gran Via de les Corts Catalanes 669 BIS. 1º. 2ª
08013. Barcelona, Spain
T +34 93 342 65 50
F +34 93 301 69 65
tornejuncosa@tjapatents.com
www.tjapatents.com

INFORME DE PATENTABILIDAD

'USO DE NANOPARTÍCULAS DE PLGA CON CLOBETASOL EN
APLICACIONES DENTALES'

02.11.2020

Este informe es informativo y no es vinculante.

Las opiniones expresadas en este informe responden a una actitud de imparcialidad y se basan en la información recibida y en el análisis realizado basado en nuestros conocimientos y experiencia profesional. Estas opiniones están sujetas a revisión en caso de que se alegan razones fundadas.

El contenido de este documento es confidencial. Queda prohibida la divulgación sin el permiso expreso del cliente y el editor.